Durham E-Theses

The kaon nucleon interaction

Graham G. Ross

How to cite:

Ross, Graham G. (1969) The kaon nucleon interaction. Doctoral thesis, Durham University.

THE KAON NUCLEON INTERACTION

Thesis submitted to the
University of Durham

by

GRAHAM G. ROSS, B.Sc.

for the Degree of Doctor of Philosophy.

Department of Physics,
University of Durham.

June 1969.

ABSTRACT

The K-matrix formalism for the low energy $\bar{K}N$ interaction is reviewed. By using the N/D method to compute the scattering matrix for left hand singularities chosen to approximate the physical singularities of the $\bar{K}N$ and $\Sigma\pi$ amplitudes the nature of the energy dependence of the inverse K-matrix elements are investigated. From this it is concluded that an effective range parameterisation should be a good approximation to the inverse K-matrix elements and that the off diagonal elements of the effective range matrix may not, à priori, be neglected.

The application of dispersion relations to the prediction of the strange particle coupling constants is discussed. A once subtracted sum rule is introduced which reduces the discrepancy in the prediction of the coupling constants due to the use of different low energy parameterisations for the $\bar{K}N$ amplitude. The resultant prediction of the coupling constants is incompatible with the SU(3) predictions.

A new S-wave zero range fit to the low energy $\bar{K}N$ data is performed. A good fit is obtained which improves on previous analyses over the low energy $\bar{K}N$

region. The values of the coupling constants predicted
by the standard dispersion relation using this
parameterisation are again incompatible with the SU(3)
predictions.

Finally the effect of the non-negligible P waves
in the isospin one channel are investigated using a
constant scattering length parameterisation for these
waves in the analysis of the low energy $\bar{K}N$ data.

Acknowledgements

I would like to thank my supervisor Dr. A.D. Martin for his friendly guidance throughout my stay at Durham. I would also like to thank Professor B.H. Bransden for his support and interest, and the members of the Physics and Mathematics Departments in the University of Durham for numerous interesting and stimulating discussions. My thanks also go to Mrs. P.A. Wilson for her care in typing this thesis.

Finally I would like to acknowledge receipt of an S.R.C. Research Studentship throughout the course of this work.

CONTENTS

CHAPTER 1

Introduction

The interactions of particles at present appear to be governed by four separate types of force which are, in descending order of strength, the strong, the electromagnetic, the weak and the gravitational forces. In this thesis we will be principally concerned with the strong interactions, although the effect of the electromagnetic interaction will be considered. The gravitational and weak forces will, in all applications considered here, be negligible.

From the analysis of scattering experiments it has been observed that it is possible to assign to the scattering states quantum numbers which are conserved in all interactions mediated by the strong force. The conserved quantum numbers so far allocated are charge (Q), parity (P), charge conjugation (C), baryon number (B) and strangeness (S). In addition to the limitations imposed by these selection rules, it is also possible to classify the interactions by appealing to the Lorentz Invariance of scattering experiments. Thus, by conservation of total angular momentum the interaction may be decomposed into partial waves and no interference is possible between partial waves corresponding to different

values of the total angular momentum. A further symmetry of

the strong interactions was discovered when it was found

that the observed particles could be fitted into

representations of SU(2), adding two more labels to the

particle, namely the total SU(2), or isospin, content I

and the third isospin component I_3. In analogy with the

angular momentum case, the interaction may be analysed in

terms of its states of definite isospin and, it is found,

strong interactions may be classified by their isospin

content, giving a further conserved quantum number I, and

the interaction is unchanged by rotations in isospin space.

It is evident that the recognition of such symmetries

yields a great simplification in the study of strong

interactions for the symmetry gives a classification of

these interactions. Accordingly higher symmetries have

been sought which, it is hoped, will encompass the

conservation laws, together with the isospin symmetry. Of

these attempts the most successful has been the SU(3)

symmetry group of Gell-Mann and Neeman[1]. Under this scheme

particles are fitted into SU(3) representations and

interactions mediated by the strong interactions are supposed

to be SU(3) invariant. This scheme has had great success in

predicting the particle multiplets but the experimental

evidence supporting the SU(3) invariance of the strong
interactions is very limited. The reason for this is
that the nucleon-nucleon and π meson-nucleon reactions,
for which there is a large amount of experimental data,
can only test the SU(2) isospin subgroup of the symmetry.
In order to test the full SU(3) symmetry it is necessary
to obtain details of the interactions involving strange
particles. Part of this thesis is devoted to the determina-
tion of the coupling of the strange particles to the
neucleons and it is evident that such a deter-mination
will be a useful test of the SU(3) predictions.

Many further symmetry schemes have been proposed which
attempt to include in the symmetry group the external
symmetries of the Lorentz group. Of these SU(6)[2], which
combines the internal symmetry SU(3), with the external
SU(2) spin group, has had some success but there are
theoretical difficulties involved in this group as it is
itself not relativistically invariant. Once again the
determination of the coupling of the strange particles to
the neucleons would provide a good test of the symmetry
scheme's predictions.

Although symmetries serve to classify the strong
interactions there still exists the problem of analysing

the dynamics of these interactions. An obvious approach

to this problem would seem to be to try to apply the

formalism of field theory, which has been so successful

in the description of the electromagnetic interaction, to

the strong interaction. However it turns out, for the π

mesons at least, that the strong coupling is of the order

of 15, and thus perturbation expansions, used successfully

in quantum electrodynamics to solve the field equations,

would not in general be expected to be of much use. Moreover

the basic Lagrangian is not at present known, there being

no classical theory of strong interactions to which to

appeal. A different approach to the problem would therefore

seem to be necessary and it was suggested by Heisenberg[3] that,

in the absence of any knowledge of the strong interaction,

a formalism should be set up which deals only with

physically observable quantities. Thus the S Matrix is

introduced which connects the incoming particle states,

before they reach the region of interaction, with the

outgoing particle states after they leave the region of

interaction. The transition probability between scattering

states will therefore be given by the square of the S matrix

elements between these states. If the ingoing and outgoing

basis states are taken to be plane wave states then it may

be shown that, as a result of the Lorentz invariance of
the interactions, the S Matrix will be a function of the
invariants formed out of the particle four momenta. A
fundamental postulate is then that the S matrix is an
analytic function of these invariants. Moreover it is
postulated that the S matrix, analytically continued in
these variables to a region where the direction of certain
particle four momenta are reversed, will then describe
the S matrix for the process involving the scattering of
the new incident state to the new outgoing state. Thus if
the original process is

$$a + b \longrightarrow c + d$$

then the S matrix for this process may be analytically
continued to the region where the direction of the momenta
of particles c and b are reversed and then it will describe
the scattering process

$$a + \bar{c} \longrightarrow d + \bar{b}$$

where the bar denotes the antiparticle is to be taken.
Similarly the S matrix is continuable to the region where
it describes the process

$$b + \bar{c} \longrightarrow d + \bar{a}$$

The analyticity postulate is made more explicit by
demanding that the only singularities of the S matrix arise

from the kinematical singularities in each channel, namely those due to the possible single and many particle states in each channel.

It is evident that, as crossing relates the singularities of each channel to those in the other channels, some sort of self consistency condition is set up and it is believed possible that the only solution to these consistency restrictions may be the physical world in which, therefore, every particle exists because of the existence of every other particle.

The postulate of the analyticity of the S matrix has been extended to analyticity in the complex angular momentum plane[4] connecting one partial wave with another. In this theory the pole in the S matrix associated with a single particle state is believed to move in the angular momentum plane, each pole tracing a trajectory throughout this plane. The trajectories thus connect particles of different spin and the associated poles are known as Regge poles. A consequence of this theory is that the high energy behaviour of the amplitude in one channel is dominated by the exchange of Regge poles in the crossed channels. The form of the high energy amplitude predicted by the Regge model is found to be in good agreement with experiment.

It is also of interest to apply the bootstrap principal to the Regge pole model and models have been evolved which satisfy the conditions of analyticity, crossing and Regge high energy behaviour. Such models are, however, still very speculative and beyond the scope of this thesis.

Experimentally, the interactions that have been most extensively studied are those involving nucleons and π mesons. Due to the fact that the only stable targets are the nuclei of atoms most scattering data involves either protons, or protons and neutrons. Moreover in order to obtain useful numbers of collisions it is necessary to produce an incident beam of high intensity. In the past the only suitable incident particles have been π mesons and nucleons. However, more recently, it has become possible to produce incident beams of K mesons and data has been obtained for the kaon-nucleon interaction. The analysis of this data is still in its infancy, and it is with this reaction, particularly in the low energy region, that this thesis will be concerned.

In table (1.1a) we list the particles which which we will primarily be concerned, together with their quantum numbers. These particles are classified by SU(3) into two octets as shown in table (1.1b). It should be noted that

Particle	Mass (MeV)	B	S	P	Q	J	I	I_3	Mass symbol
K^+	493.83	0	1	–	1	0	$\frac{1}{2}$	$\frac{1}{2}$	m
K^0	497.75	0	1	–	0	0	$\frac{1}{2}$	$-\frac{1}{2}$	m
$\bar{K}^0$	497.75	0	-1	–	0	0	$\frac{1}{2}$	$\frac{1}{2}$	m
K^-	493.83	0	-1	–	-1	0	$\frac{1}{2}$	$-\frac{1}{2}$	m
π^+	139.58	0	0	–	1	0	1	1	μ
π^0	134.98	0	0	–	0	0	1	0	μ
π^-	139.58	0	0	–	-1	0	1	-1	μ
p	938.26	1	0	+	1	$\frac{1}{2}$	$\frac{1}{2}$	$\frac{1}{2}$	M
n	939.55	1	0	+	0	$\frac{1}{2}$	$\frac{1}{2}$	$-\frac{1}{2}$	M
Σ^+	1189.47	1	-1	+	1	$\frac{1}{2}$	1	1	m_{Σ^+}
Σ^0	1192.54	1	-1	+	0	$\frac{1}{2}$	1	0	m_{Σ^0}
Σ^-	1197.41	1	-1	+	-1	$\frac{1}{2}$	1	-1	m_{Σ^-}
Λ	1115.50	1	-1	+	0	$\frac{1}{2}$	0	0	m_{Λ}

Table (1.1a)

$$B(J)^P = 1\left(\tfrac{1}{2}\right)^+$$
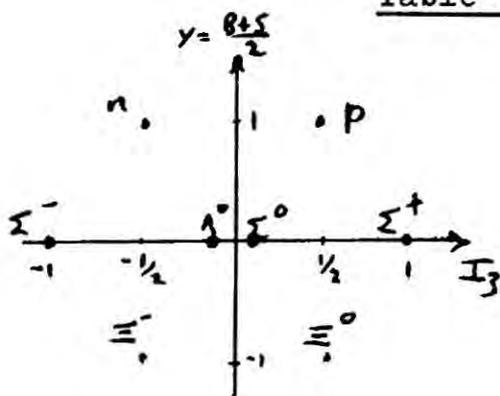
$$B(J)^P = 0(0)^-$$

Table (1.1b)
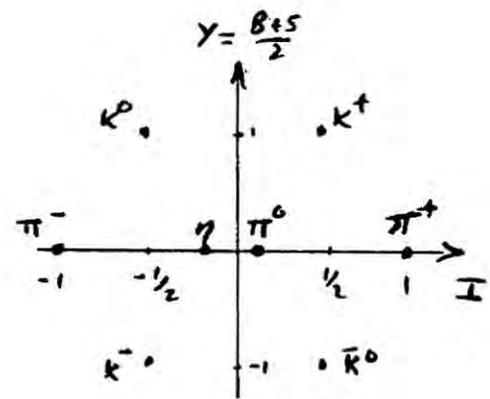
each octet is made up of particles with the same baryon number, spin and parity as shown.

As mentioned above, the determination of the coupling between the strange and non-strange particles is of fundamental importance. The normal way of determining the coupling constants, which are related to the residues of the single particle poles, is by extrapolation of the forward scattering amplitude, by means of a dispersion relation, from the physical region where data is available to the pole positions. For the π N case this extrapolation is straightforward as the experimental data is sufficient to give the discontinuity of the function across its cuts over the region of interest. However in the $\bar{K}N$ case a difficulty arises due to the presence, at the $\bar{K}N$ threshold, of the open $\Sigma\pi$ and $\Lambda\pi$ channels. Due to the fact that no experiments are, at present, possible for $\Sigma\pi$ and $\Lambda\pi$ scattering, the discontinuity across the $\Sigma\pi$ and $\Lambda\pi$ kinematic cuts below the $\bar{K}N$ threshold is experimentally unknown. Thus it is necessary to parameterise the $\bar{K}N$ amplitude in the low energy region, determine the low energy parameters by a fit to the low energy data, and use the continuation of the parameterisation below the $\bar{K}N$ threshold to predict the discontinuity across the $\Sigma\pi$ and $\Lambda\pi$ cuts. The parameterisation and fit to the data has been performed by

several people and the results applied to the prediction of the $\bar{K}N\Lambda$ and $\bar{K}N\Sigma$ coupling constants. However there is serious disagreement between the results of these analyses, it being found that the predicted values for the coupling constants lie, broadly, in two regions, one in agreement with the SU(3) prediction, and the other not. The basic reason for the difference between the predictions lies in the fact that the isospin zero $\bar{K}N$ amplitude has a resonance at a position just below the $\bar{K}N$ threshold. This resonance, which provides a large contribution to the dispersion relation prediction of the coupling constant, must be predicted by the parameterisation, and a small change in the parameters can produce a large change in the resonance contribution.

In view of the discrepancies between the existing solutions it would appear profitable to examine in detail the merits of the various parameterisations used and to investigate ways of improving them. Moreover restrictions on the solutions may be possible by applying suitable consistency tests to the fits which relate the low energy behaviour of the amplitude to that in other energy regions. This thesis is concerned with these problems and provides a new analysis of the low energy data which, it is hoped, will

finally resolve the discrepancy between the previous fits.

In Chapter 2 the formalism necessary to describe kaon
nucleon scattering is introduced and the decomposition
according to angular momentum and isospin is computed.
Finally the analyticity postulate in the complex energy
squared plane is made explicit by writing down the Mandelstam
representation for the scattering amplitude.

The parameterisation of the low energy $\bar{K}N$ amplitude
is introduced in Chapter 3 and, using a model which, it is
hoped, approximates the $\bar{K}N$ case, the validity of approxima-
tions to the full parameterisation are tested. It is
concluded that a result obtained by Nath and Shaw[5] in a more
general analysis of low energy parameterisation should not
be expected to be valid in this particular case. Lastly
a summary of the various fits that have been made to the
low energy $\bar{K}N$ data is given.

The use of dispersion relations in the determination
of the coupling constants is discussed in detail in Chapter
4 and the existing predictions listed. The SU(3) and SU(6)
values for the couplings are written down for comparison
with the predicted values. Other independent measurements
of the coupling constants are also reviewed. A new
superconvergent sum rule is proposed which, it is claimed,

provides a prediction of the coupling constant essentially independent of the unphysical region. Other consistency tests are discussed and one developed for use in future fits.

In Chapter 5 an S wave fit to all the present data in the region of kaon laboratory momentum 0-280 MeV/c is presented. New data arising from $K_2^o p$ experiments is included in the fit. The uniqueness of the fit and stability against change in parameterisation is also investigated and the coupling constant computed. Finally the consistency test developed in Chapter 4 is applied to the new solution.

Chapter 6 presents a more extensive fit to the $\bar{K}N$ data, including P waves in the parameterisation of the isospin one amplitude. Data in the region 0-280 MeV/c kaon laboratory momentum is analysed for processes involving the I=0 amplitude whilst the range is extended to 400 MeV/c for experiments involving only the I=1 reaction. Once again the stability against change of parameterisation and the uniqueness of the solution is investigated and the coupling constants evaluated.

CHAPTER 2

Kaon-Nucleon Scattering

(i) The S Matrix

If we define by $|\alpha_{in}\rangle$ and $|\beta_{out}\rangle$ the basis states which are identified asymptotically as time tends to $\pm \infty$ with free particle plane wave states, then the S matrix, by definition, transforms the "out" base to the "in" base

$$S|\beta_{out}\rangle = |\beta_{in}\rangle$$

Assuming that the states $|\alpha_{out}\rangle$ form a complete orthonormal set, conservation of probability implies the unitarity condition that

$$S^{\dagger}S = SS^{\dagger} = I \tag{2.1}$$

where $\dagger$ denotes adjoint and I is the unit matrix.

S is therefore a unitary operator and the transition amplitude between α and β may be written

$$\langle \beta_{out}|\alpha_{in}\rangle = \langle \beta_{out}|S|\alpha_{out}\rangle = S_{\beta\alpha}$$

The processes with which we will principally be concerned are those "two to two" processes involving two particle initial and final states.

$$a + b \longrightarrow c + d$$

This is illustrated in Fig. (2.1).
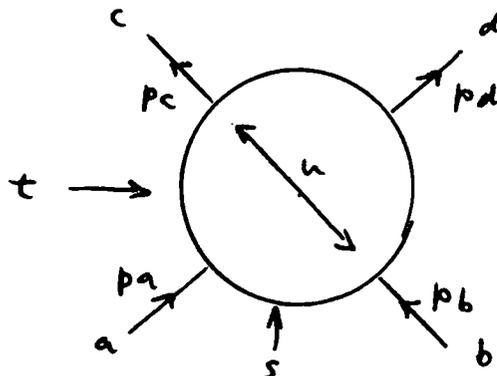
From the four momenta p_a, p_b, p_c, p_d of the individual particle plane wave states we may form the invariants s, t and u defined by

$$s = -(p_a + p_b)^2 = -(p_c + p_d)^2$$
$$t = -(p_a - p_c)^2 = -(p_b - p_d)^2 \qquad (2.2)$$
$$u = -(p_a - p_d)^2 = -(p_b - p_c)^2$$

The energy momentum conservation condition

$$p_a + p_b = p_c + p_d$$

implies the relation

$$s + t + u = m_a^2 + m_b^2 + m_c^2 + m_d^2 \qquad (2.3)$$

and so the three invariants are not independent of each other. Here m_i is the mass of particle i.

It is conventional to factor a delta function, corresponding to no scattering, out of the S matrix and, for the two to two process of Fig. (2.1) this decomposition is normally written[6]

$$S_{fi} = \delta_{fi} - \frac{i (2\pi)^4 \, \delta^{(4)}(p_c + p_d - p_a - p_b)}{n_a \, n_b \, n_c \, n_d} T_{fi} \qquad (2.4)$$

where

$$S_{fi} = {}_{out}\langle p_c p_d | S | p_a p_b \rangle_{out} = {}_{out}\langle p_c p_d | p_a p_b \rangle_{in}$$

f and i denote final and initial states and the n's are the conventional normalization factors for bosons or fermions as

the case may be, viz:

$$n_\beta = \left(\frac{\varepsilon_\beta}{m_\beta} \right)^{1/2} \qquad \text{for bosons}$$

and $\qquad n_F = (2\varepsilon_F)^{1/2} \qquad$ for fermions

with $\qquad \varepsilon^2_{\beta(F)} = \mathcal{P}^2_{\beta(F)} + m^2_{\beta(F)}$

Equation (2.4) explicitly exhibits the energy-momentum

conservation of the system.

If we express the conditions imposed by unitarity on the

T matrix by substituting equation (1.4) in (2.1) we find[7]

$$\delta_{fi} = \delta_{fi} - i(2\pi)^4 \delta^{(4)}(Q^{(i)} - Q^{(f)}) N_i N_f (T_{fi} - (T^*)_{if})$$
$$+ (2\pi)^8 N_i N_f \sum_a N_a^2 \delta^{(4)}(Q^{(i)} - Q^{(a)}) \delta^{(4)}(Q^{(a)} - Q^{(f)}) T_{fa}(T^*)_{ai}$$

where the sum over a is over all possible intermediate

states, $Q^{(a)}$ stands for the total, centre of mass,

momentum of state a, and N_a is the normalization factor

for the particles in state a . Simplifying this equation

we obtain the unitarity equation for the T matrix

$$\frac{1}{2i}(T_{fi} - T^*_{fi}) = -\frac{1}{2}(2\pi)^4 \sum_a N_a^2 \delta^{(4)}(Q^{(i)} - Q^{(f)}) T_{fa}(T^*)_{ai} \qquad (2.5)$$

The analyticity postulate states the S matrix, and thus

also the T matrix are analytic functions of the variables

s, t and u and that the only singularities are the kinematic

ones. It may be seen from (2.5) that at an energy correspond-

ing to a new allowed intermediate state, a, the left hand

side of (2.5) changes. Accordingly the T amplitude has a

singularity at such a threshold and, in fact, such a

threshold is a branch point of the T amplitude. These

branch cuts are drawn along the positive real axis in the

complex energy squared plane $S = E^2$ and define a Riemann

surface on which the amplitude is single valued. Moreover

the choice of cut direction ensures the amplitude is

hermetian analytic.

The singularity structure of the amplitude arising

from the kinematic cuts in the s and t channels at a

fixed value of $u = u_o$ is drawn in Fig. (2.2). The poles

corresponding to single particle states of mass m_s, m_t in

channel s,t respectively are also given. I_s^2 and I_t^2 give

the position of the first inelastic thresholds in the s and

t channels and Σ^2 is the sum of the masses of the four

interacting particles
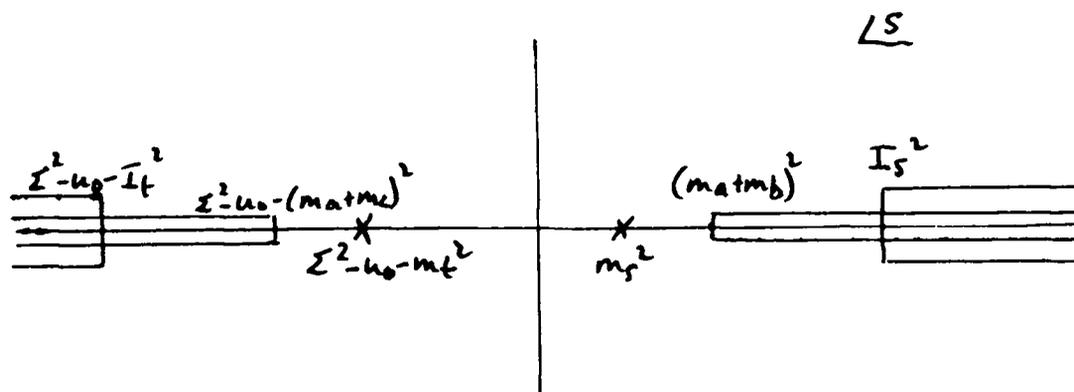
Fig. (2.2)

A resonance is given by a pole on the unphysical sheets at a complex point in the s plane.

The physical amplitude for the process

$$a + b \longrightarrow c + d$$

is defined by the relation

$$T^{Physical}_{a+b \to c+d}(s, t, u) = \lim_{\epsilon \to 0+} T(s+\iota\epsilon, t, u)$$

where s, t and u are real.

Crossing relates this amplitude to the t channel process

$$a + \bar{c} \longrightarrow \bar{b} + d$$

to give the relation

$$T_{a+b \to c+d}(s, t, u) = T^{*}_{a+\bar{c} \to \bar{b}+d}(s, t, u) \qquad (2.6)$$

Similar relations may be obtained between the amplitudes in the s and u and the t and u channels.

(ii) <u>Kinematics and Partial Wave Analysis</u>

In this section we will consider in detail the structure of the T matrix for a two to two process as shown in Fig. (2.1) where a and c are spin $\frac{1}{2}$ particles and b and d spin 0 particles. The s channel will be taken to be the physical one and particle b is assumed to be at rest in the laboratory system.

Labelling all quantities with self-explanatory superscripts we may determine the kinematical invariants as follows[7]

$$p_a^{lab} = (E_a^{lab}, \underline{p}_a^{lab}) \quad ; \quad p_a^{cm} = (E_a^{cm}, \underline{p}_a^{cm})$$
$$p_b^{lab} = (m_b, 0) \quad ; \quad p_b^{cm} = (E_b^{cm}, -\underline{p}_a^{cm})$$

Thus
$$s = -(p_a + p_b)^2$$
$$= m_a^2 + m_b^2 + 2 E_a^{lab} m_b$$

Using the invariance of the scalar product $p_a \cdot p_b$ gives

$$E_a^{lab} m_b = E_a^{cm} E_b^{cm} + (\underline{p}^{cm})^2$$

Hence

$$|\underline{p}^{cm}| = |\underline{p}_a^{lab}| \frac{m_b}{(m_a^2 + m_b^2 + 2 E_a^{lab} m_b)^{1/2}}$$

Finally using these equations we may express the momenta in terms of the invariant s

$$|\underline{p}^{cm}| = \sqrt{\frac{(s - (m_a + m_b)^2)(s - (m_a - m_b)^2)}{4s}} \qquad (2.7)$$

In order to describe the kinematics of scattering completely it is necessary to introduce one more variable apart from the invariant s. As mentioned in the previous section a suitable choice is the invariant t and we may express the scattering angle in terms of s and t

$$t = -(p_a - p_c)^2$$
$$= m_a^2 + m_c^2 + 2 (\underline{p}_a^{cm} \cdot \underline{p}_c^{cm} - E_a^{cm} E_c^{cm})$$

If Θ_{ac}^{cm} is the angle between the directions of motion of the particles a and c in the centre of mass system this equation gives

$$\cos\Theta_{ac}^{cm} = \frac{s^2 + s(2t - m_a^2 - m_b^2 - m_c^2 - m_d^2) + (m_a^2 - m_b^2)(m_c^2 - m_d^2)}{\left[(s-(m_a+m_b)^2)(s-(m_a-m_b)^2)(s-(m_c+m_d)^2)(s-(m_c-m_d)^2)\right]^{\frac{1}{2}}} \quad (2.8)$$

The S matrix may be decomposed as in (2.4) where now the Lorentz invariant quantity T_{fi} may be written in the form

$$T_{fi} = \bar{u}(p_c) \, T(s,t,u) \, u(p_a) \qquad (2.9)$$

where u(p) is the usual four spinor for spin $\frac{1}{2}$ particles and is normalised to

$$\bar{u}(p) \, u(p) = 1$$

$T(s,t,u)$ is a 4 x 4 matrix in spin space.

It may be shown[8] that the differential cross section in the center-of-mass frame is given by

$$\frac{d\sigma}{d\Omega} = \frac{m_b m_d}{16\pi^2 s} \left|\frac{Q^{(f)}}{Q^{(i)}}\right| \sum \left|\bar{u}(p_c) \, T(s,t,u) \, u(p_a)\right|^2 \qquad (2.10)$$

where the summation indicates the sum over the final spin states and the average over the initial spin states.

It is often convenient to define the scattering amplitude in a particular reference frame in such a way that

$$\frac{d\sigma}{d\Omega} = \sum \left| \frac{Q^{(f)}}{Q^{(\iota)}} \right| \; | F_{f\iota} |^2 \tag{2.11}$$

where $Q^{(\iota)}$ refers to the reference frame under consideration. Thus it may be seen from (2.10) and (2.11) that

$$F_{f\iota}^{CM} = \sqrt{m_b m_d} \; T_{f\iota} / 4\pi \sqrt{s} \tag{2.12}$$

and
$$F_{f\iota}^{lab} = \sqrt{m_b m_d} \; T_{f\iota} / 4\pi \, m_a$$

Using equations (2.11), (2.12), (2.6) and (2.5) we may write the optical theorem for these amplitudes in the form normally used.

$$
\begin{aligned}
\operatorname{Im} F_{\iota\iota}^{CM}(s) &= \frac{|q^{CM}|}{4\pi} \, \sigma_{tot}(s) \\
\operatorname{Im} F_{\iota\iota}^{lab}(s) &= \frac{|q^{lab}|}{4\pi} \, \sigma_{tot}(s)
\end{aligned} \tag{2.13}
$$

where in both cases the amplitudes have been evaluated in the forward direction and σ_{tot} is the total cross section for particles in state i.

As $T(s,t,u)$ is a Lorentz invariant quantity (strictly, it is the quantity $\bar{u}(p_c)T(s,t,u)u(p_a)$ which is Lorentz Invariant) it may be expressed as a function of the

independent kinematic invariants. In this case due to parity conservation there are only two such invariants and these may be taken[6] as the unit matrix I and $\frac{1}{2}\gamma\cdot(p_b+p_d)$ where the γ are the Dirac γ matrices so that $T(s,t,u)$ is decomposed into the form

$$T(s,t,u) = -A(s,t,u)\,I + \frac{1}{2}i\gamma\cdot(p_b+p_d)\,B(s,t,u) \qquad (2.14)$$

where A and B are scalar functions of the kinematical variables and are known as the invariant amplitudes for this process.

An alternative decomposition is given in terms of the centre of mass amplitude F_{fi}^{CM} where

$$F_{fi}^{CM} = \chi^\dagger(p_c)\,F^{CM}\,\chi(p_a) \qquad (2.15)$$

and the χ are Pauli spinors. From (2.10) and (2.11) and introducing a minus sign by convention since these amplitudes may have an arbitrary phase between them, we see that

$$\chi^\dagger(p_c)\,F^{CM}\,\chi(p_a) = -\frac{\sqrt{m_b m_d}}{4\pi\sqrt{s}}\,\bar{u}(p_c)\,T\,u(p_a) \qquad (2.16)$$

The decomposition in terms of F^{CM} is written

$$F^{CM} = f_1 + \frac{(\underline{\sigma}\cdot p_b)(\underline{\sigma}\cdot p_d)}{|p_b|\,|p_d|}\,f_2 \qquad (2.17)$$

where $\underline{\sigma}$ is the three vector of 2x2 Pauli spin matrices.

The connection between f_1, f_2 and A,B is given by

$$4\pi f_1 = \frac{\left\{[(W+m_b)^2-m_a^2][(W+m_d)^2-m_c^2]\right\}^{\frac{1}{2}}}{4W^2}\left[A+(W-M)B\right]$$

$$4\pi f_2 = \frac{\left\{[(W-m_b)^2-m_a^2][(W-m_d)^2-m_c^2]\right\}^{\frac{1}{2}}}{4W^2}\left[-A+(W+M)B\right] \qquad (2.18)$$

where $\qquad M = \dfrac{m_b + m_d}{2} \qquad , \qquad W = \sqrt{s}$

In writing down the scattering amplitude use was made of its Lorentz invariance in order to express it as a sum of scalar terms. However the Lorentz invariance may be further utilised by writing the amplitude as a series expansion in terms of a set of orthogonal vectors belonging to an irreducible representation of the Homogeneous Lorentz group. A convenient basis for this purpose is the basis of particle helicity states, where helicity is defined as the component of spin along the direction of motion. This decomposition has been carried out in detail by Jacob and Wick[9] and for the kaon-nucleon scattering case their general result reduces to

$$f_{\lambda\lambda'}(\theta,\phi) = \frac{1}{\pi}\sum_J (2J+1)\langle\lambda'|F_J^{CM}|\lambda\rangle e^{i(\lambda-\lambda')\phi}\, d_{\lambda\lambda'}^J(\theta) \qquad (2.19)$$

where λ and λ' are the helicities of the initial and final

fermions respectively, F_J^{CM} is the submatrix of F^{CM} corresponding to states of total angular momentum J, and θ and ϕ are the centre of mass scattering angles. The z axis is chosen along the initial momentum. $f_{\lambda\lambda'}$ is the scattering amplitude for scattering between states with initial and final fermion helicities λ and λ' respectively. The d-functions appropriate to kaon-nucleon scattering are

$$d_{\frac{1}{2},\frac{1}{2}}^{J}(\theta) = \frac{\cos\theta/2}{J+\frac{1}{2}}\left[P'_{J+\frac{1}{2}}(\cos\theta) - P'_{J-\frac{1}{2}}(\cos\theta)\right]$$

$$d_{-\frac{1}{2},\frac{1}{2}}^{J}(\theta) = \frac{\sin\theta/2}{J+\frac{1}{2}}\left[P'_{J+\frac{1}{2}}(\cos\theta) + P'_{J-\frac{1}{2}}(\cos\theta)\right]$$

(2.20)

Since in the present system there are only four possible helicity combinations, we may write

$$\langle f|F_J^{CM}|i\rangle = \langle f|\begin{pmatrix} f_{++}^J & f_{+-}^J \\ f_{-+}^J & f_{--}^J \end{pmatrix}|i\rangle$$

(2.21)

and

$$\langle f|F^{CM}|i\rangle = \langle f|\begin{pmatrix} f_{++} & f_{+-} \\ f_{-+} & f_{--} \end{pmatrix}|i\rangle$$

Parity conservation requires that in each of these cases there shall be only two independent amplitudes, so taking these as the two independent partial wave amplitudes $f_{l\pm}$ and the two independent amplitudes f_1 and f_2 defined in (2.17) we may write

$$f_{l\pm} = \frac{1}{2}\left(f_{++}^J \pm f_{+-}^J\right)$$

(2.22)

and

$$f_{++}(\theta,\phi) = f_{--}(\theta,\phi) = \left(f_1(\theta) + f_2(\theta)\right)\cos\frac{\theta}{2}$$

$$f_{\substack{+- \\ -+}}(\theta,\phi) = \pm e^{\mp\phi}\sin\frac{\theta}{2}\left(f_1(\theta) - f_2(\theta)\right)$$

(2.23)

$f_{\ell \pm}$ denotes a partial wave with total orbital angular

momentum ℓ and total angular momentum $J = \ell \pm \frac{1}{2}$.

From (2.18), (2.19) and (2.20) we have

$$f_{++} = \cos \frac{\theta}{2} \sum_{J} \left[P'_{J+\frac{1}{2}}(\cos\theta) - P'_{J-\frac{1}{2}}(\cos\theta) \right] f_{++}^{J} \qquad (2.24)$$

$$f_{+-} = e^{-i\phi} \sin \frac{\theta}{2} \sum_{J} \left[P'_{J+\frac{1}{2}}(\cos\theta) + P'_{J-\frac{1}{2}}(\cos\theta) \right] f_{+-}^{J}$$

which, using (2.22) and (2.23) gives us finally

$$f_1(\theta) = \sum_{\ell=0}^{\infty} f_{\ell+} P'_{\ell+1}(\cos\theta) - \sum_{\ell=2}^{\infty} f_{\ell-} P'_{\ell-1}(\cos\theta) \qquad (2.25)$$

$$f_2(\theta) = \sum_{\ell=1}^{\infty} (f_{\ell-} - f_{\ell+}) P'_{\ell}(\cos\theta)$$

The orthonormality of the Legendre polynomials may be

expressed in the form

$$\int_{-1}^{1} dz \, P'_{\ell}(z) \left[P_{\ell-1}(z) - P_{\ell+1}(z) \right] = 2\delta_{\ell\ell'}$$

and using this and (2.24) we obtain the inverse relation

$$f_{\ell\pm} = \frac{1}{2} \int_{-1}^{1} dz \left[f_1 \, P_{\ell}(z) + f_2 \, P_{\ell\pm}(z) \right] \qquad (2.26)$$

The differential cross section for states with initial

and final helicities λ and λ' are given in terms of the

amplitude $f_{\lambda\lambda'}(\theta,\phi)$, defined in (2.19) by

$$\frac{d\sigma}{d\Omega} = \left| \frac{Q^{(f)}}{Q^{(i)}} \right| \left| f_{\lambda\lambda'}(\theta,\phi) \right|^2$$

where $Q^{(f)}$ and $Q^{(i)}$ are the final and initial centre of

mass momenta respectively. If we assume the initial fermion is unpolarised and if the polarisation of the final fermion is not observed the differential cross section is given by the sum over the final helicities and average over the initial helicities. Using (2.23) to express this in terms of $f_1(\theta)$ and $f_2(\theta)$ as defined in (2.17) we obtain

$$\frac{d\sigma}{d\Omega} = \left|\frac{Q^{(f)}}{Q^{(i)}}\right| \left\{ \left| f_1(\theta) + \cos\theta f_2(\theta)\right|^2 + \left|\sin\theta f_2(\theta)\right|^2 \right\} \qquad (2.27)$$

The transverse polarisation $P(\theta)$ of the final fermion is obtained by splitting the helicity eigenstates into transverse eigenstates and computing the polarisation as follows

$$P(\theta) = \frac{\frac{d\sigma_+}{d\Omega} - \frac{d\sigma_-}{d\Omega}}{\left(\frac{d\sigma}{d\Omega}\right)_{unpolarised}}$$

where the + and − refer to the spin component along the direction $\underset{\sim}{n}_{in} \times \underset{\sim}{n}_{out}$ and $\underset{\sim}{n}_{in}$ and $\underset{\sim}{n}$ out are unit vectors along the direction of the incident and outgoing bosons respectively. Here $\underset{\sim}{n}_{in}$ is along the z axis and, using (2.23), the result may be expressed in terms of f_1 and f_2 as[10]

$$P(\theta)\left(\frac{d\sigma}{d\Omega}\right)_{unpolarised} = 2\sin\theta \, \mathcal{I}m\left\{ f_2 f_1^* \right\} \qquad (2.28)$$

(iii) <u>The Isotopic Spin Structure of the KN and $\bar{K}N$ systems</u>

From an examination of Table (1.1), it may be seen that there are two isospin kaon doublets, one with strangeness +1 and the other with strangeness -1. Moreover the doublets may be transformed into each other by the operation of going from the particle to the antiparticle.

Due to the fact that strangeness must be conserved, the final state for the scattering of K^+ mesons by nucleons must involve a strange particle with strangeness +1. There is only one such particle available besides the K^+ meson, viz. the neutral K-meson K^0. The only inelastic processes that can occur are therefore

$$K^+ + n \longrightarrow K^0 + p$$

and inelastic processes where for example extra π-mesons are present in the final state. There are thus four charge states in kaon-nucleon scattering

$$|K^+p\rangle, \quad |K^+n\rangle, \quad |K^0p\rangle \text{ and } |K^0n\rangle$$

If we regard the nucleon and kaon as isospin doublets

$$N \equiv \begin{pmatrix} |p\rangle \\ |n\rangle \end{pmatrix} \qquad K \equiv \begin{pmatrix} |K^+\rangle \\ |K^0\rangle \end{pmatrix} \tag{2.29}$$

with the usual isospin operators $\underline{t}^N$ and $\underline{t}^K$ respectively, the charge independence of KN reactions may be conveniently

exhibited by introducing a basis of states that are

eigenstates of the operators I^2 and I_3 where $\underline{I}$ is the

isospin operator and is given by

$$\underline{I} = \frac{1}{2} \underline{\tau}^N + \frac{1}{2} \underline{\tau}^k$$

All four states are then expressed in terms of

states with isotopic spin 1 and 0, obtained by coupling

the two isospin $\frac{1}{2}$ states and using the usual Clebsch-Gordon

decomposition

$$\begin{aligned}
|k^+ p\rangle &= |1,1\rangle \\
|k^0 p\rangle &= \frac{1}{\sqrt{2}} \{|1,0\rangle + |0,0\rangle\} \\
|k^+ n\rangle &= \frac{1}{\sqrt{2}} \{|1,0\rangle - |0,0\rangle\} \\
|k^0 n\rangle &= |1,-1\rangle
\end{aligned} \qquad (2.30)$$

Isotopic spin symmetry means that the S matrix is

invariant under rotations in isospin space, and therefore

that there are only two independent amplitudes involving

two particle kaon nucleon states, namely an isospin one

amplitude and an isospin zero amplitude.

It should be noted that isotopic spin symmetry is

only valid for the strong interactions and therefore the

electromagnetic effects must be included separately to

allow for the K^+, K^0 and p, n mass differences and also

for the effect of the Coulomb force.

The scattering of K^- mesons by nucleons is complicated

by the presence, even at the K^-p threshold, of two, two

particle, inelastic channels with strangeness -1. Thus
the scattering amplitude is a multichannel matrix even
at low energies. The processes allowed for K^-p scattering
are

$$
\begin{aligned}
K^- + p &\longrightarrow K^- + p \\
K^- + p &\longrightarrow \bar{K}^0 + n \\
K^- + p &\longrightarrow \Sigma^+ + \pi^-, \Sigma^0 + \pi^0, \Sigma^- + \pi^+ \\
K^- + p &\longrightarrow \Lambda + \pi^0
\end{aligned}
\qquad (2.31)
$$

plus further multiparticle processes.

As the antikaon doublet is obtainable from the kaon
doublet by particle-antiparticle conjugation, care must be
taken in the choice of the isospin wave functions in order
that both doublets may transform under isospin rotations
in a consistent fashion. Thus choosing the kaon doublet
as in (2.29) and the isospin operator $\underset{\sim}{I}$ for the $\bar{K}N$ system
as

$$
\underset{\sim}{I} = \tfrac{1}{2} \underset{\sim}{\tau}^N + \tfrac{1}{2} \underset{\sim}{\tau}^{\bar{K}}
$$

the antikaon doublet must be taken as

$$
\bar{K} \equiv \begin{pmatrix} |\bar{K}^0\rangle \\ -|K^-\rangle \end{pmatrix}
\qquad (2.32)
$$

The isospin decomposition of the four possible $\bar{K}N$
charge states is given by (2.29) and (2.32) as

$$
\begin{aligned}
|\bar{K}^0 p\rangle &= |1,1\rangle \\
|K^- p\rangle &= -\tfrac{1}{\sqrt{2}}\left\{ |1,0\rangle + |0,0\rangle \right\} \\
|\bar{K}^0 n\rangle &= \tfrac{1}{\sqrt{2}}\left\{ |1,0\rangle - |0,0\rangle \right\} \\
|K^- n\rangle &= -|1,-1\rangle
\end{aligned}
$$

Isospin symmetry thus states that there are only two independent amplitudes for processes involving two particle antikaon nucleon states. Electromagnetic effects must, once again, be included to allow for mass difference and Coulomb scattering.

The isospin decomposition must also be applied to the other channels involving the different isospin multiplets, the Λ singlet and the Σ triplet. Using the normal Clebsch-Gordon decomposition it is straightforward to compute the standard isospin basis vectors I, I_3 for these channels which gives

$$
\begin{aligned}
|1,0\rangle &= |\Lambda \pi^0\rangle \\
|0,0\rangle &= \frac{1}{\sqrt{3}} \left\{ |\Sigma^+ \pi^-\rangle - |\Sigma^0 \pi^0\rangle + |\Sigma^- \pi^+\rangle \right\} \\
|1,0\rangle &= \frac{1}{\sqrt{2}} \left\{ |\Sigma^+ \pi^-\rangle - |\Sigma^- \pi^+\rangle \right\}
\end{aligned}
\tag{2.34}
$$

In order to tabulate the isospin independent amplitudes for the low energy $\bar{K}N$ amplitude where only two particle channels are open we introduce the notation

$$
\begin{aligned}
|a_0\rangle &= \frac{1}{\sqrt{2}} \left\{ |K^- p\rangle - |\bar{K}^0 n\rangle \right\} \\
|b_0\rangle &= \frac{1}{\sqrt{3}} \left\{ |\Sigma^+ \pi^-\rangle - |\Sigma^0 \pi^0\rangle + |\Sigma^- \pi^+\rangle \right\} \\
|a_1\rangle &= \frac{1}{\sqrt{2}} \left\{ |K^- p\rangle + |\bar{K}^0 n\rangle \right\} \\
|b_1\rangle &= \frac{1}{\sqrt{2}} \left\{ |\Sigma^+ \pi^-\rangle - |\Sigma^- \pi^+\rangle \right\} \\
|c_1\rangle &= |\Lambda \pi^0\rangle
\end{aligned}
\tag{2.35}
$$

for our basis states, the subscript referring to the total isospin.

The T matrix is block diagonal in these states and may be written as

$$\langle a_I \mid T \mid b_{I'} \rangle = T_{ab}^{(I)} \, \delta_{I\bar{I}'} \qquad\qquad (2.36)$$

with analagous symbols for the other elements of the matrix T.

(iv)   The Mandelstam Representation

Mandelstam[11] has given a prescription for obtaining the analytic properties of each of the elements of the Dirac matrix T(s,t,u) defined by (2.14), considered as function of two independent kinematic variables simultaneously. He conjectures that, apart from possible subtractions if the integrals do not converge, an amplitude for the process shown in Fig. (2.1) with spin as in section (ii) would have the form

$$A^I(s,t,u) = \sum_\gamma \frac{\alpha_\gamma^I}{m_\gamma^2 - s} + \frac{1}{\pi^2} \int_{(m_\Lambda + \mu)^2}^\infty ds' \int_{4\mu^2}^\infty dt' \frac{A_{23}^I(t',s')}{(t'-t)(s'-s)}$$

$$+ \frac{1}{\pi^2} \int_{(M+m)^2}^\infty du' \int_{(m_\Lambda+\mu)^2}^\infty ds' \frac{A_{13}^I(u',s')}{(u'-u)(s'-s)} + \frac{1}{\pi^2} \int_{(M+m)^2}^\infty du' \int_{4\mu^2}^\infty dt' \frac{A_{12}^I(u',t')}{(u'-u)(t'-t)} \qquad (2.37)$$

and a similar expression for $B^{(I)}(s,t,u)$ where m, M, μ are the masses of the kaon, nucleon and π meson respectively.

The spectral functions A_{ij} are by assumption real and are non vanishing only within certain boundaries which may be calculated by means of a prescription given by Mandelstam and which approach the limits of integrations only asymptotically. The sum is over the Σ and Λ pole terms.

Although it is believed that the Mandelstam representation may follow from imposing causality on S matrix theory, no complete proof of this exists and in our subsequent work we will treat (2.37) as a postulate defining the analytic properties of our scattering amplitude explicitly.

CHAPTER 3

The Parameterisation of the Low Energy $\bar{K}N$ Amplitude

(i) The K Matrix

Unitarity, as expressed for the total amplitude by (2.5), may be written in a particularly simple way for the partial wave amplitudes $f_{\ell\pm}$ as defined in (2.22). This is done using the partial wave projection (2.26) together with equations (2.17), (2.16) in equation (2.15). Assuming two particle elastic scattering only the result may be written in the form

$$\mathfrak{Im} \, f_{\ell\pm}^{-1} = -k\,\Theta_k \qquad , \qquad k \equiv |\underset{\sim}{k}| \qquad (3.1)$$

Here $\underset{\sim}{k}$ is the centre of mass momenta for the elastic process and Θ_k is unity above the elastic threshold and zero otherwise. Equation (3.1) expresses the unitarity of the partial wave amplitude exactly in the region below the first inelastic threshold.

For scattering which involves more than one two particle channel, the amplitude becomes a matrix in channel space, and unitarity for the partial wave matrix amplitude may be written

$$\mathfrak{Im} \, T_{\ell\pm}^{-1} = -k\,\Theta \qquad (3.2)$$

Here k is now the diagonal matrix whose elements are the channel centre of mass momenta and Θ is a diagonal

matrix whose elements are unity above the channel threshold and zero otherwise. This equation expresses two body unitarity and is exact below three particle thresholds.

It is evident from (3.2) that we may write $T_{\ell\pm}$ in the form

$$T_{\ell\pm}^{-1} = K_{\ell\pm}^{-1} - ik \tag{3.3}$$

where, below three particle thresholds, $K_{\ell\pm}$ is a real matrix. Thus this expression for the partial wave amplitudes, first introduced for $\bar{K}N$ scattering by Dalitz and Tuan[12], explicitly constructs an amplitude which is unitary below three particle thresholds.

The choice of the branch of continuation below threshold of a channel momentum on the physical sheet may be made by considering the T-matrix element $\langle j | T | i \rangle$. This corresponds to a wave function for which there is an incident wave of unit amplitude in channel i and otherwise outgoing waves $\exp(ik_j r)/r$ in all channels. If the channel j is closed then the momentum k_j must be taken to have the value $+i|k_j|$ so that the outgoing wave in channel j is replaced by a damped exponential wave $\exp(-|k_j| r)/r$.

The obvious disadvantage of (3.3) is that there are an infinity of channels to be considered even though the energy is such that only several channels are open, and the calculation of the T matrix elements requires the K matrix

elements for all conceivable channels. Accordingly it is usual to define the reduced K-matrix K_R which is defined for those channels which, in the energy range of interest, are open for at least part of the range. Equation (3.3) will now become

$$T_{\varrho\pm}^{-1} = K_R^{-1} - ik \qquad (3.4)$$

where now T, K_R and k have their dimension equal to the number of channels in the subset to be considered.

With some algebraic manipulation[13] it follows from (3.3) and (3.4) that K and K_R are related by

$$(K_\varrho)_{ij} = K_{ij} + i K_{i\tau} \left[(I - ikk)^{-1} k \right]_{\tau\sigma} K_{\sigma j} \qquad (3.5)$$

where i, j refer to channels in the subset and τ, σ refer to channels outside the subset.

We now consider the restrictions imposed on the K-matrix and the reduced K-matrix by the supposed invariance of the S matrix under time reversal. If we denote our basis states by $|J, m, \eta\rangle$ where J and m label the total angular momentum and the third component of angular momentum, and η the remaining quantum numbers necessary to specify the state, then under time reversal these states are transformed[14] by the operator T where

$$T |J, m, \eta\rangle = (-1)^{J-m} |J, -m, \eta\rangle$$

and we have used the phase convention of ref (14).

If strong interactions are time reversal invariant then the S matrix must satisfy

$$\bar{T} \, S \, T^{-1} = S^\dagger$$

This implies a similar condition on the K matrix and we may therefore write

$$\langle Jm\eta | K_{\ell\pm} | Jm'\eta' \rangle = \langle Jm\eta | \bar{T}^{-1} K_{\ell\pm} \bar{T}^{-1} T | Jm'\eta' \rangle$$

as

$$\langle Jm\eta | K_{\ell\pm} | Jm'\eta' \rangle = (-1)^{m-m'} \langle J-m'\eta' | K_{\ell\pm} | J-m\eta \rangle \qquad (3.6)$$

However we know that

$$\langle Jm\eta | K_{\ell\pm} | Jm'\eta' \rangle = \delta_{mm'} \langle J\eta | K_{\ell\pm} | J\eta' \rangle$$

and therefore (3.6) may be finally written as

$$\langle J\eta | K_{\ell\pm} | J\eta' \rangle = \langle J\eta' | K_{\ell\pm} | J\eta \rangle \qquad (3.7)$$

Thus time reversal invariance of the S matrix implies that $K_{\ell\pm}$ is symmetric. It may therefore be diagonalised by an orthogonal transformation and, by (3.3), this will also diagonalise $T_{\ell\pm}$.

We make use of this property when we apply the K matrix to the $\bar{K}N$ interaction. A convenient set of states which diagonalises the T and the K matrices is that given in (2.34) and, following (2.35) we introduce the notation

$$\langle a_I | T | b_I \rangle = T_{ab}^{(I)} \delta_{II'}$$
$$\langle a_I | K | b_I \rangle = K_{ab}^{(I)} \delta_{II'} \qquad (3.8)$$

where I denotes the total isospin and a,b,c the channels
$\bar{K}N$, $\Sigma\pi$ and $\Lambda\pi$ respectively.

Before considering explicit parameterisations of the
K matrix it is necessary to know more about the singularities
of the partial wave amplitudes and this will be considered
in the next section.

(ii) The Singularity Structure of the Partial Wave Amplitudes

In Chapter 2 we introduced the idea of the analyticity
of the scattering amplitude in the invariant variables
s,t and u. This idea was made more explicit by postulating
the Mandelstam Representation (2.37) for the invariant
amplitudes A^I and B^I defined by (2.14). In this section
we wish to use the Mandelstam Representation to deduce the
singularity structure of the Partial Wave Amplitudes.
Using equations (2.18) and (2.26) we know that, for the
process shown in Fig. (1.1), the partial wave amplitudes
$f_{\ell\pm}$ may be written as

$$f_{\ell\pm} = \frac{1}{32\pi W^2} \left[\left\{ \left[(W+m_b)^2 - m_a^2\right]\left[(W+m_d)^2 - m_c^2\right] \right\}^{1/4} \left[A_\ell + (W-M)B_\ell\right] \right.$$
$$\left. + \left\{ \left[(W-m_b)^2 - m_a^2\right]\left[(W-m_d)^2 - m_c^2\right] \right\}^{1/4} \left[-A_{\ell\pm_1} + (W+M)B_{\ell\pm_1}\right] \right] \quad (3.9)$$

where $\quad (A_\ell; B_\ell) = \int_{-1}^{1} dx\, P_\ell(x)\, (A; B)$

Equation (3.9) may be rewritten, taking a factor outside both terms

$$f_{\ell t} = \frac{1}{8\pi}\left[\left\{[(W+m_b)^2 - m_a^2][(W+m_d)^2 - m_c^2]\right\}\left\{A_\ell + (W-M)B_\ell\right\}\right.$$
$$\left. + kq\left\{-A_{\ell t_1} + (W+M)B_{\ell t_1}\right\}\right]\left[\left\{(W+m_b)^2 - m_a^2\right\}\left\{(W+m_d)^2 - m_c^2\right\}\right]^{-\frac{1}{2}} \quad (3.10)$$

where k and q are the initial and final centre of mass momenta respectively.

We now observe that the Mandelstam representation (2.36) may be written in the form

$$A(s,t,u) = \text{Pole terms} + \frac{1}{\pi}\int dt' \frac{a_1(s,t')}{t'-t} + \frac{1}{\pi}\int du' \frac{a_2(s,u')}{u'-u} \quad (3.11)$$

where

$$a_1(s,t') = \frac{1}{\pi}\int ds' \frac{A_{23}(t',s')}{s'-s} + \frac{1}{\pi}\int du' \frac{A_{12}(u',t')}{u'+t'+s-\Sigma}$$
$$a_2(s,u') = \frac{1}{\pi}\int ds' \frac{A_{13}(u',s')}{s'-s} + \frac{1}{\pi}\int dt' \frac{A_{12}(u',t')}{u'+t'+s-\Sigma} \quad (3.12)$$

and $\quad \Sigma = \sum_i m_i^2$

with a similar expression for B(s,t,u)

Moreover by crossing a_1 and a_2 are related by

$$a_1(s,t') = \pm a_2(s,t')$$

depending on whether A(B) is symmetric or antisymmetric under crossing.

If we now consider the functions $A / (kq)^\ell$ and $B / (kq)^\ell$ we see that, from equations (3.10), (3.11) and (3.12), we may write them as

$$\frac{A_\ell(s)}{(kq)^\ell} = \frac{1}{\pi} \int dt' \, a_1(s,t') \, I_\ell(t',s) \tag{3.13}$$

where

$$I_\ell(t',s) = \frac{1}{(kq)^\ell} \int_{-1}^{1} d(\cos\theta) \, P_\ell(\cos\theta) \left[\frac{1}{(t'+k^2+q^2-2kq\cos\theta)} + \frac{(-1)^\ell}{(t'+k^2+q^2+2kq\cos\theta)} \right]$$

and similarly for $B_\ell(s)/(kq)^\ell$.

I_ℓ contains no singularities other than those arising from the vanishing denominators in the Mandelstam representation and, since

$$\frac{1}{2} \int_{-1}^{1} \frac{P_\ell(z)}{(y-x)} \, dx = Q_\ell(y)$$

the integral will vanish at k = 0, q = 0 like $(kq)^\ell$, so that no pole is introduced by dividing by this factor in (3.13).

Also, since I_ℓ is a function only of even powers of $(kq)^\ell$ no branch points occur arising from these kinematical factors. Hence $A_\ell/(kq)^\ell$ and similarly $B_\ell/(kq)^\ell$ are free from kinematical singularities. Finally, from equation (3.10) it is evident that $f_{\ell\pm}/(kq)^\ell$ will also be free of kinematical singularities. The apparent irrationality cut for

$$(m_b - m_a)^2 \leqslant s \leqslant (m_c - m_d)^2$$

is cancelled by the other terms in the expression.

The other singularities in the Partial Wave amplitude $f_{\ell\pm}$ may arise in two ways. Firstly the multiplying

factors in equation (3.10) give rise to a pole at s = 0 and a cut from $-\infty < s \leq 0$. Secondly singularities may arise due to the pole terms or the cut in u, t in the Mandelstam relations for A^T and B^T, and these singularities are known as dynamical singularities. By using equation (3.12) the positions of the dynamical singularities may be determined from the singularity structure of A^T and B^T and this has been done in detail for the process

$$\bar{K} + N \longrightarrow \bar{K} + N$$

by MacDowell[15] and for the processes

$$\bar{K} + N \longrightarrow \Sigma + \pi$$

and

$$\bar{K} + N \longrightarrow \Lambda + \pi$$

by Moorhouse[16]. They find the dynamical singularities for the $\bar{K}N$ and $\widehat{\Sigma\pi}$ channels of the s wave amplitude are as follows

(i) $\bar{K} + N \longrightarrow \bar{K} + N$

The singularities due to the t cut $(4\mu^2 \leq t \leq \infty)$ in A^T, B^T are the following cuts in the s plane

$$-\infty \leq s \leq 0 \qquad |s| = M^2 - m^2$$

$$\left[\sqrt{M^2 - \mu^2} - \sqrt{m^2 - \mu^2} \right]^2 \leq s \leq \left[\sqrt{M^2 - \mu^2} + \sqrt{m^2 - \mu^2} \right]^2$$

The singularity due to the u cut $((M+m)^2 \leq u \leq \infty)$ is the following cut in the s plane.

$$I = 0 : \quad -\infty \leq s \leq 2(m^2 + M^2) - (m_\Sigma + \mu)^2$$

$$I = 1 : \quad -\infty \leq s \leq 2(m^2 + M^2) - (m_\Lambda + \mu)^2$$

These singularities are sketched together with the kinematical

singularities in Fig. (3.1a).

(ii) $\bar{K} + N \longrightarrow \Sigma + \pi$
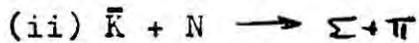
The singularities arising from the nucleon pole in the

u channel are two cuts in the s plane

$$-\infty \lesssim s \lesssim 0$$

$$1.31 \; Gev^2 \lesssim s \lesssim 1.57 \; Gev^2$$

The u channel cut $(M+\mu)^2 \lesssim s \lesssim \infty$ gives the s channel

cut $$-\infty \lesssim s \lesssim \sim 0.24 \; Gev^2$$

plus a region of the s plane to which the amplitude may

be non-continuable. In Fig. (3.1b) the singularities for

this amplitude are shown and this region is the region

bounded by the curve α.

Finally the cuts due to the t channel singularity

$t_0 \lesssim t \lesssim \sqrt{s}$ where t_0 is an anamalous threshold and is given

by $$t_0 = m^2 + \mu^2 + 2m\mu \cos 26°$$

give a cut

$$-\infty \lesssim s \lesssim 0$$

and another region of possible non continuability bounded

by the curve β as shown in Fig. (3.1b).

(iii) $\Sigma + \pi \longrightarrow \Sigma + \pi$
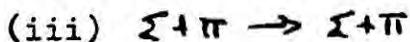
The u channel pole at $u = m_\Sigma^2$ gives the cuts

$$-\infty \lesssim s \lesssim 0$$

and $\dfrac{(m_\Sigma^2 - \mu^2)^2}{m_\Sigma^2} \lesssim s \lesssim m_\Sigma^2 + 2\mu^2$

and the pole at $u = m_\Lambda^2$ gives the cuts

$$-\infty \lesssim s \lesssim 0$$

$$\left(\dfrac{m_\Sigma^2 - \mu^2)^2}{m_\Lambda^2}\right) \lesssim s \lesssim 2m_\Sigma^2 - m_\Lambda^2 + 2\mu^2$$

The u cut $\left(I = 0 : (m_\Sigma + \mu)^2 \lesssim u \lesssim \infty ; \ T = 1 : (m_\Lambda + \mu)^2 \lesssim u \lesssim \infty \right)$

in A^T, B^T give the following cuts in the S plane

$$I = 0 : \quad -\infty \lesssim s \lesssim (m_\Sigma - \mu)^2$$

$$I = 1 : \quad -\infty \lesssim s \lesssim 2m_\Sigma^2 + 2\mu^2 - (m_\Lambda + \mu)^2$$

There is an anamalous threshold for the t-cut in A^T, B^T

$\left(3\mu^2 \lesssim t \lesssim \infty\right)$ and this cut gives the following cuts

$$-\infty \lesssim s \lesssim 0$$

$$|s| = m_\Sigma^2 - \mu^2$$

$$m_\Sigma^2 - \tfrac{1}{2}\mu^2 - (m_\Sigma^2 \mu^2 - \tfrac{3}{4}\mu^4)^{1/2} \lesssim s \lesssim m_\Sigma^2 - \tfrac{1}{2}\mu^2 + (m_\Sigma^2 \mu^2 - \tfrac{3}{4}\mu^4)^{1/2}$$

These singularities are sketched in Fig. (3.1c). For the $\Lambda\pi$ channel the general features of the S wave singularity structure are essentially the same and will not be listed here.

(a)

(b)
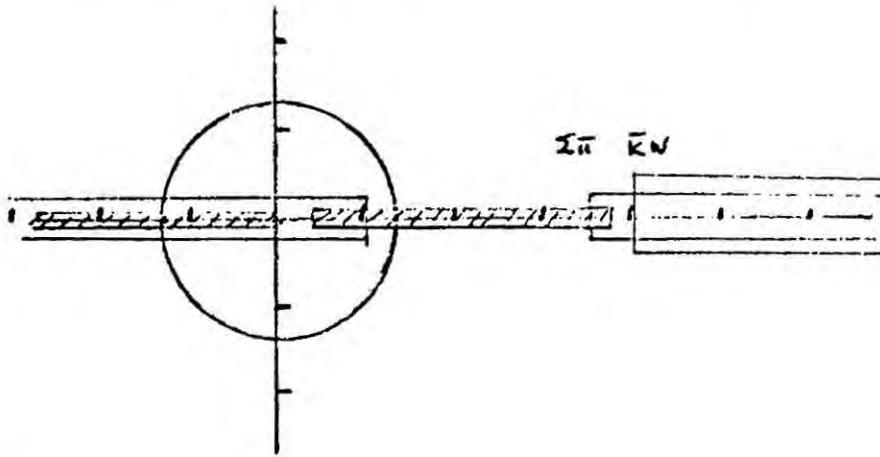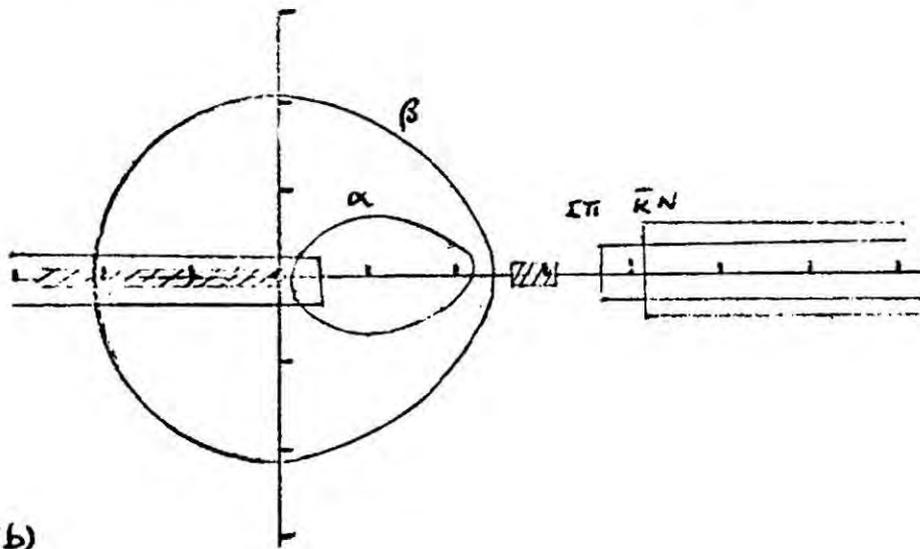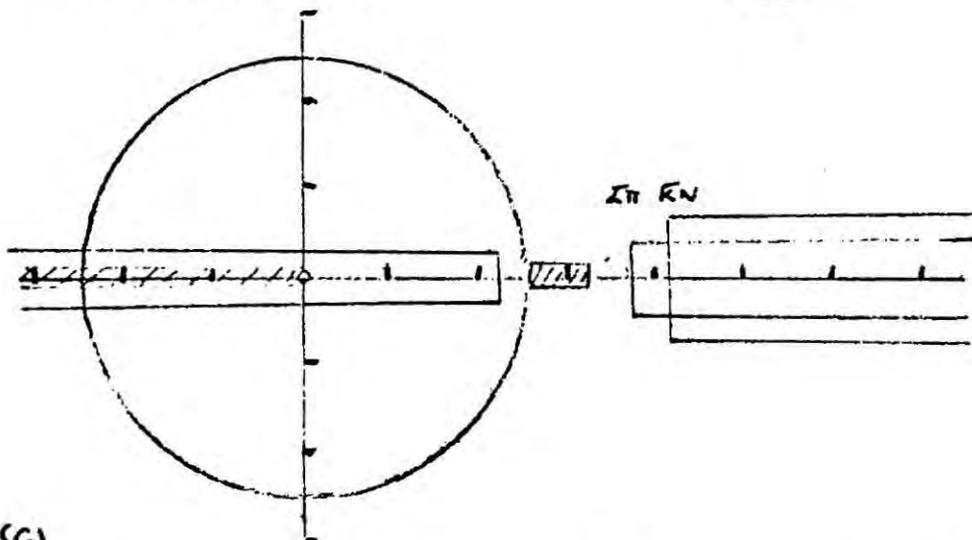
(c)

Fig(3.1) The scale is marked in units of 0.5 Gev.²

(iii) The Parameterisation of the Partial Wave Amplitudes

In the previous section we found that the partial wave amplitude $f_{\ell t}$ has a kinematical cut which may be removed by multiplying by the factor $(kq)^{-\ell}$. For the many channel case we may define a new partial wave matrix $\pi_{\ell t}$ without the kinematical cut by the equation

$$\pi_{\ell \pm} = (k)^{-\ell} \, T_{\ell \pm} (k)^{-\ell} \qquad (3.14)$$

k being the diagonal matrix of channel centre of mass momenta. Equation (3.3) becomes

$$\pi_{\ell \pm}^{-1} = \mathbb{I}K_{\ell \pm}^{-1} - ik^{2\ell+1} \qquad (3.15)$$

where we have defined the new K matrix $\mathbb{I}K_{\ell t}$ by

$$\mathbb{I}K_{\ell \pm} = (k)^{-\ell} \, K_{\ell \pm} \, (k)^{-\ell} \qquad (3.16)$$

This new K matrix, with the threshold singularities removed, may be written[17] as a power series in the channel momenta

$$\mathbb{I}K_{\ell \pm}^{-1} = M_{\ell t} + \tfrac{1}{2}(k^2-k_0^2)^{1/2} \, r_{\ell \pm} (k^2-k_0^2)^{1/2}$$
$$+ (k^2-k_0^2) \, P_{\ell \pm} (k^2-k_0^2) + \cdots \qquad (3.17)$$

where M, r, P ..... are real, symmetric, energy independent matrices whose elements may be used to parameterise the scattering process, and k_0^2 is k^2 evaluated at the point about which the series expansion is being made. This expansion, of course, breaks down when, with decreasing energy a dynamical singularity is reached.

A parameterisation of the K matrix in which only the first term, the M matrix, is kept of the series (3.17) is known as a zero range parameterisation, whilst if the first two terms of the series, namely M and r, are kept the parameterisation is called an effective range parameterisation.

The extraction of the threshold behaviour and the expansion of (3.17), of course apply equally well to the reduced K matrix K_R and henceforth we will use the expression, the K matrix, to refer to the reduced K matrix. The subset of channels on which this reduced K matrix is defined will be specified where necessary.

For the one channel case (3.15) may be written

$$\pi_{\ell\pm} = \left[\frac{1}{A} - i k^{2\ell+1} \right]^{-1} \tag{3.18}$$

where
$$1/A = 1/1K_{\ell\pm}$$

A is real and has the dimensions of length. The effective range expansion of A is then given by

$$\frac{1}{A} = \frac{1}{A_0} + \frac{1}{2} r k^2 \tag{3.19}$$

where A_0 and r are real constants and are known as the scattering length and effective ranges for this one channel amplitude.

The form (3.18) may also be written for the elastic amplitude in the many channel case but by (3.5), in

general, A will be complex due to the presence of the
other inelastic channels. Once again A may be
expanded in the form (3.17) where A_o and r will now
be complex constants and are known as the complex
scattering length and complex effective range for the
many channel process. It should be noted that, in
this formalism, only the elastic unitarity cut is
explicitly built into the amplitude.

The expansion of the K matrix in the form of
(3.17) was first discussed in the multichannel
potential model by Ross and Shaw[17]. Subsequently
Nath and Shaw[18] investigated the expansion for a
scattering amplitude with various left-hand singularities
using the multichannel N/D formalism to compute the
K matrix given these singularities. As a result of
their work they suggested that, in a process for which
the effective range expansion is sufficient to describe
the energy variation of the K matrix in the energy
range of interest, a good approximation in general
is expected to be one in which r is taken as diagonal.

In the rest of this section, we will review the
N/D formalism and apply the method to left hand
singularities which may be taken, from the discussion

of Section (ii), as appropriate to the $\bar{K}N$ case. As a
result of this we suggest that the approximation of a
diagonal r matrix should not be expected to be valid
for $\bar{K}N$ scattering. We also attempt to interpret the
physical meaning of the various terms in the effective
range expansion, and to investigate the possible
effects of the crossed $(\bar{\pi}\pi)$ cut in the $\bar{K}N$ elastic
amplitude.

The N/D approach to determining the T matrix
given its left hand singularities consists in writing
the T matrix in the form

$$T_{\ell\pm} = N_{\ell\pm} D_{\ell\pm}^{-1} \tag{3.20}$$

where $N_{\ell\pm}$ and $D_{\ell\pm}$ are square matrices of the same
dimension as $T_{\ell\pm}$ and, it is supposed, the decomposition
can be made in such a way that $N_{\ell\pm}$ has only the left hand
singularities, namely those arising from the cross
channels, whilst $D_{\ell\pm}$ has only the right hand singularities
arising from the direct channel poles and cuts.
Suppressing the angular momentum labels on the matrices
we observe that unitarity, as expressed by equation
(3.2) may be written, using (3.15), as

$$\mathrm{Im}\,T^{-1} = [\mathrm{Im}\,D]\,N^{-1} = -k^{2\ell+1}\theta \tag{3.21}$$

where we have assumed, for simplicity, that the left
and right hand cuts do not overlap. If we also assume
that the left hand cuts lie along the real axis we
may by (3.15) also write

$$\Im\, N = [\Im\, T] D \tag{3.22}$$

this latter equation being true over the left hand cut
energy region.

We now suppose that the asymptotic behaviour of
N and D are such that it is possible to write a
dispersion integral for N, and a dispersion integral
for D with one subtraction in such a way that the
contribution to the integrals from the portion at
infinity is negligible. Without loss of generality
D may be normalised to the unit matrix at its
subtraction point. Thus N and D are given by

$$D(s) = 1 - \frac{(s-s_0)}{\pi}\, P\!\!\int_R [k(s')]^{2\ell+1} N(s') \frac{ds'}{(s'-s)(s'-s_0)} \tag{3.23}$$
$$- i\, [k(s)]^{2\ell+1} N(s)$$

$$N(s) = \frac{1}{\pi} \int_L [\Im\, T(s')] D(s') \frac{ds'}{(s'-s)} \tag{3.24}$$

for $s > s_{threshold}$

Here P denotes that the Principal value integration should be performed and the R and L beneath the integral signs denote that the integrals are over the right and left hand cuts respectively. The solutions to these integral equations may be shown to be independent of the subtraction point s_o of the integral equation for D.

From (3.22) and (3.24) we may compute the reduced K matrix as defined in (3.15) to be

$$K_{\ell\pm}^{-1} = [\text{Re}\, D] N^{-1} + i(k^{2\ell+1} - k^{2\ell+1}\Theta) \qquad (3.25)$$

Although, in general solutions to the coupled integral equations (3.24) are complicated and may have to be obtained numerically, when the left hand cut is approximated by a series of poles the solution may be obtained analytically. Accordingly, we will examine the two channel S wave case, where the left hand cut is approximated by a pole in the S plane at the same position, $-s_1$, in each channel. Near this pole the T matrix will be given by

$$T(s) \approx \frac{g}{(s+s_1)} \qquad (3.26)$$

where g is a two by two symmetric matrix of constants.

The position of the pole and the values of g will be chosen to approximate the physical case of $\bar{K}N$ scattering. Subsequently we will add a further pole in one channel to investigate the possible effect of a left hand cut extending, in one channel, very near to the right hand cuts. For simplicity we consider the case where equal mass scattering occurs in either channel, the mass of the particles in channel i being given by m_i. The diagonal matrix of channel centre of mass momentum then becomes

$$k_{ij}(s) = \tfrac{1}{2} \, \delta_{ij} \, \sqrt{s - 4m_i^2}$$ (3.27)

Using (3.26) and (3.27) in equations (3.23), (3.24) and (3.25), $IK(s)$ may immediately be written down as

$$IK^{-1}(s) = g^{-1}(s+s_1) - \frac{(s+s_1)^2}{\pi} P \int_0^\infty \frac{k(s')\theta}{(s'+s_1)^2(s'-s)} ds' + i\left(k(s) - k(s)\theta\right)$$ (3.28)

where we have chosen the subtraction point $s_0 = -s_1$.

The integrals in this equation may be performed analytically to give

$$\left[IK^{-1}(s)\right]_{ij} = (g^{-1})_{ij}(s+s_1) - \frac{\delta_{ij}}{2}\left[\sqrt{s+4m_i^2}\right.$$
$$\left. - \sqrt{4m_i^2-s}\,\theta_{ij} - (s+s_1)\cdot\frac{1}{2\sqrt{s_1+4m_i^2}}\right] + i\left(k(s) - k(s)\theta\right)$$ (3.29)

This may now be written in a form suitable for comparison
with (3.17) if we use (3.27) to write all quantities
in terms of channel momenta

$$[K^{-1}(s)]_{ij} = [4(g^{-1})_{ij} h_{io}^2 - \tfrac{1}{2} \delta_{ij} h_{io}]$$
$$+ [4(g^{-1})_{ij} + \delta_{ij} \cdot \tfrac{1}{2h_{io}}] k_i^2 \quad (3.30)$$

where we define h_{io} by the equation

$$4h_{io}^2 = s_1 + 4m_i^2 \quad (3.31)$$

If we define the matrix $(h_0)_{ij} = \delta_{ij} h_{io}$ and evaluate
the series (3.17) about the point $s=s_r$ we may rewrite
(3.30) in an analagous way to (3.17) as

$$K^{-1}(s) = g^{-1}(s+s_r) - m^2 h_0^{-1} + \frac{(s_r-s_1)}{8} h_0^{-1}$$
$$+ \tfrac{1}{2}(k^2-k_0^2)^{1/2} [8g^{-1} + h_0^{-1}](k^2-k_0^2)^{1/2} \quad (3.32)$$

where $\quad (m^2)_{ij} = m_i^2 \delta_{ij}$

The one pole approximation to the left hand cut
is therefore equivalent to the expansion (3.17) with
only the first two terms non zero, and we may make the
identification

$$M = g^{-1}(s_1+s_r) - m^2 h_0^{-1} + \frac{(s_r-s_1)}{8} h_0^{-1} \quad (3.33)$$

$$r = 8g^{-1} + h_0^{-1} \quad (3.34)$$

Using (3.33) in (3.34) r may be obtained in terms of M as

$$r = 8\left[M + \left(m^2 - \frac{(s_T - s_l)}{8}\right)h_0^{-1}\right]/(s_l + s_T) + h_0^{-1} \quad (3.35)$$

If we now consider the effect of moving the left hand cut position, that is the position, $-s_l$, of the equivalent pole, then M, which is essentially fixed by the scale of the interaction, will remain constant through the corresponding variation in g, and (3.35) will give the variation of r, the effective range matrix. It may be seen therefore that for a distant left-hand cut, the dominant term in (3.35) will be the term in h_0^{-1} and therefore

$$r = 2h_0^{-1} \quad (3.36)$$

In this situation, r is evidently diagonal and its elements will be inversely proportional to the square root of the distance of the left hand cut from the region about which the expansion (3.17) is made. r will thus give a measure of the range of the "potential" induced by the crossed channels.

If the left hand cut, and therefore the position of the equivalent pole, $-s_l$, is allowed to approach the physical region, it is evident from (3.31) that

(3.36) may no longer be taken as good approximations to the effective range, and that the full equation (3.35) must be considered. It is evident that, provided the M matrix is not diagonal, there is no reason for assuming a diagonal r matrix in this case.

It is of interest to apply the above discussion to the case of $\overline{K}N$ scattering. A good, equal mass, approximation to the singularity structure of Fig.(3.1) is obtained by choosing the masses m_i as follows

$$m_1 = 0.7 \text{ Gev}$$
$$m_2 = 0.65 \text{ Gev} \tag{3.37}$$

This gives the cut structure of Fig. (3.2)
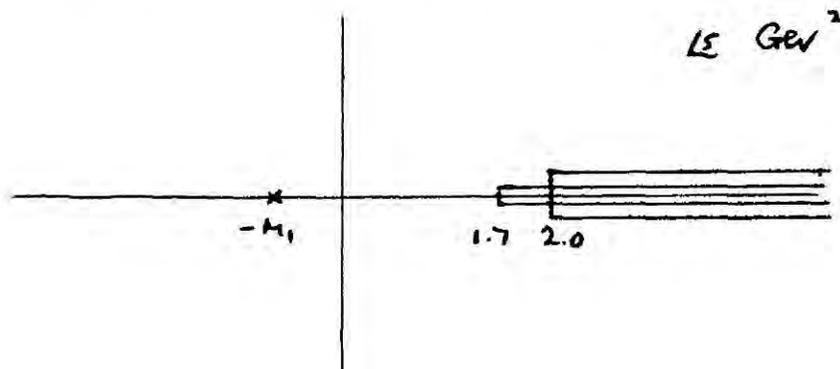
Fig (3.2)

In order to investigate the possible forms and values of r for an expansion about $S_T = 4m_1^2$, the M matrix was fixed at a physically reasonable value, and (3.35) used to compute r for various values of S_1.

By a physically reasonable set of values for the elements of M we mean those obtained by Kim in a fit to the low energy $\bar{K}N$ data. A detailed account of this fit is given in the next section. The values obtained for the elements of r were plotted in Fig. (3.3) against a range of values of S_1. For comparison the values obtained by Kim for his (diagonal) effective range parameters are indicated also in Fig. (3.3). It may be seen from this plot that, for S_1 lying in a considerable range of the physical left hand cut (Fig. (3.1)), the off diagonal elements may not be considered as negligible. Thus it may be concluded that, for the $\bar{K}N$ case, there is no a priori reason for negglecting these off diagonal elements.

In the $\bar{K}N$ case it may be seen, Fig. (3.1), that the left hand cut in the $\bar{K}N \to \bar{K}N$ channel extends past the right hand $\Sigma\pi$ and $\Lambda\pi$ unitarity cuts. It is therefore of interest to investigate the possible effect of this cut on the validity of a two term effective range expansion of the form given by (3.32). Accordingly a two pole left hand cut is used in the N/D equations (3.24). D is normalised to unity at the position of the first pole, $- S_1$, and thus from (3.23) N will have the form
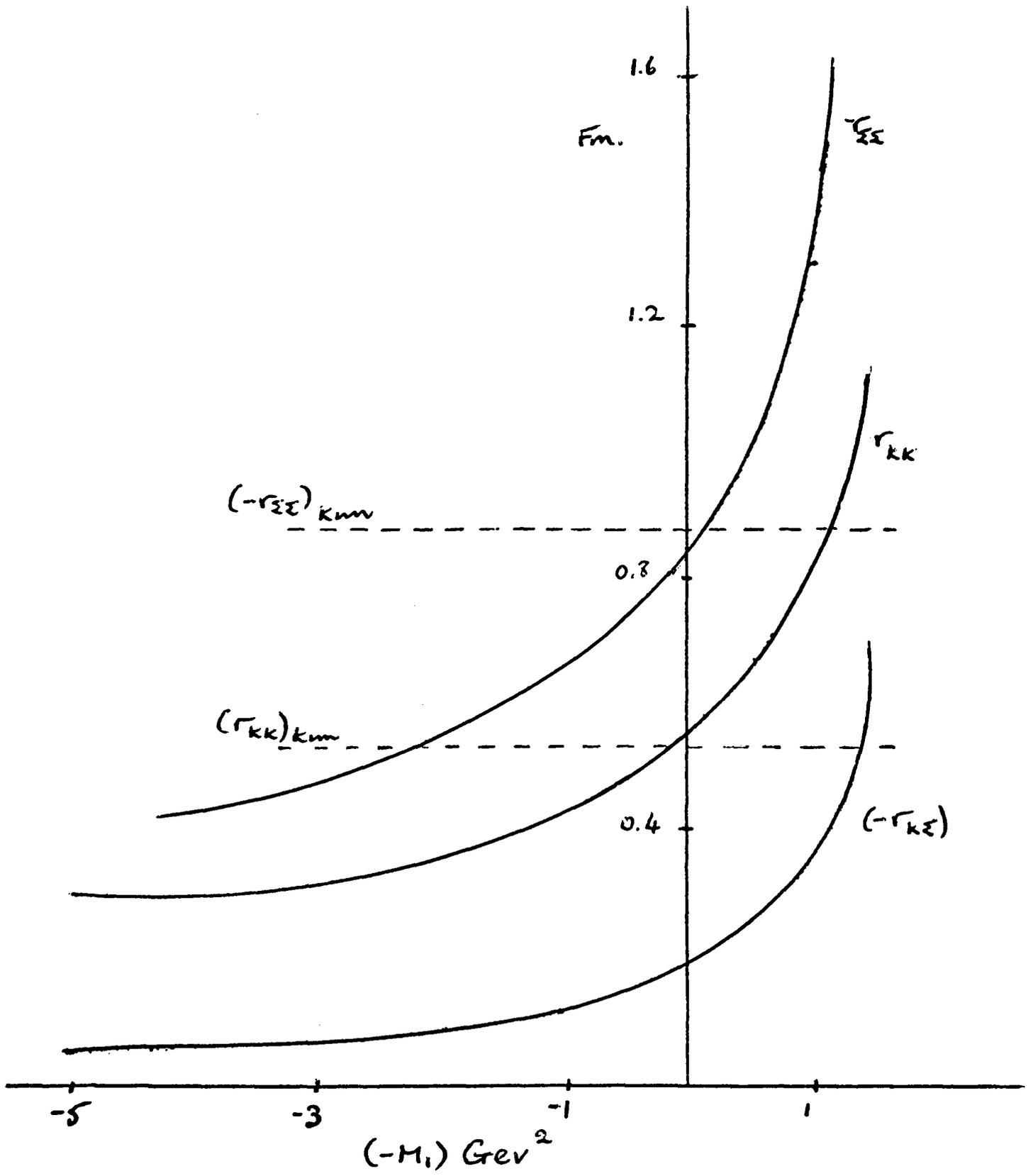
Fig (3.3)

$$N(s) = \frac{g_1}{(s+S_1)} + \frac{g_2 D(-S_2)}{(s+S_2)} \tag{3.38}$$

g_1 and g_2 are both two by two matrices whose elements give the residues at the pole positions $-S_1$ and $-S_2$ respectively. g_1 will be a real symmetric matrix and approximate the contribution of the dominant left hand cut, whilst g_2 will have only one non-zero element, $(g_2)_{11}$, and will approximate the effect of the crossed $\pi\pi$ cut in the $\bar{K}N$ amplitude, the magnitude of whose discontinuity is believed to be small. Using (3.38) in (3.24) with $s_0 = -S_1$ we obtain

$$D(s) = 1 - \frac{(s+S_1)}{\pi} P \int_0^{\infty} k(s') \left[\frac{g_1}{(s'+S_1)} + \frac{g_2 D(-S_2)}{(s'+S_2)} \right] \frac{ds'}{(s'-s)(s'+S_1)} - i k(s) \left[\frac{g_1}{(s+S_1)} + \frac{g_2 D(-S_2)}{(s+S_2)} \right] \tag{3.39}$$

The integrals in (3.39) may be performed analytically and the value of $D(-S_2)$ is got by solving (3.39) for $D(s)$ at $s = -S_2$.

Using the resulting expression for $D(s)$ and knowing $N(s)$ from (3.38) the K matrix elements may be easily obtained via equation (3.25). In Figs. (3.4) and (3.5) we plot the K matrix elements vs. $\left(k_1^2 - k_{10}^2 \right)$ for a range of values of the parameter $(g_2)_{11}$ which determines the contribution of the pole

at $(-S_2)$. The values of m_1 and m_2 are given by (3.37) and S_2 is fixed at

$$S_2 = -1.6 \text{ Gev}^2$$

S_1 is taken to be

$$S_1 = 0.0 \text{ Gev}^2$$

for Fig. (3.5) and to be

$$S_1 = 5.0 \text{ Gev}^2$$

for Fig. (3.4). Using (3.33) the values of g_1 are varied to give Kims result for $g_2 = 0$ and then the effect of non zero (g_2) investigated.

It may be seen from Fig. (3.4) and Fig. (3.5) that, although the values of the effective range terms are changed by the addition of the extra pole, the effective range expansion remains a good approximation to the energy dependence of the M matrix elements over a considerable momentum range. Near $S = -S_2$ of course the M matrix elements blow up but this effect is reduced when S_1 moves near the physical threshold. Accordingly it is concluded that an effective range expansion with the full effective range matrix r considered, should be a good parameterisation to the low energy $\bar{K}N$ amplitude. However the use of this parameterisation to continue below the $\bar{K}N$ threshold should be treated with caution due to the possible effects of the t channel $(\pi\pi)$ cut.
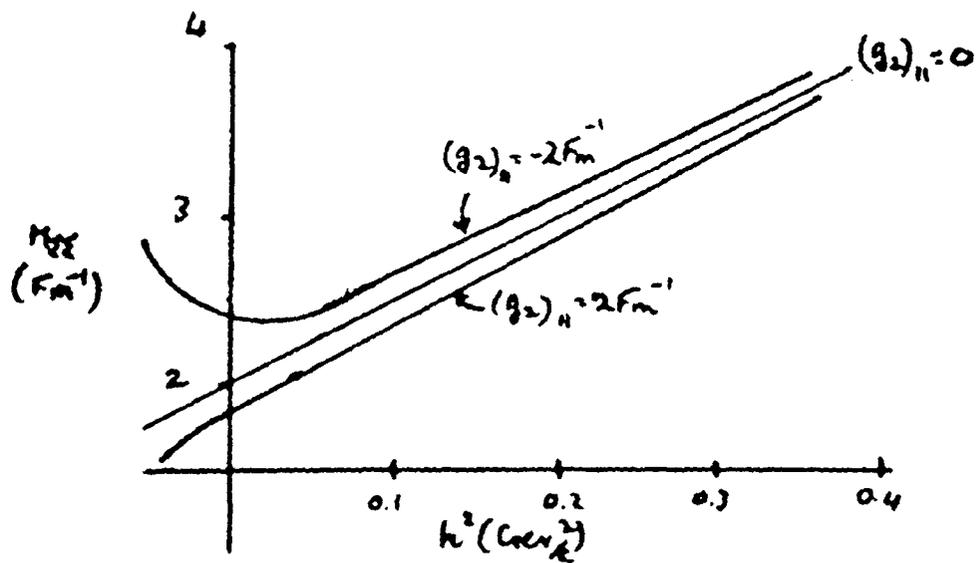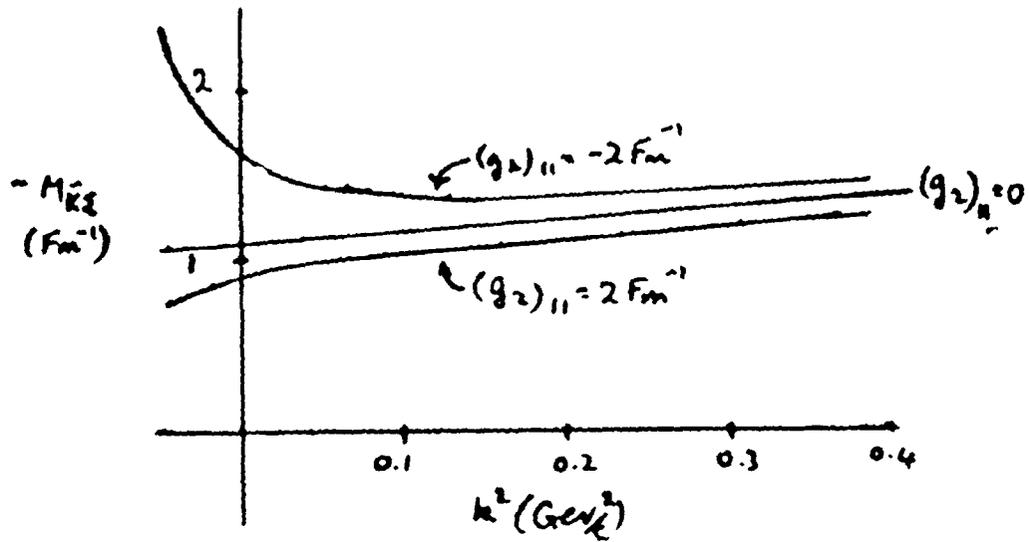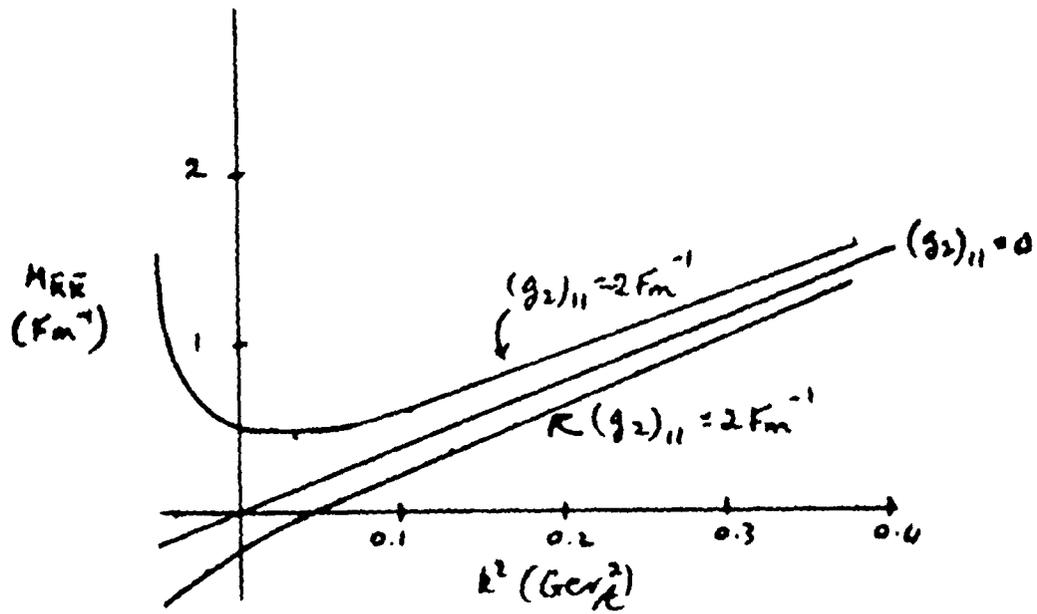
Table (3.4)
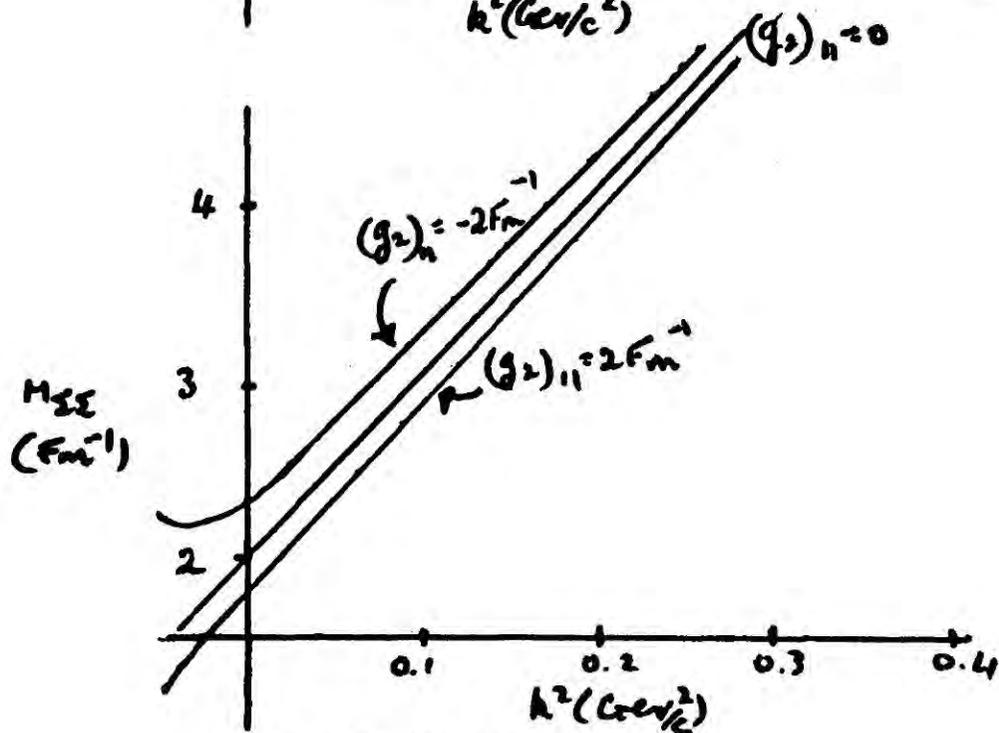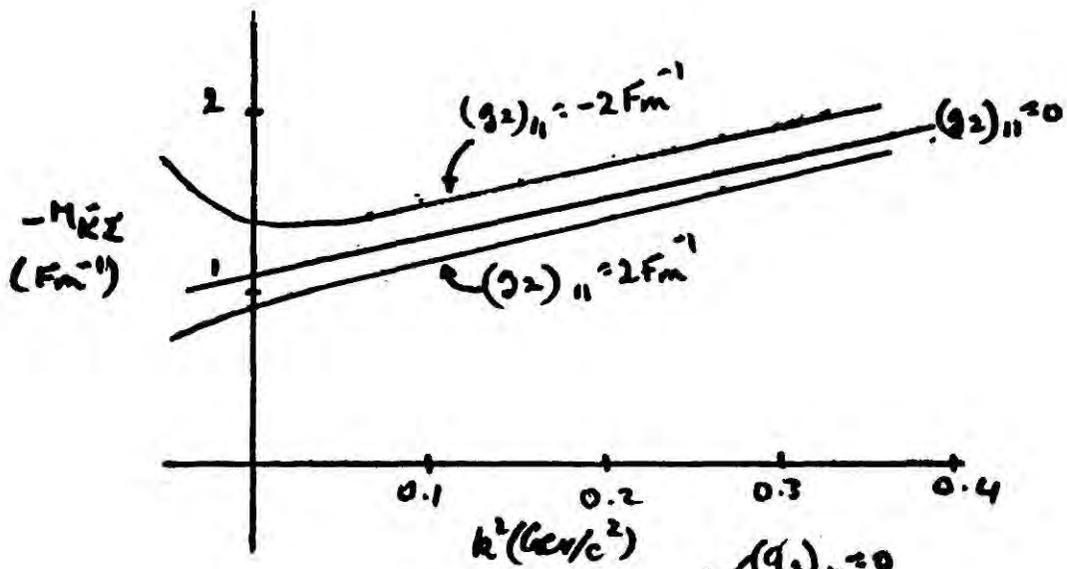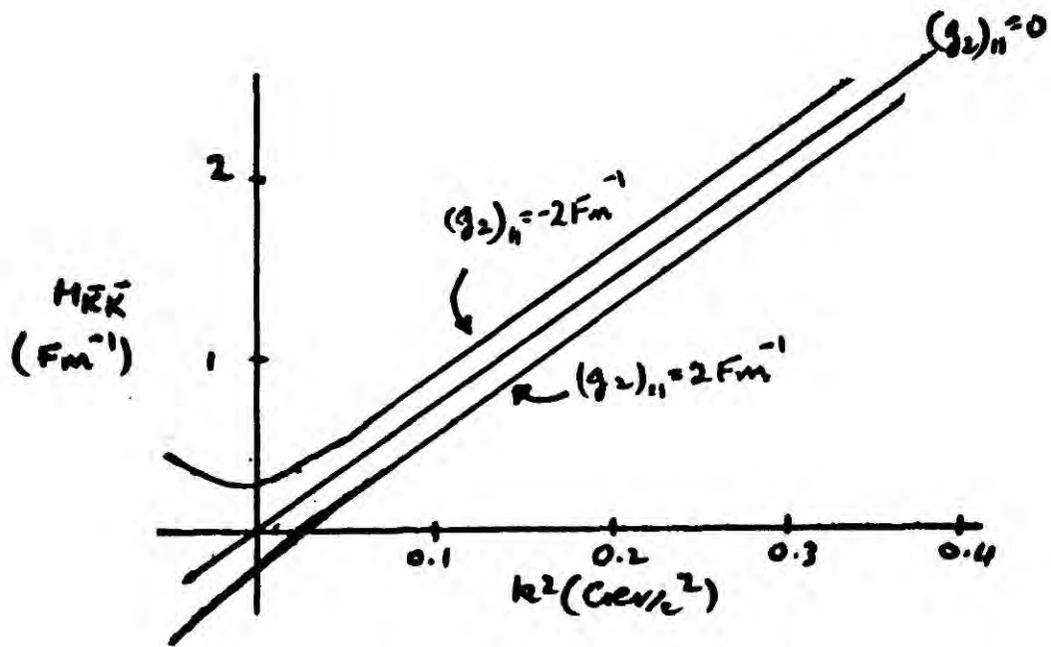
Table (3.5)

(iv) Resonances

In S matrix theory a stable particle is associated with a pole on the real axis below the unitarity cut. For a resonance, however, its mass is such that it is energetically possible for it to decay into at least one multiparticle channel. Thus the resonance cannot, by unitarity, correspond to a pole on the real axis. It is, in fact, believed that a resonance corresponds to a pair of complex conjugate poles P and P' on the unphysical sheets of the amplitude, the complex conjugate condition being necessary to satisfy the hermetian analytic property of the scattering amplitude.

If we denote the pole position, P, by $s_P = s_R - i\gamma$ where γ is real and positive then this pole will be much nearer the physical region as defined in Chapter 2 than its complex conjugate partner P' at $s_{P'} = s_R + i\gamma$ Thus, for physical s near s_R, the partial wave amplitude $f_{\ell\pm}$ will be approximately given by

$$f_{\ell\pm}(s) \approx \frac{-g(s_P)}{s_R - s - i\gamma} \qquad (3.40)$$

where the residue function $g(s)$ has been approximated by its value at the pole $g(s_P)$.

(3.40) is the standard Breit-Wigner resonance
formula with a resonance width Γ given by

$$\Gamma = \gamma / \sqrt{s_R}$$

Here Γ is the width of the resonance peak at half
maximum.

The extrapolation of the residue function g(s)
to the physical region may be improved over (3.40) by
considering the kinematical singularities of the
amplitudes. This may conveniently be done using the
K matrix[13] and writing the effective range expansion
for the one channel reduced K matrix, (3.19),

$$K_{\ell\pm}^{-1} = \frac{1}{a} + \frac{1}{2} r k^2$$

gives, using (3.14) and (3.15) the partial wave
amplitude as

$$f_{\ell\pm} = \frac{k^{2\ell}}{\frac{1}{a} + \frac{1}{2} r k^2 - i k^{2\ell+1}}$$

For the case where $a > 0$ and $r < 0$ this may be written
in the Breit-Wigner form of (3.40) as

$$f_{\ell\pm} = k^{2\ell} \frac{(-\frac{2}{r})}{k_R^2 - k^2 - i\gamma'}$$

where $\quad k_R^2 = -\frac{2}{ra} \quad$ and $\quad \gamma' = -\frac{2k^{2\ell+1}}{r}$

We observe that γ', which is related to the width,
is now energy dependent with the threshold factor $k^{2\ell+1}$

The effective range expansion for the K matrix can
be equivalently written

$$\mathbb{K}_{\ell\pm} = \frac{-2k^{2\ell}/r}{k_{\lambda}^2 - k^2}$$

and so the resonance is associated with a pole on the
real axis in the single channel K matrix.

The many channel case may similarly be treated[13]
using the K matrix formalism. Thus we write the T
matrix in the form obtained by solving (3.4)

$$T_{\ell\pm} = K_{\ell\pm} \left(1 - \iota k K_{\ell\pm}\right)^{-1} \qquad (3.41)$$

From this equation it is apparent that a pole may occur
in two ways. Firstly, as in the one channel case,
the K matrix elements may themselves have a pole at
the resonant position on the real axis

$$\left(K_{\ell\pm}\right)_{ij} = \frac{\sqrt{\Gamma_i \Gamma_j}/2}{E_r - E} \qquad (3.42)$$

This gives the partial wave scattering matrix $T_{\ell\pm}$ in
the form

$$\left(T_{\ell\pm}\right)_{fi} = \frac{\sqrt{\Gamma_f \Gamma_i}}{E_r - E - \iota \Gamma/2} \qquad (3.43)$$

where $\quad \Gamma = \sum_i \Gamma_i$

This is the multichannel Breit-Wigner resonances formula.
Γ is the total width of the resonance and Γ_i the
partial decay width of the resonance into channel i.
A resonance produced in such a manner is known, in
the notation introduced by Dalitz, as a scattering
resonance.

If the resonance lies close to a threshold (for
channel i, say), then it will be essential to take the
threshold behaviour into account. This is done via
(3.16) whence we get instead of (3.42) the form
for the K matrix

$$\left(K_{\ell\pm}\right)_{ij} = \frac{k_i^{\ell}\sqrt{\Gamma_i\Gamma_j}\,/2}{E_r - E} \qquad (3.44)$$

which gives

$$\left(T_{\ell\pm}\right)_{ij} = \frac{\sqrt{\Gamma_i\Gamma_j}\,k_i^{\ell}}{E_r - E - i\Gamma/2} \qquad (3.45)$$

where

$$\Gamma = \sum_{i \neq j} \Gamma_j + \Gamma_i k_i^{\ell}$$

The second way in which a resonance may arise
is through the effect of the closed channels and not
through the K matrix elements having poles. This may
be seen by defining a reduced K matrix K_o on the open

channels only. Then by (3.5)

$$(K_0)_{ij} = K_{ij} + i K_{i\ell} \left[(I - \iota k K)^{-1} k \right]_{\ell\sigma} K_{\sigma j}$$

where i and j refer to the open channels and ℓ and σ refer to the closed channels. Thus the factor in the square brackets may be written

$$\left[(I - \iota k K)^{-1} k \right]_{\ell\sigma} = \left[(I + |k| K)^{-1} k \right]_{\ell\sigma}$$

where i |k| is the continuation of the channel momenta matrix for the closed channels. It is evident that a pole in this term will result in a resonance form in the scattering amplitude, even though the K matrix elements themselves do not have a pole. Such a resonance is known as a virtual bound state resonance and may be characterised by the condition

$$\det (I + |k| K) = 0 \tag{3.46}$$

(v) <u>Survey of the low energy $\bar{K}N$ data</u>

For reactions involving negative K mesons incident on protons the following processes have been studied

(a) $\quad K^- p \rightarrow K^- p$

(b) $\quad K^- p \rightarrow \bar{K}^0 n$

(c) $\quad K^- p \rightarrow \Sigma^+ \pi^-$ $\qquad$ (3.47)

(d) $\quad K^- p \rightarrow \Sigma^0 \pi^0$

(e) $\quad K^- p \rightarrow \Sigma^- \pi^+$

(f) $\quad K^- p \rightarrow \Lambda \pi^0$
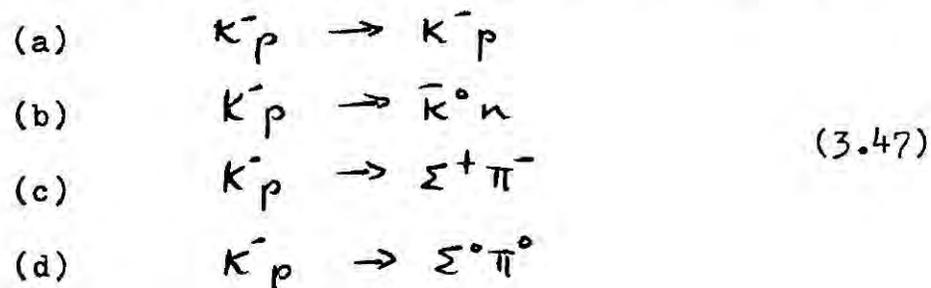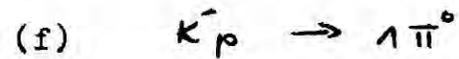
Humphrey and Ross[E1] performed one of the earliest detailed investigations of the low energy $\bar{K}N$ reaction, obtaining total cross sections for the processes (a) – (f) in the K^- lab momentum range 0-275 Mev/c. They also obtained sufficient statistics to obtain the differential cross section for elastic $K^- p$ scattering in the range of $\cos \Theta_{C.M.}$. $-1 \leqslant \cos \Theta_{CM} \leqslant 0.966$ where $\Theta_{C.M.}$ is as defined in (2.8). Subsequently Sakitt et al.[E2] studying the processes (a), (c) and (e) obtained total cross sections for these processes in the momentum range 0-300 Mev/c and also the differential cross sections for elastic $K^- p$ scattering in the same range as above. They were also able to measure the differential cross sections for the processes (c) and (e) averaged over two momentum ranges and with $\cos \Theta_{C.M.}$ in the range $- 0.8 \leqslant \cos \Theta_{C.M.} \leqslant + 0.8$. From an examination of this angular distribution they were able to deduce that reactions (a), (c) and (e) must proceed principally through the S-wave interaction. More recently Kim[E3] has performed an experiment in the K^- lab momentum region 0-280 Mev/c and has obtained data for the processes (a) – (f) with considerably

better statistics than those previously mentioned.
He obtains the differential cross section to good
accuracy for elastic scattering for nine momentum
ranges and split up into seven angular ranges in the
range $-0.965 \leqslant \cos \theta_{C.M.} \leqslant 0.965$.

The differential cross section for the processes
(c) and (e) is also obtained but over a restricted
angular range and with poor statistics. However,
once again it appears that the interaction for
processes (a) - (e) is pure S wave in the energy range
considered. Total cross sections are obtained for
all the processes (a) - (f).

Further data on the low energy K^-p interaction
has been obtained by Kittel et al.[E4] who obtained
considerably more statistics for the charge exchange
reaction (b) in the momentum range 0 - 300 Mev/c.

In the higher energy region corresponding to K^-
lab momentum between 250 and 500 Mev/c, Watson[E5] et al.
have obtained 10,000 events for the processes (a) - (f)
together with the multipion process

$$K^-p \rightarrow \Lambda \pi^+ \pi^-$$ (3.48)

From the differential cross section data for all
processes, and the polarisation data for the process

$K^- p \rightarrow \Lambda \pi$ it was found necessary to include S, P and D waves in order to explain the angular distributions. The presence of the D wave may be explained by the existence of an Isospin one $D_{3/2}$ resonance at an energy of 1520 Gev, denoted henceforth as the $Y_0^*(1520)$.

In discussing the possible experimental processes available for the study of the $\bar{K}N$ interaction we have so far only considered the scattering of K^- by protons. However it is possible to obtain information on the scattering of $\bar{K}^0$ mesons on protons via the interactions of K_2^0 mesons on protons, where the K_2^0 is defined as a linear superposition of K^0 and $\bar{K}^0$ states

$$|K_2^0\rangle = \frac{1}{\sqrt{2}} \left\{ |K^0\rangle - |\bar{K}^0\rangle \right\} \qquad (3.49)$$

It should be mentioned that it is the $K_2^0 - p$ interaction that is experimentally available for measurement for, in the preparation of a beam of K mesons a production process such as

$$\pi^- p \rightarrow K^0 \Lambda$$

is used. However the K^0 decays through the weak interactions which, to a good approximation, conserve the CP quantum number. Accordingly the K^0 should be written in terms of CP eigenstates as

$$|K^0\rangle = \frac{1}{\sqrt{2}} \left\{ |K_1^0\rangle + |K_2^0\rangle \right\} \qquad (3.50)$$

where

$$|K_1^0\rangle = \frac{1}{\sqrt{2}} \left\{ |K^0\rangle + |\bar{K}^0\rangle \right\} \qquad (3.51)$$

It is found that the weak decay times of the $|K_1^0\rangle$ and $|K_2^0\rangle$ states differ by a factor of six hundred and thus the $|K_2^0\rangle$ state, which is the longer lived one, will remain for scattering experiments.

The reactions studied involving the $K_2^0 p$ initial state are

$$\begin{array}{lll}
(g) & K_2^0 p \rightarrow K_2^0 p & \\
(h) & K_2^0 p \rightarrow K_1^0 p & \\
(i) & K_2^0 p \rightarrow \Sigma^0 \pi^+ & (3.52) \\
(j) & K_2^0 p \rightarrow \Lambda \pi^+ &
\end{array}$$
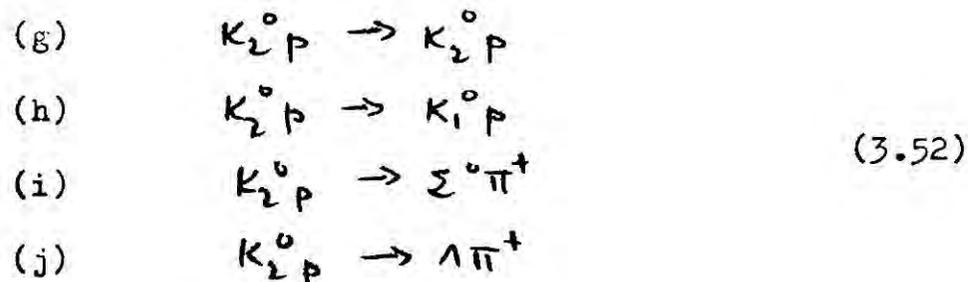
Kadyk[E6] et al. have obtained data for the processes (g) – (j) in the kaon lab momentum range 0-550 Mev/c. They obtain differential cross section data for the processes (f), (h), (i) and (j) together with polarisation data, from the decay of the Λ particle, for the processes (f) and (j). From an analysis of the angular distribution it is apparent that there is a significant amount of P wave, even at kaon lab momentum 100 Gev/c, in the processes (f) and (j).

Finally Sayer[E7] et al. have obtained measurements of the total $K_2^0 p$ cross section in the momentum range $0 \sim 350$ Mev/c.

(vi) <u>Survey of the fits to the low energy $\bar{K}N$ data</u>

For the low energy region corresponding to the kaon lab momentum 0-550 Mev/c it is apparent from the discussion of the previous section that the important channels open in the range are the $\bar{K}N$, $\Sigma\pi$ and $\Lambda\pi$ channels of (2.34) together with the $\Lambda\pi^+\pi^-$ channel of (3.48). Ignoring, for the present, this latter process, we may define the reduced K matrix on the states of (2.34) and, adopting the notation of (3.8), write

$$\langle a_I \mid \mathbb{K}_{\ell\pm} \mid b_{I'} \rangle = \mathbb{K}_{\ell\pm}{}^{(I)}_{ab} \; \delta_{II'} \qquad (3.53)$$

where, as before, I denotes isospin and a, b and c refer to the $\bar{K}N$, $\Sigma\pi$ and $\Lambda\pi$ channels respectively.

It is evident, therefore, that an S wave zero range parameterisation of low energy $\bar{K}N$ scattering will contain 3 I=0 and 6 I=1 parameters whilst an effective range parameterisation will double the number.

The initial analysis of the $\bar{K}N$ low energy data did not have sufficient data to determine the nine zero

range parameters uniquely and a more economical
parameterisation was used, namely the complex scattering
length parameterisation introduced in section (iii).
In this parameterisation the $\bar{K}N$ elastic amplitudes are
given by

$$T_{aa}^{(I)} = \frac{A_I}{1 - ik A_I} \qquad (3.54)$$

where $A_I = a_I + ib_I$ is the complex scattering length
with a_I and b_I real parameters and k is the centre of
mass momentum for the $\bar{K}N$ channel. In order to describe
the processes of (3.47) it is necessary to introduce
two further parameters and a convenient choice for
these are ϵ and ϕ_{th} defined as

$$\epsilon = \frac{\sigma(K^-p \rightarrow \Lambda\pi^0)}{\sigma^{I=1}(\text{All hyperons})} \qquad (3.55)$$

$$\phi \equiv \text{Arg}\left[\frac{T_{ab}^{(0)}}{T_{ab}^{(1)}}\right] = \phi_{th} + \text{Arg}\left[\frac{1 - ik A_1}{1 - ik A_0}\right] \qquad (3.56)$$

$$(\phi_{th} = \phi_{K^-p \text{ threshold}})$$

Thus there are a total of six parameters necessary
to describe the processes of (3.40). In performing a
fit to the data the effects of the Coulomb interaction
and the K^-p, $\bar{K}^0 n$ mass differences are corrected for,
using the method of Appendix I.

Several constant length fits have been performed, the latest of which is by Kim[E3] who analysed the data of ref.(E3) for the K^- lab momentum range 0-280 Mev/c. Of the two fits he obtained one was subsequently ruled out by comparing its predictions of the $K_2^o p$ interaction with experiment. The remaining fit gives the following values for the six S-wave parameters

$$a_o = -1.67 \pm 0.04 \qquad\qquad b_o = 0.71 \pm 0.04$$

$$a_1 = -0.07 \pm 0.06 \qquad\qquad b_1 = 0.68 \pm 0.03$$

$$\epsilon = 0.31 \pm 0.02 \qquad\qquad \phi = -53.8^o$$

More recently Kim[19] has reanalysed the low energy $\bar{K}N$ data (E3,E5) extending the range of K^- laboratory momentum to 0-550 Mev/c. The presence of the $D_{3/2}$ I=0 520 Mev resonance, requires that S, P and D waves are included in a parameterisation to the amplitude in this energy region. For the S waves and resonant I=1, $P_{3/2}$ wave Kim used a multichannel effective range expansion, omitting however the off-diagonal elements of the effective range matrix r. The remaining P waves were parameterised in the zero range approximation. A Breit-Wigner resonant form with an energy dependent width was used for the I=0 $D_{3/2}$ amplitude and a constant scattering length form for the I=1 $D_{3/2}$ amplitude. The other D waves were omitted. The total number of

parameters was therefore 44 and Kim obtained a unique

solution for the parameters.

The nine S wave M matrix elements and the five

S wave r matrix elements he obtains are as follows

$(fm)^{-1}$ fm

$M^{o}_{\bar{K}K}$ 0.0 ± 0.02 $r^{o}_{\bar{K}K}$ 0.54 ± 0.08

$M^{o}_{\bar{K}\Sigma}$ -1.11 ± 0.04

$M^{o}_{\Sigma\Sigma}$ 2.04 ± 0.10 $r^{o}_{\Sigma\Sigma}$ -0.89 ± 0.31

$M^{'}_{\bar{K}K}$ -3.60 ± 0.02 $r^{'}_{\bar{K}K}$ -0.13 ± 0.07

$M^{'}_{\bar{K}\Sigma}$ -2.86 ± 0.03

$M^{'}_{\bar{K}\Lambda}$ 2.08 ± 0.07

$M^{'}_{\Sigma\Sigma}$ -1.40 ± 0.06 $r^{'}_{\Sigma\Sigma}$ -0.78 ± 0.23

$M^{'}_{\Sigma\Lambda}$ 1.81 ± 0.04

$M^{'}_{\Lambda\Lambda}$ -2.31 ± 0.11 $r^{'}_{\Lambda\Lambda}$ -1.22 ± 0.45

where we have introduced an obvious notation for the

matrix elements.

A feature of both the scattering length and K

matrix fits is that they predict a virtual bound state

I=0 resonance which is interpreted as the $Y^{*}_{o}(\sim 1405)$

I=0 $S_{\frac{1}{2}}$ resonance experimentally observed in three

particle production processes. However the position E_{r}

and with Γ for this resonance differ between the two

solutions. They are

$$E_r = 1410.7 \pm 1.0 \text{ Mev} \qquad \Gamma = 36.4 \pm 3.2 \text{ Mev}$$

for the constant scattering length parameterisation and

$$E_r = 1403 \pm 3 \text{ Mev} \qquad \Gamma = 50 \pm 5 \text{ Mev}$$

for the K Matrix solution.

CHAPTER 4

Dispersion Relations and Sum Rules

(i) The Forward $K^{\pm}p$ Dispersion Relations

In order to evaluate the coupling constants $g_{\bar{K}N\Lambda}$ and $g_{\bar{K}N\Sigma}$, which are associated with the residues of the single particle Λ and Σ poles in the $\bar{K}N$ amplitude, it is necessary to know the amplitude in the neighbourhood of these poles. However, as the lie below the physical K^-p threshold, it is necessary to extrapolate the amplitude from the region where it is given by experiment to the pole positions. It is well known[20] that this extrapolation cannot be done without introducing infinite uncertainty in the result unless either the amplitude is known exactly over some range, or it is known to some finite accuracy over an infinite range. As experiment will only determine the amplitude to a finite accuracy, extrapolation to the poles will only be possible using the knowledge of the amplitude over an infinite range. This is conveniently done using Cauchy's integral representation and in this section we apply this technique

to the kaon-nucleon scattering amplitude in the forward direction.

For the scattering amplitude in which the s channel is elastic K^-p scattering then the corresponding u channel will be elastic K^+p scattering. This is shown in Fig. (4.1)
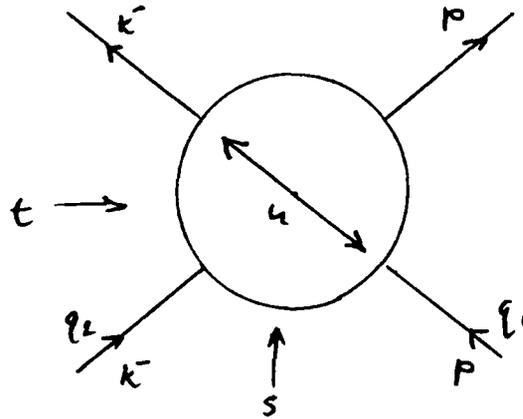
Fig. (4.1)

As we will be working in the forward direction we have $t = 0$. It is customary and convenient in this kind of problem to take the kaon laboratory energy as the energy variable and, using (2.7), we may write s and u in terms of ω as

$$s = M^2 + m^2 + 2M\omega$$
$$u = M^2 + m^2 - 2M\omega \qquad (4.1)$$

We denote the conventional laboratory system amplitudes evaluated in the forward direction by $F_\pm (\omega)$

where the + and - refer to K^+p and K^-p scattering
amplitudes respectively. The physical amplitudes
are obtained as limiting values of the amplitude $F_{\mp}(z)$,
where z represents complex values of ω.

Thus

$$F_{\mp}(\omega) = \lim_{\epsilon \to 0+} F_{\mp}(\omega+\iota\epsilon) \tag{4.2}$$

and from (2.6) crossing symmetry implies

$$F_+(z) = F_-^*(-z) \tag{4.3}$$

Since in the forward direction t is fixed as
zero, in order to determine the singularity structure
of the amplitude it is only necessary to look for the
available intermediate states in the s and u channels.
Thus the s channel gives rise to poles at $s = m_\Lambda^2$
and $s = m_\Sigma^2$ and a cut for $s \geqslant (m_\Lambda + \mu)^2$ whilst the u
channel gives a cut $u \geqslant (M + m)^2$. Hence from (4.1) we
may derive the structure in the complex ω plane shown
in Fig. (4.2).

Fig. (4.2)

Here

$$\omega_{\Lambda,\Sigma} = \frac{m_{\Lambda,\Sigma}^2 - M^2 - m^2}{2M}$$

and
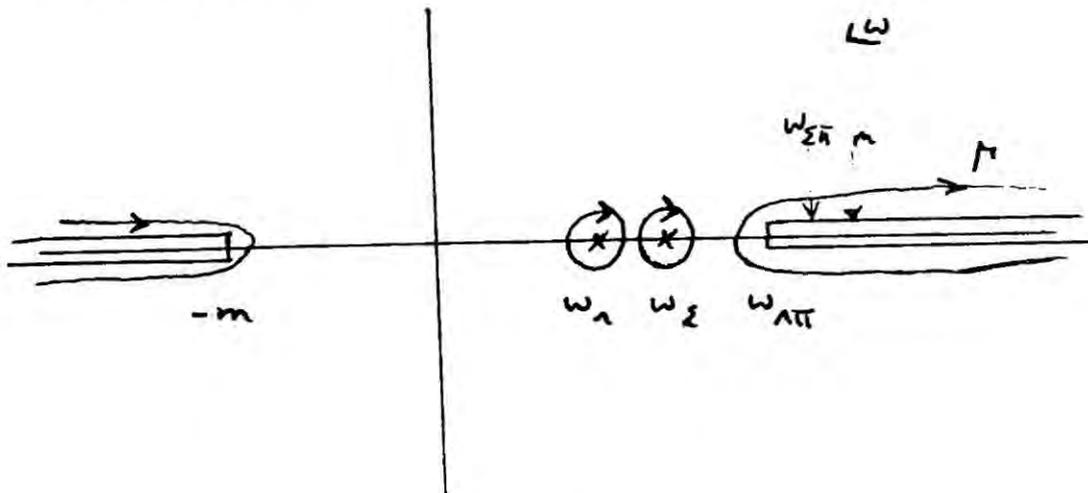
$$\omega_{\Lambda\pi} = \frac{(m_\Lambda + m_\pi)^2 - M^2 - m^2}{2M}$$

We now apply Cauchy's theorem to the analytic function $F_-(\omega)$ using the contour Γ shown in Fig. (4.2) and closing it by means of an infinite circle. Thus we have

$$F_-(z) = \frac{1}{2\pi i} \int_\Gamma dz' \frac{F_-(z')}{(z'-z)}$$

If we assume for the moment that the contribution of the infinite circle vanishes this gives

$$F_-(z) = \sum_Y{}' \frac{A_Y}{(\omega_Y - z)} + \frac{1}{\pi} \int_{\omega_{\Lambda\pi}}^\infty d\omega' \frac{\mathrm{Im}\,F_-(\omega')}{(\omega'-z)} + \frac{1}{\pi} \int_{-\infty}^{-m} d\omega' \frac{\mathrm{Im}\,F_+(\omega')}{(\omega'+z)}$$

where $A_{\Lambda,\Sigma}$ are residues of the hyperon poles. Using the crossing relation (4.3) this becomes

$$F_-(z) = \sum_Y \frac{A_Y}{(\omega_Y - z)} + \frac{1}{\pi} \int_{\omega_{\Lambda\pi}}^\infty d\omega' \frac{\mathrm{Im}\,F_-(\omega')}{(\omega'-z)} + \frac{1}{\pi} \int_m^\infty d\omega' \frac{\mathrm{Im}\,F_+(\omega')}{(\omega'+z)}$$

A similar dispersion relation may be written down for $F_+(z)$.

We now take the limiting values of z as shown in (4.2) and use the relation

$$\frac{1}{\omega'-\omega \pm i\epsilon} = \frac{P}{(\omega'-\omega)} \mp i\pi \delta(\omega'-\omega)$$

where P denotes the Principal value integral is to be

taken. Thus the two dispersion relations may be written for $\omega \geqslant m$

$$\text{Re } F_{\pm}(\omega) = \sum_{\gamma} \frac{A_{\gamma}}{(\omega_{\gamma} \pm \omega)} + \frac{1}{\pi} \int_{\omega_{A\pi}}^{m} d\omega' \frac{\Im m F_{-}(\omega')}{(\omega' \pm \omega)}$$

$$+ \frac{P}{\pi} \int_{m}^{\infty} d\omega' \left\{ \frac{\Im m F_{-}(\omega')}{(\omega' \pm \omega)} + \frac{\Im m F_{+}(\omega')}{(\omega' \mp \omega)} \right\} \qquad (4.4)$$

Conventionally we write

$$F_{\pm}(\omega) = D_{\pm}(\omega) + \iota A_{\pm}(\omega)$$

where $D_{\pm}(\omega)$ and $A_{\pm}(\omega)$ are real. Also, since we are working in the forward direction, the optical theorem (2.13) may be applied giving

$$A_{\pm}(\omega) = \frac{k_{L}}{4\pi} \sigma_{T}^{\pm}(\omega)$$

where k_{L} is the kaon laboratory momentum and $\sigma_{T}^{\pm}(\omega)$ are the $K^{\pm}p$ total cross sections. Thus (4.4) may be rewritten

$$D_{\pm}(\omega) = \sum_{\gamma} \frac{A_{\gamma}}{(\omega_{\gamma} \pm \omega)} + \frac{1}{\pi} \int_{\omega_{A\pi}}^{m} d\omega' \frac{A_{-}(\omega')}{(\omega' \pm \omega)} \qquad (4.5)$$

$$+ \frac{P}{4\pi^{2}} \int_{m}^{\infty} d\omega' \, k_{L}' \left\{ \frac{\sigma_{T}^{-}(\omega')}{(\omega' \pm \omega)} + \frac{\sigma_{T}^{+}(\omega')}{(\omega' \mp \omega)} \right\}$$

In order to connect the pole residues with the conventional coupling constants defined in field theory we assume the interaction Lagrangian

$$\mathcal{L}_{I} = \sqrt{4\pi} \left\{ g_{K^{-}p\Lambda} \, \overline{\psi}_{p} \gamma_{5} \psi_{\Lambda} \phi_{K} + g_{K^{-}p\Sigma^{0}} \, \overline{\psi}_{p} \gamma_{5} \underline{t} \cdot \underline{\psi}_{\Sigma} \phi_{K} \right\}$$
$$+ h.c.$$

where $g_{\bar{K}p\gamma}$ is the renormalised, unrationalised, pseudo-

~~scalar~~ coupling constant. Using techniques familiar

for the πNN case, cf. ref.(21), this gives the

contribution to $F_-(\omega)$ from the pole terms as

$$F_-(\omega) = \sum_{\gamma}' g^2_{k\bar{p}\gamma} \frac{\bar{u} \gamma_5 (q_1 + q_2 + m_\gamma) \gamma_5 u}{(q_1 + q_2)^2 - m_\gamma^2}$$

Using (4.1) this may be written

$$F_-(\omega) = \sum_{\gamma}' g^2_{k\bar{p}\gamma} \frac{\bar{u}(m_\gamma - \not{q}_1 - \not{q}_2)u}{M^2 + 2M\omega + m^2 - m_\gamma}$$

$$= \sum_{\gamma}' g^2_{k\bar{p}\gamma} \frac{m_\gamma - M - \omega}{2M(\omega - \omega_\gamma)}$$

where ω_γ is as defined above.

Identifying A_γ with the residue of this pole

gives

$$A_\gamma = g^2_{k\bar{p}\gamma} \frac{(M - m_\gamma)^2 - m^2}{4M^2} \qquad (4.6)$$

It is apparent that the validity of (4.5) depends

on the asymptotic behaviour of the amplitude which

must be such that the contribution from the integral

over the infinite circle should vanish and the integrals

in (4.5) should be convergent. Current theory and

experiment suggest that, as $\omega \to \infty$, $\sigma_T^{\pm}(\omega)$ tend to

constant values. It is therefore to be expected that

the integrals in (4.4) will not in fact converge and
therefore it is necessary to replace (4.5) by a
dispersion relation with a subtraction made at $\omega = \omega_0$

$$D_{\pm}(\omega) = D_{\pm}(\omega_0) \pm (\omega_0 - \omega) \sum_{\gamma} \frac{A_{\gamma}}{(\omega_{\gamma} \pm \omega)(\omega_{\gamma} \pm \omega_0)}$$

$$\pm \frac{(\omega_0 - \omega)}{\pi} \int_{\omega_{\pi\pi}}^{m} \frac{A_-(\omega') d\omega'}{(\omega' \pm \omega)(\omega' \pm \omega_0)} \pm (\omega_0 - \omega) \frac{P}{4\pi^2} \int_m^{\infty} \frac{k_L' \bar{\sigma_T}(\omega') d\omega'}{(\omega' \pm \omega)(\omega' \pm \omega_0)} \quad (4.7)$$

$$\mp (\omega_0 - \omega) \frac{P}{4\pi^2} \int_m^{\infty} \frac{k_L' \sigma_T^+(\omega') d\omega'}{(\omega' \mp \omega)(\omega' \mp \omega_0)}$$

If we set $\omega_0' = -\omega_0$ and make use of the crossing relation
(4.2) the second of these relations may be written
in the form.

$$\sum_{\gamma} \frac{A_{\gamma}}{(\omega_{\gamma} - \omega)(\omega_{\gamma} + \omega_0)} = \frac{D_-(\omega) - D_+(\omega_0)}{(\omega + \omega_0)} - \frac{1}{\pi} \int_{\omega_{\pi\pi}}^{m} \frac{A_-(\omega')}{(\omega' - \omega)(\omega' + \omega_0)} d\omega'$$

$$+ \frac{P}{4\pi^2} \int_m^{\infty} \frac{k_L' \sigma_T^+(\omega') d\omega'}{(\omega' + \omega)(\omega' - \omega_0)} - \frac{P}{4\pi^2} \int_m^{\infty} \frac{k_L' \bar{\sigma_T}(\omega') d\omega'}{(\omega' - \omega)(\omega' + \omega_0)} \quad (4.8)$$

Finally if $\omega_0 = \omega$ we obtained the dispersion relation
as generally used to obtain the coupling constants.

$$\sum_{\gamma} \frac{A_{\gamma}}{\omega_{\gamma}^2 - \omega^2} = \frac{D_-(\omega) - D_+(\omega)}{2\omega} - \frac{1}{4\pi^2} \int_m^{\infty} \frac{k_L'(\sigma_-(\omega') - \sigma_+(\omega'))}{\omega'^2 - \omega^2} d\omega'$$

$$- \frac{1}{\pi} \int_{\omega_{\pi\pi}}^{\infty} \frac{A_-(\omega')}{\omega'^2 - \omega^2} d\omega' \quad (4.9)$$

It should be noted that the physical integral in these equations now has an integrand of the asymptotic form

$$[\sigma_-(\omega) - \sigma_+(\omega)]/\omega \qquad \text{as} \quad \omega \to \infty$$

The convergence of the dispersion integrals depends on the asymptotic behaviour of this quantity and this will be discussed in the next section, together with the Regge parameterisation of the high energy amplitudes, which are used in the dispersion relations for energies above those experimentally available.

(ii) <u>The High Energy behaviour of the scattering amplitude</u>

Experimentally, total cross sections such as

$\sigma_{tot}(pp)$, $\sigma_{tot}(p\bar{p})$, $\sigma_{tot}(\pi p)$ and $\sigma_{tot}(Kp)$ are observed to be roughly constant above a few Gev (cosmic ray data shows no great change in $\sigma_{tot}(pp)$ and $\sigma_{tot}(\pi p)$ upto 10^4 Gev).

According to the optical theorem (2.13)

$$\mathcal{I}m\, T_u(s) = \frac{q_{cm}\sqrt{s}}{m_b} \sigma_{tot}(s)$$

and thus provided the total cross section approaches a constant value, the imaginary part of the forward

elastic amplitude is proportional to s at high energies. By observing that the real part should not grow arbitrarily larger than the imaginary part and combining this condition with forward dispersion relations Pomeranchuk[22] obtained the result that, for the process

$$A + B \quad \longrightarrow \quad A + B$$

$$\lim_{\omega \to \infty} \left[\sigma_{tot}(AB) - \sigma_{tot}(\bar{A}B) \right] = 0$$

For K^-p scattering this implies

$$\lim_{\omega \to \infty} \left[\sigma_{tot}(K^-p) - \sigma_{tot}(K^+p) \right] = 0$$

Thus Pomeranchuk's condition on the total cross section ensures that the dispersion integrals derived in the previous section are convergent and that the contribution of the integral over the infinite circle vanishes.

As mentioned in the introduction it was found that the contribution of a Regge pole exchanged in the t channel dominates the s channel asymptotic behaviour in the near forward direction. The form of the contribution to the high energy s channel amplitude from a t channel Regge pole is given explicitly by

$$F^{Regge}(\omega) = -c(t) \left(\frac{\omega}{\omega_0} \right)^{\alpha(t)} \left[\frac{\tau + \exp(-\pi\alpha(t))}{\sin \pi\alpha(t)} \right] \quad (4.10)$$

In this formula $\alpha(t)$ is the trajectory function and gives the pole position as a function of t in the angular momentum plane. C(t) is a function of t whose form is known, $\mathcal{C}$ is the signature factor and is ± 1 depending on whether the Regge pole has positive or negative signature, and ω_0 is a scale factor. Thus, in the analysis of the high energy behaviour of an amplitude, only the high lying trajectories need be considered. It is found[23] that the high energy near forward amplitude for the processes involving KN and $\overline{K}$N channels may be described in terms of six Regge poles. These are the P, the P' and the R (or A_2), all with even signature and the ρ, the ω, and the ϕ, all with odd signature. Normally the contributions of the ω and the ϕ whose quantum numbers are the same are taken together.

The KN and $\overline{K}$N amplitudes of interest, together with the contribution of the various Regge poles to them, are listed below

$$A(K^-p \to K^-p) = A_P + A_{P'} + A_\omega + A_\rho + A_R$$

$$A(K^-n \to K^-n) = A_P + A_{P'} + A_\omega - A_\rho - A_R \qquad (4.11)$$

$$A(K^+p \to K^+p) = A_P + A_{P'} - A_\omega - A_\rho + A_R$$

$$A(K^+n \to K^+n) = A_P + A_{P'} - A_\omega + A_\rho - A_R$$

Here $A_{P,P'...}$ represents the contribution as given
in (4.10) to the amplitude from the P, P' ...
Regge poles.

Phillips and Rarita[23] have analysed the available
high energy KN, $\bar{K}N$ data, together with the πN data
which is governed by the P, P' and ρ Regge poles,
to determine the functions $\alpha(t)$ and $C(t)$ for the
Regge poles listed above, and any reference to Regge
poles in future will assume the solution obtained by
them.

(iii) Application of $\bar{K}N$ dispersion relations to the
      prediction of coupling constants

In section (i) the standard dispersion relation
(4.9) was derived for the K^-p scattering amplitude.
A similar derivation may be followed for the K^-n
scattering amplitude with the difference that, since
it is a pure isospin one amplitude, the Λ pole does
not contribute. Thus the Λ and Σ pole terms may be
isolated by writing the dispersion relations for the
linear combinations $\left[(K^{\pm}p) - (K^{\pm}n)/2\right]$ and $(K^{\pm}n)$
corresponding to states of the $\bar{K}N$ system of isospin
I=0 and I=1 respectively.

In order to evaluate the dispersion relation
(4.9) it is necessary to know the cross sections over
the entire extent of the cut, and the real part at
the subtraction point. Conventional applications of
the relations normally make the subtraction at the
$K^{\pm}p$ threshold, namely $\omega = m$. Here the real parts are
accurately known from the low-energy parameterisations.
The integral over the unphysical region $\omega_{\Lambda\pi} \lesssim \omega \lesssim m$
must be estimated by analytically continuing the
amplitude $A_-(\omega)$ into this region by means of the
low-energy parameterisations. As this parameterisation
is based on a fit to the data up to some energy ω_1
it is usual to use this parameterisation to also evaluate
the relevant integral up to ω_1. From the discussion
of the previous chapter, it is evident that there is
no unique solution for the fit to the low energy K^-p
amplitude. Accordingly the relation should be evaluated
using each parameterisation separately and the results
compared. Details of this comparison will be given
later in this section.

It should be mentioned here that it is not obvious
whether the isospin multiplet mass differences, which
are due to the electro-magnetic interaction, should be

included in the dispersion relation predictions for
the strong interaction couplings. In all applications
of dispersion relations in this thesis it will be
assumed that the mass differences should not be
included in the low energy parameterisations but it
should be noted that this convention may not be used
by all authors. However the difference introduced
in the estimation of the coupling constants by including
the mass differences is, in general, small.

The K^+p amplitude has, however, no such degeneracy
of solutions, and a unique scattering length fit has
been obtained by Goldhaber[24] et al. They found that the
experimental data on K^+p scattering for kaon laboratory
momenta $k \leqslant 642$ Mev/c are well represented by an S
wave effective range parameterisation with

$$A_1 = (-0.29 \pm 0.015) \text{ fm} \quad R_1 = (0.5 \pm 0.15) \text{ fm.}$$

Recently Martin and Perrin[25] have reanalysed the
low energy K^+p data and have obtained a unique solution
with S-wave parameters given by

$$A_1 = (-0.32 \pm 0.01) \text{ fm.} \quad R_1 = (0.31 \pm 0.15) \text{ fm.}$$

However all the results to be quoted will have used the
older solution by Goldhaber. Martin and Perrin find
that using their solution in a dispersion relation
prediction of g_Λ^2 raises its value by about 2 from the

from the value predicted using the Goldhaber solution.

The low energy K^+n interaction is known less reliably, since it must be deduced primarily from studies of K^+ interactions with neutrons bound in nuclei. Experimental invormation on the $K^{\pm}n$ total cross sections comes mainly from the comparison of the $K^{\pm}p$ and $K^{\pm}d$ total cross sections by means of the Glauber[26] formula with certain modifications introduced by Wilkin[27] to restore charge independence.

From an analysis of K^+d processes upto 812 Mev/c Stenger et al.[28] have found that the I=0 S-wave amplitude is small and consistent with a pure scattering length of magnitude

$$A_o = (0.04 \pm 0.04) \text{ fm.}$$

This solution is normally used at low energies in the dispersion calculations but it should be noted that Stenger et al. found that P and D waves are important in the I=0 state. Finally the low energy K^-n amplitude is obtained directly from the $\bar{K}N$ parameterisation. It should be noted that there is no experimental data for the K^-n process below 0.6 Gev/c and all information in this region comes from the fits to the K^-p data alone.

Experimental $K^{\pm}N$ total cross sections for kaon
laboratory energies upto 20 Gev are given in refs.
(E8,E9,E10). In the kaon laboratory momenta region
0.6 to 3.3 Gev/c recent experiments[E8] have determined
the total cross section very accurately, with
statistical errors of the order of 1%. Between 3.3
and 6 Gev/c the data available[E9] is somewhat older
and the errors are rather large compared with the
previous set. However the data does join smoothly
with the lower end. Finally in the range 6 Gev/c to
20 Gev/c only one experiment[E10] has been performed
but this has good statistical accuracy and joins
smoothly onto the data of the second group. Above
the energy region accessible to experiment the Regge
form is used for the amplitude.

In Table (4.1) we list the predictions obtained,
using the dispersion relation (4.9) with $\omega = m$, for
the coupling constants g_{Λ}^2 and g_{Σ}^2. Here g_{Λ} and g_{Σ}
stand for $g_{\Lambda K p}$ and $g_{\Sigma^0 K p}$ respectively.

Apart from an improvement in the data, the main
differences between the results are due to the use
of different parameterisations of the low-energy $\bar{K}N$
interaction and the type of parameterisation assumed

Analysis	$\overline{K}N$ parameterisation	g_Λ^2	g_Σ^2
Zovko[31]	Kim C.S.L.[E3]	$g_\Lambda^2 + g_\Sigma^2$	$\lesssim 9.6$
	Sakitt et al. C.S.L.[E2]	$g_\Lambda^2 + g_\Sigma^2$	$\lesssim 8.2$
Lusignoli et al.[32]	Kim C.S.L.[E3]	3.9 ± 0.8	$\lesssim 2.5$
	Sakitt et al. C.S.L.[E2]	4.2 ± 0.9	$\lesssim 0.4$
Carter[33]	Kim C.S.L.[E3]	4.9 ± 0.9	$\lesssim 3.0$
Davies et al.[34]	Kim C.S.L.[E3]	5.0 ± 1.7	$\lesssim 3.0$
Kim[E3,19]	Kim C.S.L.[E3]	4.0 ± 0.9	$\lesssim 2.4$
	Kim KM.[19]	13.5 ± 2.1	0.2 ± 0.4
Martin and Poole[35]	Kim C.S.L.[E3]	4.1	–
Rood[29]	Rood KM.[29]	6.2 ± 1.0	–
Carter[36]	Kim C.S.L.[E3]	5.2 ± 0.9	$\lesssim 3.0$
Queen et al.[37]	Kim C.S.L.[E3]	3.9 ± 0.6	$\lesssim 3.1$
	Kittel-Otter E.R.[30]	5.2 ± 0.9	$\lesssim 1.0$
	Kim KM.[19]	11.9 ± 0.7	0.4 ± 0.6
Granovskii and Starikov[38]	Kim C.S.L.[E3]	5.9 ± 1.3	$\lesssim 1.3$

Notation: C.S.L. = Constant Scattering Length
E.R. = Scattering length with effective range terms
KM = K-matrix

Table (4.1)

is listed in each case. The reason that the low

energy contribution is so important is that large

cancellations occur between the various terms in

(4.9) and so the relatively small term coming from

the integral over the region below the $\bar{K}N$ threshold

becomes important. Moreover, as mentioned in the

previous chapter, the parameterisations predict a

virtual bound state resonance, the Y_0^*, at a position

just below the $\bar{K}N$ threshold and the contribution of

the resonance to the integral is very sensitive to its

width and position as predicted by the parameterisation.

This effect is clearly seen in Table (4.1) where there

are listed two distinct predictions for the coupling

constant g_Λ, and the difference between these predictions

clearly exceeds the total statistical error in their

estimations. The first prediction $g_\Lambda^2 \simeq 5$ is obtained

using the various scattering length fits which generally

predict a narrow Y_0^*, whilst the other prediction

$g_\Lambda^2 \simeq 12.5$ is obtained using Kim's K-matrix fit which

predicts a broader Y_0^* resonance.

Finally it should be mentioned that there is also

a $P_{3/2}$ $I = 1$ scattering resonance in the $\bar{K}N$ amplitude

at a point below the $\bar{K}N$ threshold. As most of the

low energy parameterisations do not include its

effect it is consequently not in general included in the dispersion relation. The sign of its contribution may be obtained by considering the multichannel Breit Wigner P wave resonance form

$$T_{ii}(E) = \frac{\frac{1}{2} \Gamma_i k_i^2}{E_r - E - \frac{1}{2} i \sum_j \Gamma_j k_j^3}$$

where j runs over the $\bar{K}N$, $\Sigma\pi$ and $\Lambda\pi$ channels and i is the $\bar{K}N$ elastic channel. By unitarity Γ_i must be positive and thus below the $\bar{K}N$ threshold the contribution of this resonance to the elastic amplitude will be

$$T_{ii}(E) = \frac{-\frac{1}{2} \Gamma_i |k_i|^2}{E_r - E - \frac{1}{2} \Gamma_i |k_i|^3 - \frac{1}{2} i \sum_{j \neq i} \Gamma_j k_j^3} \tag{4.12}$$

Comparison of (4.12) with (4.6) and (4.9) indicates that the residues of the Σ and Y_i^* poles in the $\bar{K}N$ amplitude have the same sign and thus the values obtained for g^2_{Σ} will be an upper limit when the Y_i^* is not included in the parameterisation. This is indicated in Fig. (4.1).

(iv) <u>Unitary symmetry predictions of g^2_{Λ} and g^2_{Σ}</u>

The unitary symmetry model proposes that all particles should transform under SU(3) as irreducible

representations of SU(3). Accordingly the pseudo-scalar mesons are grouped under an octet representation of SU(3) as are the baryons. If now we construct interactions among the various unitary multiplets which are invariant under the transformations of SU(3) it is possible to obtain relations between these interactions.

Accordingly we may construct an interaction Hamiltonian density in the form

$$H = g_1 \bar{B} \gamma_5 D^a B P_a + g_2 \bar{B} \gamma_5 F^a B P_a$$

where B_a and P_a are the baryon fields and pseudo scalar meson fields with unitary indices a which transform via the regular representation. F and D represent the two independent types of coupling possible because of the two $\underset{\sim}{8}$ representations in the reduction of the product $\underset{\sim}{8} \otimes \underset{\sim}{8}$

$$\underset{\sim}{8} \otimes \underset{\sim}{8} = \underset{\sim}{27} \oplus \underset{\sim}{10} \oplus \underset{\sim}{10}^* \oplus \underset{\sim}{8}_1 \oplus \underset{\sim}{8}_2 \oplus \underset{\sim}{1}$$

These $\underset{\sim}{8}$ representations generate two identity representations in $\underset{\sim}{8} \otimes \underset{\sim}{8} \otimes \underset{\sim}{8}$. Since $\underset{\sim}{8} \otimes \underset{\sim}{10}$, $\underset{\sim}{8} \otimes \underset{\sim}{10}^*$ and $\underset{\sim}{8} \otimes \underset{\sim}{27}$ do not contain $\underset{\sim}{1}$.

From this Hamiltonian it is straightforward[39] to obtain the coupling constants g_A^2 and g_Z^2 in terms of the pseudoscalar πNN coupling constant $g_{\pi NN}^2$

$$g_\Lambda^2 = \tfrac{1}{2}(1+2\alpha)^2 \, g_{\pi NN}^2$$

$$g_\Sigma^2 = (1-2\alpha)^2 \, g_{\pi NN}^2$$

where $\alpha = \frac{F}{f+d}$ gives the fraction of F-type coupling. The value obtained for $g_{\pi NN}^2$ is

$$g_{\pi NN}^2 = 14.6 \pm 0.6$$

Although the value of α is not determined by SU(3) symmetry alone, if one assumes the validity of SU(6) symmetry, then α is fixed at 0.4 and the unitary predictions for the coupling constants are

$$g_\Lambda^2 = 15.8$$

$$g_\Sigma^2 = 0.6$$

If we do not assume SU(6) symmetry we may still determined the range of possible values for the coupling constants by varying α over its allowed range. This is done in Fig. (4.3).

Finally by eliminating α from the equations for the coupling constants a prediction is obtained for the quantity $g_\Lambda^2 + g_\Sigma^2$

$$g_\Lambda^2 + g_\Sigma^2 \geq \tfrac{1}{2} g^2$$
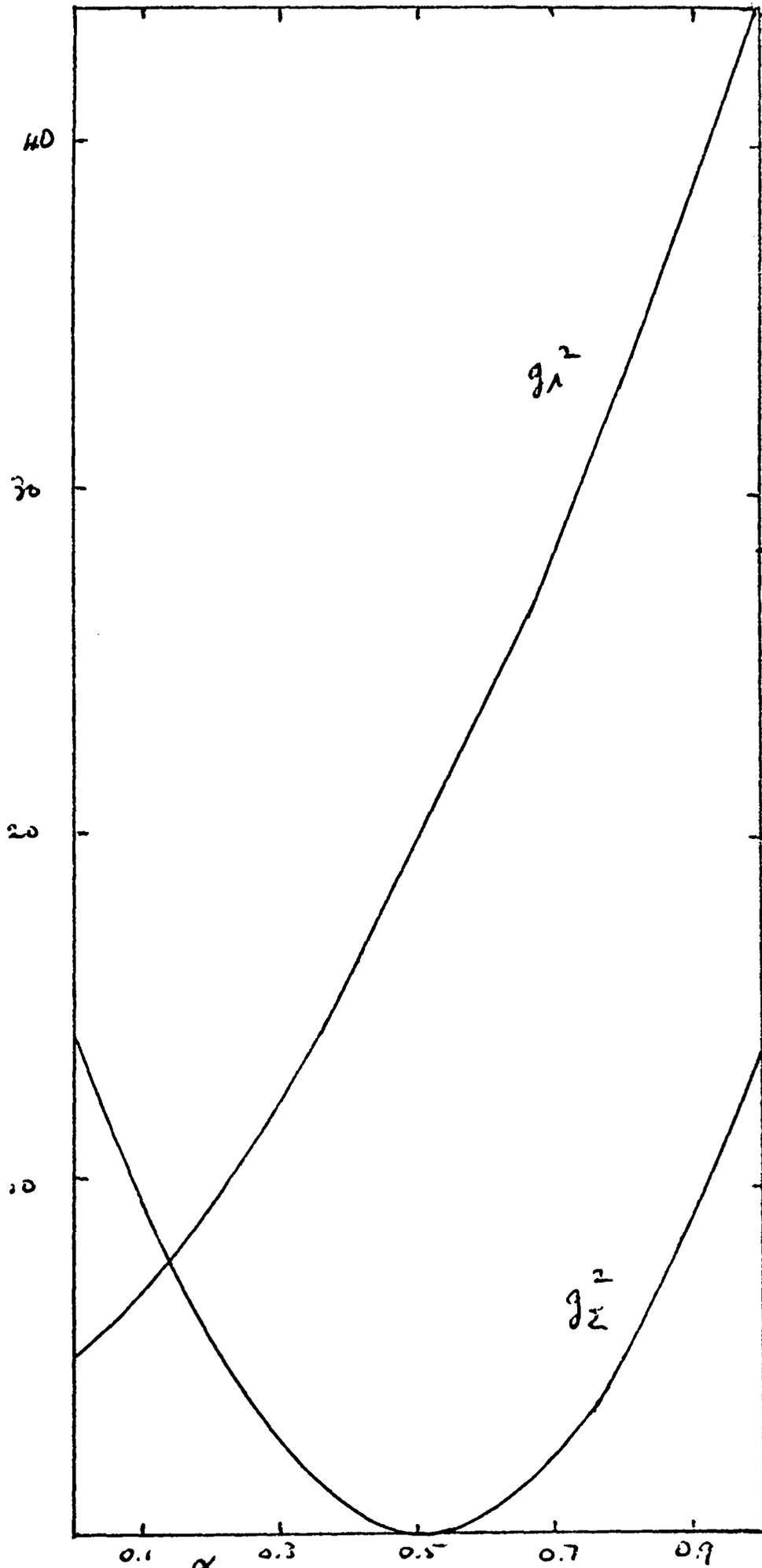
Fig (4.3)

It is apparent that the dispersion relations predictions of the coupling constants obtained using the constant scattering length parameterisation for the low energy $\overline{K}N$ interaction are not consistent with pure SU(3) symmetry whilst those obtained using Kim's K matrix fit do lie in the range (Fig.(4.3)) allowed by pure SU(3) symmetry. Moreover the value obtained using Kim's K-matrix fit are compatible with the SU(6) predictions.

At this point it is convenient to review the alternative methods that have been used to determine the $\overline{K}N\Lambda$ coupling constants. The main predictions come from the analysis of strange particle photoproduction and associated production. Generally an isobaric model is used to analyse the data. This model consists of evaluating the contributions to the production amplitude from simple Feynman diagrams with single particle intermediate states. The most significant results in this field have been obtained by Nelipa[40] who analysed the data from the processes $\gamma + p \rightarrow K^+ + \Lambda$ and who obtained the result

$$9.21 \leqslant g_\Lambda^2 \leqslant 9.61$$

and by Thom[41] whose analysis of the same data yielded

the value
$$\varepsilon^2_{\Lambda} = 5.43$$

It turns out that the determination of $\varepsilon^2_{\Sigma^0}$ is
impossible to do with any accuracy the only result
obtainable being
$$g_{\Sigma^0}^2 < g_{\Lambda}^2$$

The overall conclusion of these estimates of the coupling
constants is that there appears to be a strong violation
of SU(3) symmetry.

It is interesting to note here that another test
of SU(3) invariance involving K mesons has been derived
by Levinson[42] et al. who show that SU(3) invariance
implies the inequalities

$$\frac{d\sigma(1)}{d\Omega} \gtrless \frac{1}{2} \frac{d\sigma(3)}{d\Omega} + \frac{3}{2} \frac{d\sigma(2)}{d\Omega} \pm \left[3 \frac{d\sigma(2)}{d\Omega} - \frac{d\sigma(3)}{d\Omega} \right]$$

where 1, 2 and 3 label the final states $\pi^+ + n$, $K^+ + \Lambda$
and $K^+ + \Sigma^0$ in $\gamma + p$ photoproduction. At 3.4 Gev and
4.0 Gev these reactions have been analysed by Elings[43]
et al. who found the inequalities very well satisfied.
One might conjecture that, if the apparent violation
of SU(3) symmetry at low energies turns out to be true,
whilst the above analysis suggests SU(3) is good at
high energies, the answer may be that symmetry breaking
terms, which have to account for the π meson K-meson
mass difference, will have small effects at higher
energies where the mass difference becomes negligible.

More recently Boyarski[44] et al. have measured the
cross sections for the above reactions in the photon
energy range 5, 8, 11 and 16 Gev and they find the
inequalities satisfied in the squared momentum transfer
region $(-t) < 0.2$ Gev^2. However for $(-t) < 0.1$ Gev^2
there is a marked violation of the inequality which,
they suggest, may be due to the large π-K symmetry
breaking becoming apparent at low momentum transfer.

(v) A Superconvergent dispersion relation[49]

For an analytic function which is known exactly over
its cuts every dispersion relation written for the
function, or for the function multiplied by any other
analytic function, will give the same result for the
analytic continuation throughout the cut plane of
its variables. However, if, as is the situation in
practice, the function is known over certain regions
with greater accuracy than elsewhere, an improvement
in the accuracy of the prediction for the continued
function may be obtained by multiplying the amplitude
by an analytic function which weights the contributions
to the dispersion integral in such a way as to suppress

the poorly known data.

In the case of the $K^{\pm}N$ dispersion relations discussed in section (i) it was observed that the main uncertainty in the prediction of the coupling constants was due to the differences in the various predictions of the unphysical $\bar{K}N$ amplitudes arising from the various fits. Accordingly, if the contribution of this unphysical region could be suppressed, a more accurate prediction for the coupling constant might be possible. It was, however, observed in section (i) that one subtraction at least is necessary in order to ensure the convergence of the integrals. It would be possible to add weight to the contribution of particular regions to the dispersion integral by making further subtractions in these regions, but at each subtraction point the real part of the amplitude must be known and knowledge of real parts is, at present, very poor. A way out of this impasse was suggested, in a different context, by Igi[45] who proposed that Cauchys theorem should be applied to $\left\{ F_-(\omega) - F_-^{Regge}(\omega) \right\}$ where $F_-^{Regge}(\omega)$ is the Regge contribution to the scattering amplitude. It is apparent from (4.10) that the Regge term has a cut

running along the positive real axis and starting at $\omega=0$. The singularities of $F_-(\omega)$ are, as before, given by Fig. (4.2).

Applying Cauchy's theorem to a contour Γ' which encloses the Regge cut as well as those shown in Fig. (4.2) and closing by an infinite circle we obtain the relation

$$\int_{-\alpha}^{\infty} \mathcal{I}m \left[F_-(\omega) - F_-^{Regge}(\omega)\right] d\omega = 0 \qquad (4.13)$$

where we have assumed that the function $\left[F_-(\omega) - F_-^{Regge}(\omega)\right]$ decreases faster than $\frac{1}{\omega}$ at infinity. This leads to the relation

$$\sum_\gamma \pi A_\gamma + \int_{\omega_{int}}^{m} A_-(\omega') d\omega' + \frac{1}{4\pi} \int_m^N k_i' \left(\sigma_-(\omega') - \sigma_+(\omega')\right) d\omega' \qquad (4.14)$$
$$- \left[\sum_i \frac{\mathcal{I}m c_i}{\alpha_i+1} N^{\alpha_i+1}\right] = 0$$

where we have used the explicit form for the Regge poles as given in (4.10) with $\alpha_i = \alpha_i(0)$ and the optical theorem (2.13). The only terms contributing to the sum over Regge poles in this equation are the ω and ρ Regge terms, the others disappearing due to their crossing properties as given by (4.11). The quantity N is the

value of ω above which the contribution of the term

$$\int_{\omega_N}^{\infty} \partial_n \left[F_-(\omega) - F_-^{Regge}(\omega) \right] d\omega - \int_{-N}^{-\infty} \partial_n \left[F_-(\omega) - F_-^{Regge}(\omega) \right] d\omega$$

to the relation (4.13) may be neglected. It should

be noted that only those Regge poles which have a value

of α greater than -1 will contribute significantly

to (4.14) for large values of N.

The relation (4.14) evidently satisfies our

requirement of reducing the contribution of the low

energy unphysical region to the determination of A_y.

However, when a detailed comparison of the magnitudes

of the various terms is made, it is observed that, at

a value of N given by 10 Gev., the contribution of the

Regge term will be -27 mb Gev^{-2}. The contribution of

the pole terms, assuming the coupling constants are

in the range covered by Table (4.1), would vary between

1.5 and 3.0 mb Gev^{-2}. It is evident that the uncertainty

in the Regge term, which may be estimated at approximately

10%, will make it impossible to determine the value

of the coupling constants to the accuracy needed to

distinguish between the two solutions.

The difficulty in using the high energy information to evaluate the coupling constants may be overcome by making a subtraction in the sum rule (4.13). If the subtraction point ω is below the Regge region the subtraction will reduce in the sum rule the integral over the Regge term and consequently reduce the error introduced by the Regge term. Moreover the sum rule may be evaluated for several values of the subtraction point, giving several determinations of the coupling constants and consequently improving the accuracy to which they are determined.

The sum rule may be derived as follows: Cauchy's integral form is written for the amplitude combination $F_+(\omega) - F_+^{Regge}(\omega)$ to give

$$F_+(\omega) - F_+^{Regge}(\omega) = \frac{1}{2\pi i} \int_{\Gamma'} \frac{[F_+(\omega') - F_+^{Regge}(\omega')]}{(\omega' - \omega)} d\omega' \quad (4.15)$$

where the contour Γ' encloses the singularities of the amplitudes on the physical sheet and is closed by an infinite circle.

If we assume that the difference between the amplitude and the Regge term decreases faster than a constant at infinity then the integral over the infinite

circle will be negligible and the sum rule may be written

$$D_+(\omega) - D_+^{Regge}(\omega) = \frac{P}{\pi} \int_{-\infty}^{\infty} \frac{\Im m \left\{ F_+(\omega') - F_+^{Regge}(\omega') \right\}}{(\omega' - \omega)} d\omega' \qquad (4.16)$$

Once again we introduce the cut off point W such that the term

$$\frac{1}{\pi} \int_{-\infty}^{-W} \frac{\Im m \left\{ F_+(\omega') - F_+^{Regge}(\omega') \right\}}{(\omega' - \omega)} d\omega' + \frac{1}{\pi} \int_{W}^{\infty} \frac{\Im m \left\{ F_+(\omega') - F_+^{Regge}(\omega') \right\}}{(\omega' - \omega)} d\omega'$$

may be neglected, and we use the crossing relation (4.3) to write the sum rule (4.18) in the form

$$D_+(\omega) - D_+^{Regge}(\omega) = \frac{P}{\pi} \int_{0}^{W} \left[\frac{A_+(\omega')}{(\omega' - \omega)} + \frac{A_-(\omega')}{(\omega' + \omega)} \right] d\omega'$$
$$+ \frac{P}{\pi} \int_{0}^{W} \left[\frac{A_+^{Regge}(\omega')}{(\omega' - \omega)} + \frac{A_-^{Regge}(\omega')}{(\omega' + \omega)} \right] d\omega' \qquad (4.17)$$

From (4.10) we know that the contribution to $A_-^{Regge}(\omega)$ is given by

$$A_-^{Regge}(\omega) = \sum_{i} c_i \left(\frac{\omega}{\omega_0} \right)^{\alpha_i} \qquad (4.18)$$

where $\alpha_i = \alpha_i(0)$ is evaluated in the forward direction. With this definition of the Regge term we have

$$A_+^{Regge}(\omega) = \sum_i c_i \tau_i' \left(\frac{\omega}{\omega_0}\right)^{\alpha_i} \qquad (4.19)$$

and $\tau_i' = \pm 1$ depending on whether the Regge pole is even or odd in signature. Using these forms the integral in (4.17) over the Regge term may be written as

$$\sum_i \frac{2c_i}{(\omega_0)^{\alpha_i}} \frac{P}{\pi} \int_0^W \frac{(\omega')^{\alpha_i+1}}{\omega'^2-\omega^2} d\omega' + \sum_j \frac{2\omega c_j'}{(\omega_0)^{\alpha_j}} \frac{P}{\pi} \int_0^W \frac{(\omega')^{\alpha_j}}{\omega'^2-\omega^2} d\omega' \qquad (4.20)$$

where the summations over i and j represent the contributions of the Regge poles of even, odd signature respectively.

These integrals may be performed analytically using the result[46]

$$\int_0^W \frac{\omega'^{\alpha_i+1}}{\omega'^2-\omega^2} d\omega' = \omega^{\alpha_i} \frac{\pi}{2} \cot \frac{\pi\alpha_i}{2} - \frac{(W)^{\alpha_i}}{\alpha_i} F\left(1, -\frac{\alpha_i}{2}, 1-\frac{\alpha_i}{2}, \frac{\omega^2}{W^2}\right) \qquad (4.21)$$

$$\frac{\alpha_i}{2} + 1 > 0 \qquad\qquad \omega^2 < W^2$$

where $F(a,b,c;z)$ is the hypergeometric function. This gives for the integral (4.20) over the Regge terms

$$\sum_i c_i\left(\frac{\omega}{\omega_0}\right)^{\alpha_i}\cot\frac{\pi\alpha_i}{2} \;-\;\frac{2}{\pi}\sum_i\frac{c_i}{\alpha_i}\left(\frac{\omega}{\omega_0}\right)^{\alpha_i}F\left(1,-\frac{\alpha_i}{2},1-\frac{\alpha_i}{2},\frac{\omega^2}{W^2}\right)$$

$$+\sum_j c_j\left(\frac{\omega}{\omega_0}\right)^{\alpha_j}\cot\frac{\pi(\alpha_j-1)}{2}\qquad\qquad (4.22)$$

$$-\frac{2}{\pi}\frac{\omega}{W}\sum_j\frac{c_j}{(\alpha_j-1)}\left(\frac{\omega}{\omega_0}\right)^{\alpha_j}F\left(1,-\frac{\alpha_j}{2}+\frac{1}{2},-\frac{\alpha_j}{2}+\frac{3}{2};\frac{\omega^2}{W^2}\right)$$

However from (4.10) we have

$$D_+^{Regge}(\omega)=\sum_i c_i\left(\frac{\omega}{\omega_0}\right)^{\alpha_i}\cot\frac{\pi\alpha_i}{2}+\sum_j c_j\left(\frac{\omega}{\omega_0}\right)^{\alpha_j}\cot\frac{\pi(\alpha_j-1)}{2}\qquad (4.23)'$$

and so using (4.17),(4.22),(4.23) the final form of
the sum rule may be written[48] as

$$-D_+(\omega)+\frac{1}{\pi}\int_{\omega_{\pi}}^{W}\left[\frac{A_+}{(\omega'-\omega)}+\frac{A_-}{(\omega'+\omega)}\right]d\omega'+\sum_\gamma\frac{A_\gamma}{(\omega_\gamma+\omega)}$$

$$=\frac{2}{\pi}\left[\sum_i\frac{c_i}{\alpha_i}\left(\frac{W}{\omega_0}\right)^{\alpha_i}F\left(1,-\frac{\alpha_i}{2},-\frac{\alpha_i}{2}+1;\frac{\omega^2}{W^2}\right)\right.\qquad (4.24)'$$

$$\left.-\frac{\omega}{W}\sum_j\frac{c_j}{(\alpha_j-1)}\left(\frac{W}{\omega_0}\right)^{\alpha_j}F\left(1,-\frac{\alpha_j}{2}+\frac{1}{2},-\frac{\alpha_j}{2}+\frac{3}{2},\frac{\omega^2}{W^2}\right)\right]$$

From the discussion of section (i) it is evident
that for $K^{\pm}p$ scattering the significant Regge poles
contributing to the sum rule are the P, P',A_2 with
even signature and the ρ, ω with odd signature. The ϕ
contribution is assumed to be contained in that of
the ω.

Using the solution of Phillips and Rarita it is
possible to work out the Regge contribution to the
sum rule. However due to the errors in determining these

contributions it is statistically better to use their values as constraints on the possible values of the Regge contributions. Accordingly the hypergeometric functions are expanded as a power series in x where $x = \omega + \omega_\Lambda$. This gives for the sum rule $(4.24)'$

$$-D_+(\omega) = \frac{1}{\pi} \int_{\omega_{\Lambda\pi}}^{\omega} \left[\frac{A_+(\omega')}{(\omega'-\omega)} + \frac{A_-(\omega')}{(\omega'+\omega)} \right] d\omega'$$
$$+ \sum_{\gamma} \frac{A_\gamma}{(\omega_\gamma+\omega)} + \sum_{n=0} b_n x^n \qquad (4.23)$$

Using Phillips and Rarita the coefficients b_n may be calculated. For W=6 Gev. we find

$$b_0^\rho = 18.51 \quad b_1^\rho = 0.96 \quad b_2^\rho = -0.42 \quad b_3^\rho = 0.005 \text{ etc}$$

where b_n is written in units Gev^{-n-1}.

In the present analysis b_n is set equal to b_n^ρ for $n \geqslant 3$ whilst the remaining three b_0, b_1, b_2 are left as free parameters. They will be determined by using the condition that the sum rule (4.23) is satisfied for a range of values of ω but their possible values will be restrained using the values $b_0^\rho, b_1^\rho, b_2^\rho$ as constraints accurate to an estimated 10%.

The pole term contributions $\sum_{\gamma} \frac{A_\gamma}{(\omega_\gamma+\omega)}$ come from both the Λ and Σ poles. However as A_Σ is proportional to g_Σ^2 which, cf. Table (4.1), is small and as the Λ and Σ

poles are close together we make the approximation that the two poles may be considered as one at the Λ pole position.

Thus

$$\frac{A_\Lambda}{(\omega_\Lambda+\omega)} + \frac{A_\Sigma}{(\omega_\Sigma+\omega)} = \frac{A_\Lambda}{(\omega_\Lambda+\omega)} + \frac{A_\Sigma}{(\omega_\Lambda+\omega)}\left(\frac{\omega_\Lambda+\omega}{\omega_\Sigma+\omega}\right) \quad (4.24)$$

$$\simeq \frac{A_\Sigma+A_\Lambda}{(\omega_\Lambda+\omega)}$$

Using average values for g_Λ^2 and g_Σ^2 from Table (4.1) the magnitude of the error introduced in making the approximation (4.24) is found to be

$$\frac{A_\Sigma\,(\omega_\Lambda\omega_\Sigma)}{(\omega_\Lambda+\omega)(\omega_\Sigma+\omega)} \simeq -0.04\,\frac{A_\Sigma+A_\Lambda}{(\omega_\Lambda+\omega)}$$

for $\omega \simeq m$

Using (4.6) we find

$$A_\Sigma + A_\Lambda \simeq -0.06\left(g_\Lambda^2 + 0.84\,g_\Sigma^2\right) \quad (4.25)$$

$$\equiv G.$$

where we have defined a fourth parameter G which is to be determined by the fit to the sum rule predictions. The remaining terms to be evaluated in the sum rule are the real part $D_+(\omega)$ and the integral over the low energy region of the imaginary parts of the $K^\pm_p$ amplitudes.

$$\frac{P}{\pi}\int_{\omega_{th}}^{W}\left[\frac{A_+(\omega')}{(\omega'-\omega)} + \frac{A_-(\omega')}{(\omega'+\omega)}\right]d\omega'$$

The magnitude of $D_+(\omega)$ is calculated using the available K^+p differential cross section data together with the knowledge of the imaginary part of the amplitude obtained from the total cross sections via the optical theorem. The sign is fixed by use of a forward dispersion relation and this has been done by Martin and Poole in ref.(47).

Finally, in order to evaluate the integrals for the range of values of ω for which the real part is known they are split into two energy ranges, the low energy range where the low energy parameterisation is used to predict the amplitude and the high energy range where the imaginary part is obtained from the total cross section.

Thus

$$\frac{P}{\pi}\int_{\omega_{\Lambda\pi}}^{W}\left[\frac{A_+(\omega')}{(\omega'-\omega)} + \frac{A_-(\omega')}{(\omega'+\omega)}\right]d\omega' = \frac{1}{\pi}\int_{\omega}^{0.58\,GeV}\frac{A_-(\omega')}{(\omega'+\omega)}\,d\omega'$$

$$+ \frac{1}{\pi}\int_{m}^{0.58\,GeV}\frac{A_+(\omega')}{(\omega'-\omega)}\,d\omega' + \frac{P}{\pi}\int_{0.58\,GeV}^{W=6GeV}\frac{k_L'}{4\pi}\left\{\frac{\sigma_+(\omega')}{(\omega'-\omega)} + \frac{\sigma_-(\omega')}{(\omega'+\omega)}\right\}d\omega'$$

$$(4.26)$$

where k_L is the kaon laboratory momentum. The technique used in evaluating the Principal value integral numerically is given in Appendix 2. Finally the data used in evaluating the integrals over the physical

region is, as mentioned in section (i) given by refs.
(E8,E9,E10).

Using (4,24), (4,25), (4.26) we write the sum
rule (4.23) in the form

$$-D_+(\omega) = \frac{1}{\pi} \int_{\omega_{A\pi}}^{0.58} \frac{A_-(\omega')}{(\omega'+\omega)} \, d\omega' + \frac{1}{\pi} \int_{0.58}^{\omega=6\,GeV} \frac{A_-(\omega')}{(\omega'+\omega)} \, d\omega'$$

$$+ \frac{P}{\pi} \int_{m}^{\infty} \frac{A_+(\omega')}{(\omega'-\omega)} \, d\omega' - \sum_{n=3}^{\infty} b_n x^n \qquad (4.27)$$

$$= -\frac{G}{x} + b_0 + b_1 x + b_2 x^2$$

and tabulate the contributions to the left hand side
for the available range of ω in Table (4.2). $-D_+$,
U, Σ_- and Σ_+ give the partial contributions to the sum
rule generated by the first four separate terms in the
left hand side of equation (4.27). The contribution
U from the unphysical region of the K^-p reaction is
worked out in two ways; firstly using Kim's K Matrix
fit and secondly using the Constant Scattering Length
fit of Kim. In the last column of Table (4.2) we list
f, the total contribution to the left hand side of
(4.27) arising from the sum of the terms D_+, U, Σ_-
and Σ_+, for the K Matrix extrapolation.

The errors for the integrals over the cross-
sections may be estimated using the quoted errors on
the cross sections assuming no correlation between the

errors on different measurements. From these errors,
together with the error in the determination of the
real part, the final error in f was estimated and
this is also tabulated in Table (4.2).

We thus have a total of eighteen points for
the sum rule (4.27) and four free parameters. These
eighteen points together with the three data points
supplied by the fits of Phillips and Rarita give a
total of 21 data points. If, using the tabulated
errors, we form, as in Appendix 3 the Chisquared
function $\chi^2(b_o,b_1,b_2,G)$ we may minimise this function
to give predictions for the quantities b_o,b_1,b_2,G.
For the solution using Kim's K Matrix fit we obtain a
unique minimum with $\chi^2(min) = 17.3$ for 18 degrees of
freedom with the prediction

$$\varepsilon_\Lambda^2 + 0.84\, \varepsilon_\Sigma^2 = 5.7 \pm 3.8$$

$$b_o = 18.10 \pm 0.31, \quad b_1 = 0.92 \pm 0.09,$$

$$b_2 = -0.46 \pm 0.04$$

(4.28)

Here the quoted errors are related to the diagonal
elements of the error matrix (cf. Appendix 3).

When the calculation was repeated using the
C.S.L. extrapolation to compute U it was found

Units : Gev^{-1}.

k (Gev/c)	$-D_+$	Σ_+	Σ_-	U KK	(CSL)	f
0.14	2.11	7.85	8.05	0.73	(0.57)	18.74±0.48
0.175	2.43	7.84	8.02	0.73	(0.57)	19.02±0.43
0.205	2.34	7.85	7.99	0.72	(0.56)	18.90±0.35
0.235	2.31	8.12	7.96	0.71	(0.55)	19.10±0.33
0.265	2.19	8.17	7.93	0.70	(0.54)	18.99±0.35
0.355	2.33	8.07	7.81	0.67	(0.52)	18.88±0.24
0.52	2.31	8.73	7.55	0.60	(0.47)	19.19±0.26
0.642	2.23	8.59	7.35	0.56	(0.44)	18.73±0.23
0.78	2.36	9.10	7.12	0.51	(0.40)	19.09±0.18
0.81	2.36	9.19	7.07	0.50	(0.39)	19.12±0.26
0.86	2.33	9.31	6.99	0.49	(0.38)	19.12±0.20
0.96	2.08	9.55	6.83	0.46	(0.36)	18.92±0.20
1.2	2.48	9.33	6.47	0.40	(0.31)	18.68±0.21
1.36	2.53	8.97	6.24	0.37	(0.29)	18.11±0.25
1.455	3.91	8.92	6.12	0.35	(0.28)	19.30±0.56
1.96	2.36	8.45	5.52	0.28	(0.22)	16.61±1.32
3.0	5.30	6.65	4.61	0.20	(0.16)	16.76±1.67
3.46	3.80	5.48	4.30	0.18	(0.14)	13.76±2.02
4.97	7.50	-2.18	3.53	0.13	(0.10)	8.98±2.68

Table (4.2)

$$g^2_\Lambda + 0.84 \, g^2_\Sigma = 4.5 \pm 3.8$$

<div align="right">(4.29)</div>

$$b_o = 18.07 \qquad b_1 = 0.92 \qquad b_2 = -0.46$$

with $\chi^2(min) = 17.2$.

It is apparent, from these results, that the sum rule prediction is much less sensitive to the extrapolation over the unphysical region than the dispersion relation prediction. From equations (4.26) and (4.29) we conclude that

$$g^2_\Lambda + 0.84 \, g^2_\Sigma = 5.1 \pm 4.0$$

where the main contribution to the error is the uncertainty in the determination of $D_+(\omega)$. Once again it may be seen that the prediction is incompatible with SU(3) invariance.

(vi) **Consistency tests of the low energy $\bar{K}N$ parameterisations**

In the previous section, predictions for the coupling constants were obtained from the superconvergent sum rule by varying the subtraction point ω . This variation altered the proportional contribution of the various energy regions and, as the experimental measurements are coupled with errors, provided independent

evaluations of the sum rules which could not only be
used to determine the coupling constants, but also
test the self consistency of the data in various
regions. However, due to the small low energy contribu-
tion built into the sum· rule, this is not the most
effective relation to test the low energy $\bar{K}N$ parameterisa-
tion. A better one is the dispersion relation (4.8)
obtained in section (i) with two subtraction points ω
and ω_0 viz:

$$\sum_{Y} \frac{A_Y}{(\omega_Y - \omega)(\omega_Y + \omega_0)} = \frac{D_-(\omega) - D_+(\omega_0)}{(\omega + \omega_0)} - \frac{P}{\pi} \int_{\omega_{A\pi}}^{\omega_-} \frac{A_-(\omega') d\omega'}{(\omega' - \omega)(\omega' + \omega_0)}$$

$$+ \frac{P}{\pi} \int_{m}^{\omega_+} \frac{A_+(\omega')}{(\omega' + \omega)(\omega' - \omega_0)} d\omega' \qquad (4.28)$$

$$+ \frac{P}{4\pi^2} \int_{\omega_+}^{\infty} \left\{ \frac{k_L' \sigma_T^+(\omega')}{(\omega' + \omega)(\omega' - \omega_0)} - \frac{k_L' \sigma_T^-(\omega')}{(\omega' - \omega)(\omega' + \omega_0)} \right\} d\omega'$$

If, for a fixed ω_0, ω is varied in the energy
range below the K^-p threshold the contribution of the
unphysical integral, which is dominated by the $Y_0^*(1405)$,
will be greatly altered. This should be balanced by
a variation in the contributions from the other terms
the change mainly arising from the integrals over the
physical regions and thus, theoretically, the

consistency of the low energy parameterisation with
the total cross section data should be tested.

This dispersion relation was first investigated
by Martin et al.[50] but, as we will have occasion to
use it to test the solutions found in the next
chapter, we will discuss its application in detail.
Moreover at $\omega = \omega_o = m$ the relation becomes the
standard dispersion relation and this will also be
used in the next chapter to obtain values for the
coupling constants.

Using the $K^{\pm}p$ and $K^{\pm}n$ data in the combination
$\left[(K^{\pm}p) - \frac{1}{2}(K^{\pm}n) \right]$ the Λ pole may be isolated and, using
(4.28), the dispersion relation may be written in
the form

$$g_{\Lambda}^2 = u(\bar{K}N) + Low(\bar{K}N) + Low(KN) + \sigma + Regge \qquad (4.29)$$

where $u(\bar{K}N)$ = integral over the $\bar{K}N$ unphysical region
+ the term involving $D_-(\omega)$.

Low $(\bar{K}N)$ = integral over A_- from m to $\omega_- = 574$
Mev determined from the K^-p parameters.

Low (KN) = integral over A_+ from m to $\omega_+ = 811$
Mev determined from the known KN parameters

+ the term involving $D_+(\omega_0)$

$\mathcal{S}$ = integrals over $A_{\pm}$ from $\omega_{\pm}$ to 20 Gev evaluated from the available total cross section data, Regge = integrals over $A_{\pm}$ from 20 Gev to ∞ evaluated using Regge pole parameters.

For the consistency test in the evaluation of these terms ω_0 is chosen to be 498 Mev and ω is varied over the energy range below the KN threshold. For the standard dispersion relation $\omega = \omega_0 = m$ and it should be noted that care must be taken in evaluating the unphysical integral contained in the $U(\overline{K}N)$ term. This is because at the $\overline{K}N$ threshold the imaginary part of the amplitude $A_-(\omega)$ has an infinite derivative and, accordingly, the numerical method of evaluating the Principal integral as given in Appendix 2 will not converge. The difficulty is overcome by expanding the integrand, near the $\overline{K}N$ threshold, in a power series in orders of the $\overline{K}N$ channel lab. momentum. The integration of terms of this series may be performed analytically and thus the total integral computed.

In Table (4.3) we list the contributions to (4.29) for the Constant Scattering length and K Matrix

ω Mev	Low(KN)	ϵ	Regge	C.S.L.		KK	
				Low($\bar{K}N$) + u($\bar{K}N$)	$g^2_\wedge$	Low($\bar{K}N$) + u($\bar{K}N$)	$g^2_\wedge$
400	6.85	−8.29	−1.05	4.99	2.5	11.66	9.2
425	7.36	−8.93	−1.13	5.89	3.2	13.31	10.6
450	7.83	−10.14	−1.19	6.81	3.3	15.07	11.6
475	8.29	−11.58	−1.26	7.84	3.2	16.98	12.5
498	8.69	−13.22	−1.31	8.99	3.1	18.99	13.1
520	9.06	−15.28	−1.38	10.41	2.8	21.29	13.7

Table (4.3)

solutions of Kim. In this calculation using the K

Matrix parameterisation the I=0 $D_{3/2}$ wave has been

omitted for the reason that the parameterisation

used for this wave is an energy dependent Breit-Wigner

with width Γ of the form

$$\Gamma \propto \left[q^2 / (x^2 + q^2) \right]^2 q$$

The best fit value of x = 0.54 fm^{-1} gives this

width a spurious pole in the unphysical region and

is therefore an unsuitable parameterisation for con-

tinuation to the unphysical region.

It may be seen from Table (4.3) that the Constant

Scattering length predictions of the coupling constant

at various energies vary less than those of the

K-Matrix predictions. However, as the typical error

in the evaluation of g_Λ^2 at each energy is ± 3, it

might appear that both variations are consistent with

constant values. That this is not so, as emphasised

by Queen[51] et al., is due to the fact that the errors

in calculating g_Λ^2 at adjacent values of the parameter

ω are strongly correlated. Using the estimation of

these errors obtained by Queen[51] et al., Martin[50] et al.

conclude that Kim's K-matrix solution is inconsistent

with the dispersion relation (4.28) whilst the
Constant scattering length solution is consistent
within the estimated errors.

Finally, to conclude this section, we would like
to briefly review other consistency tests applied to
the $\overline{K}N$ low-energy amplitude.

Chan and Meiere[52] evaluated a dispersion relation
for the function

$$T_\beta(\omega) \equiv \frac{F_-(\omega)}{(\omega - m)^{2\beta}(\omega - \omega_0)^\beta} \qquad (4.30)$$

at the K^+p threshold $\omega = -m$ and for several different
values of β in the range $0 \lesssim \beta \lesssim 1$; ω_0 was chosen
at the $\Sigma\pi$ threshold. The denominator in (4.30) is
chosen so that it introduces a short cut joining the
branch points at ω_0 and m and therefore the numerator
$\mathcal{I}m T_\beta$ in the dispersion relation integrals is
proportional to $\underline{A_+}$ in the K^+p physical regions whereas
in the K^+p unphysical region it is proportional to
$(A_- \cos\beta\pi + B_- \sin\beta\pi)$. Chan and Meiere found that
the prediction for g^2_Λ obtained from the above relation
was for variation of β consistent with a constant
value for Kim's K Matrix parameterisation but not

consistent with a constant for Kim's Constant scattering length solution. However, as pointed out by Martin et al.[50], their result depends on the fact that the constant scattering length parameterisation does not give the $\Sigma\pi$ unitarity cut and is therefore an unsuitable parameterisation near the $\Sigma\pi$ threshold where the imaginary part should vanish like q_Σ. If this behaviour is enforced on the constant scattering length solution it is found that the prediction for g_Λ^2 using the dispersion relation for (4.30) and varying β, is consistent with a constant value.

Queen et al.[53] have also investigated the consistency of the low energy $\overline{K}N$ parameterisation using a derivative sum rule for $dg_\Lambda^2/d\omega$. They find that the KK parameters are inconsistent and that better agreement with a zero derivative is obtained using the Constant Scattering Length parameters. However the errors in the sum rule limit the strength of their result.

Lastly Liu[54] has investigated the $K^{\pm}p$ sum rule obtained from the function

$$\frac{F_-(\omega) - F_+(\omega)}{(\omega^2 - \omega_0^2)^\beta (\omega^2 - m^2)^{1-\beta}}$$

where ω_0 is chosen in the unphysical region near the

$\overline{KN}$ threshold. Due to the fact that both $D_+(\omega)$ and

$D_-(\omega)$ are needed below their physical thresholds, the

resultant errors introduced mask the result but Liu

finds an indication that the prediction obtained for

g_Λ^2 from Kim's K Matrix solution should be lowered.

CHAPTER 5

S Wave K-matrix analysis of the low energy $\bar{K}N$ data

(i) Choice of Parameterisation

The constant scattering length and effective range K matrix analyses of the $\bar{K}N$ data were introduced in Chapter 3. From the use of various consistency relations derived using the analytic properties of the scattering amplitude it was shown in Chapter 4 that the constant scattering length solution appears to be more consistent with the high energy data than does Kim's K-matrix fit, but, due to experimental errors, this result is not conclusive. From a theoretical point of view, a parameterisation which explicitly exhibits the unitarity of the $\Sigma\pi$ and $\Lambda\pi$ processes as well as the elastic $\bar{K}N$ process would be preferable in any analysis of the data and especially if the parameterisation is to be used in the extrapolation of the amplitude below the elastic cut towards the $\Sigma\pi$ and $\Lambda\pi$ thresholds. For this reason it is preferable to attempt a parameterisation using the K-matrix formalism.

Kim's K-matrix fit is based on this formalism, but his analysis suffers from several disadvantages. As mentioned in Chapter 2, the analysis of data in the region 0-550 Mev/c kaon lab. momenta necessitates the inclusion

of S, P and D waves. In any parameterisation of
these partial waves involving a series expansion in
the channel centre of mass momenta it is necessary,
in general, to include those terms in the parameterisa-
tion of each partial wave which correspond to the same
order of channel momenta in the experimental points
to be predicted. This criterion leads, however, to an
unmanageable number of parameters and this number
must be reduced by appealing to other features of the
interaction.

In the analysis performed by Kim this has been
done by including effective range terms only in the
resonant D_{03} and P_{13} channels, together with the non-
resonant S waves. For the other waves, when not
neglected completely, they are only included in a
zero range parameterisation. A further assumption
is that all effective range matrices are diagonal.
This assumption has already been examined in Chapter 2
where it was concluded that, for the $\bar{K}N$ case, the off
diagonal elements could not be neglected.

It is evident therefore that the parameterisation
adopted by Kim depends on several assumptions which

are difficult, à priori, to justify. Thus it may be
that the solutions obtained, in particular for the
effective range parameters, may be spurious in the
sense that the analysis is incorrectly parameterised
and the observed energy variation of the experimental
data is being forced into the effective range parameters
that are specified rather than the neglected parameters.
The importance of the I=0 S wave effective ranges in
determining the coupling constant g_Λ^2 is illustrated in
Fig. (5.0) where the value obtained for g_Λ^2 via the
standard dispersion relation is plotted against changes
in the three I=0 effective ranges using the K-matrix
fit of Kim. In particular it should be noted that, for
a variation of $r_{K\Sigma}^0$ from +0.2 fm to -0.2 fm, a range
that would seem to be reasonable from Fig. (3.3), the
value of g_Λ^2 varies between 11 and 17.5.

From the above discussion of the ambiguities
inherent in an S, P, D wave analysis of the data up
to 550 Mev/c it is relevant to ask whether it is possible
to obtain a unique, pure S-wave, K-matrix fit of the
data in the region where S-waves are expected to be
dominant, namely in the region 0-280 Mev/c of the kaon
lab. momenta. Moreover it should be noted that in this
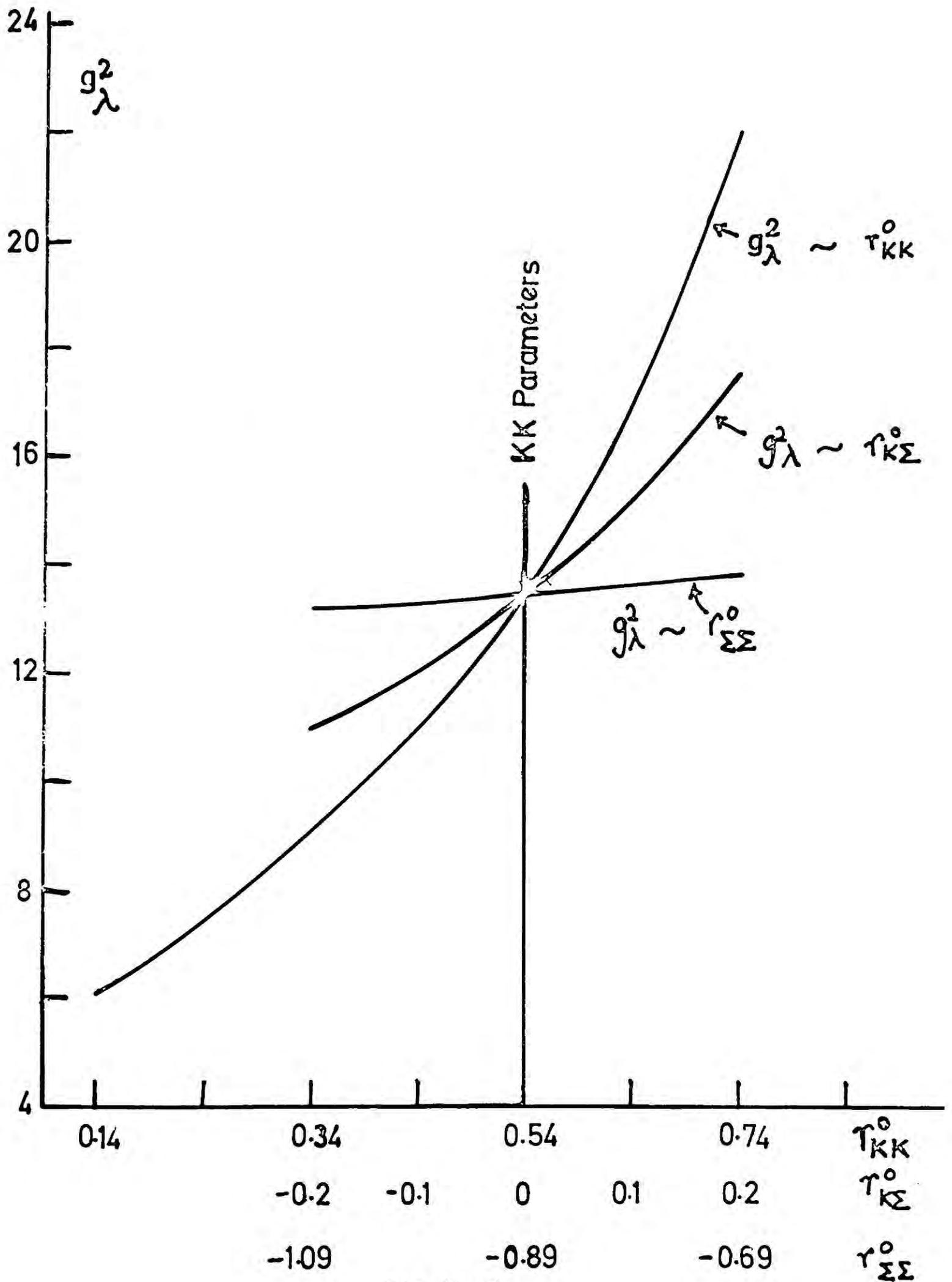
Fig (5.0)

energy region the multipion production, such as $\Lambda\pi^+\pi^-$, is observed to be negligible and so three particle channels can be neglected in this energy range. In the range fitted by Kim this is no longer true and the analysis of him ignores, in the S and P waves, the non-negligible three particle processes. Accordingly, a zero range parameterisation of the K matrix is used in a fit to all the available data in this energy range, including the recent $K_2^o p$ data of refs. (E6,E11). Moreover the solution obtained is tested against change of the parameterisation first to see if the data justify the total number of parameters used and second to study the stability of the predicted solutions. In the next section we give details of this parameterisation and in section (iii) we give the results of the fit and compare it in detail with the other fits that have been performed.

(ii) <u>Application of the zero range parameterisation</u>

Using the basis (2.35) which neglects the K^-p, $\bar{K}^o n$ mass difference, it is apparent that the S-wave K matrix is given by 3 I=0 and 6 I=1 zero range parameters, namely,

$$
\begin{pmatrix} K^{o}_{\bar{K}\bar{K}} & K^{o}_{\bar{K}\Sigma} \\[2mm] K^{o}_{\bar{K}\Sigma} & K^{o}_{\Sigma\Sigma} \end{pmatrix}
\begin{pmatrix} K'_{\bar{K}\bar{K}} & K'_{\bar{K}\Sigma} & K'_{\bar{K}\Lambda} \\[2mm] K'_{\bar{K}\Sigma} & K'_{\Sigma\Sigma} & K'_{\Sigma\Lambda} \\[2mm] K'_{\bar{K}\Lambda} & K'_{\Sigma\Lambda} & K'_{\Lambda\Lambda} \end{pmatrix}
\tag{5.1}
$$

where we have introduced the subscripts $\bar{K}, \Sigma, \Lambda$ to denote the $\bar{K}N, \Sigma\pi$ and $\Lambda\pi$ channels of definite isospin as given in (2.35). The Coulomb and mass difference corrections of Appendix 1 are most easily expressed in terms of the $\bar{K}N$ scattering lengths and thus it is convenient to write the $\bar{K}N$ scattering lengths in terms of the k-matrix elements. The isospin I S-wave complex $\bar{K}N$ scattering length is defined by A_I where

$$
T^{(I)}_{\bar{K}\bar{K}} = \frac{A_I}{1 - ik A_I}
\tag{5.2}
$$

and k is the centre of mass momentum in the $\bar{K}N$ channel.

It is also necessary, in order to analyse the experimentally observed processes of (3.47), and (3.52) to know the amplitudes $T^{I}_{\bar{K}\Sigma}$ and $T'_{\bar{K}\Lambda}$. These may be expressed in terms of the complex scattering lengths as

$$
\begin{aligned}
T^{I}_{\bar{K}\Sigma} &= \frac{M_I}{1 - ik A_I} \\[3mm]
T'_{\bar{K}\Lambda} &= \frac{N_1}{1 - ik A_1}
\end{aligned}
\tag{5.3}
$$

where N_I and N_1 are the reaction amplitudes for $\Sigma\pi$

and $\Lambda\pi$ production respectively.

Using (3.15) to express the T-matrix in terms

of the K-matrix we may express the scattering lengths

and reaction amplitudes as defined in (5.2) and (5.3)

in terms of the K-matrix elements as follows

$$A_0 = K_{\bar{K}\bar{K}}^{\,o} + \frac{i}{\Delta_0}\, q_\Sigma \left(K_{\bar{K}\Sigma}^{\,o}\right)^2$$

$$M_0 = \frac{1}{\Delta_0}\, K_{\bar{K}\Sigma}^{\,o} \tag{5.4}$$

where

$$\Delta_0 = 1 - i q_\Sigma\, K_{\Sigma\Sigma}^{\,o}$$

And

$$A_1 = K_{\bar{K}\bar{K}}' + \frac{1}{\Delta_1}\Big\{ q_\Sigma q_\Lambda \big[(K_{\bar{K}\Sigma}')^2 K_{\Lambda\Lambda}' + (K_{\bar{K}\Lambda}')^2 K_{\Sigma\Sigma}'$$
$$- 2 K_{\bar{K}\Sigma}' K_{\bar{K}\Lambda}' K_{\Sigma\Lambda}' \big] + i\big[q_\Sigma (K_{\bar{K}\Sigma}')^2 + q_\Lambda (K_{\bar{K}\Lambda}')^2 \big]\Big\} \tag{5.5}$$

$$M_1 = K_{\bar{K}\Sigma}' + \frac{i}{\Delta_1}\, q_\Lambda \left(K_{\bar{K}\Lambda}' K_{\Sigma\Lambda}' - K_{\bar{K}\Sigma}' K_{\Lambda\Lambda}' \right)$$

$$N_1 = K_{\bar{K}\Lambda}' + \frac{i}{\Delta_1}\, q_\Sigma \left(K_{\bar{K}\Sigma}' K_{\Sigma\Lambda}' - K_{\bar{K}\Lambda}' K_{\Sigma\Sigma}' \right)$$

where

$$\Delta_1 = 1 + q_\Lambda q_\Sigma \big[(K_{\Sigma\Lambda}')^2 - K_{\Sigma\Sigma}' K_{\Lambda\Lambda}' \big] - i\left(q_\Sigma K_{\Sigma\Sigma}' + q_\Lambda K_{\Lambda\Lambda}' \right)$$

and q_Λ and q_Σ are the $\Lambda\pi$ and $\Sigma\pi$ centre of mass momenta

respectively.

Using (5.4) and (5.5) together with (5.2) and

(5.3) the isospin amplitudes may be computed from the

K-matrix parameters of (5.1). We now derive the

expressions for the experimentally measured cross

sections.

Using (2.35) the initial K^-p scattering state may

be written in the form

$$|K^-p\rangle = \frac{1}{\sqrt{2}} \left\{ |a_0\rangle + |a_1\rangle \right\} \tag{5.6}$$

After this state becomes $T|K^-p\rangle$ where

$$T|K^-p\rangle = \frac{1}{\sqrt{2}} \left\{ T^0_{\bar{K}\bar{K}} |a_0\rangle + T^0_{\bar{K}\Sigma} |b_0\rangle + T'_{\bar{K}\bar{K}} |a_1\rangle + T'_{\bar{K}\Sigma} |b_1\rangle + T'_{\bar{K}\Lambda} |c_1\rangle \right\}$$

Using (2.35) again this may be written

$$T|K^-p\rangle = \frac{1}{2} \left\{ \left(T^0_{\bar{K}\bar{K}} + T'_{\bar{K}\bar{K}} \right) |K^-p\rangle + \left(-T^0_{\bar{K}\bar{K}} + T'_{\bar{K}\bar{K}} \right) |\bar{K}^0 n\rangle \right\}$$

$$+ \left(\frac{1}{\sqrt{6}} T^0_{\bar{K}\Sigma} + \frac{1}{2} T'_{\bar{K}\Sigma} \right) |\Sigma^+\pi^-\rangle + \left(\frac{1}{\sqrt{6}} T^0_{\bar{K}\Sigma} - \frac{1}{2} T'_{\bar{K}\Sigma} \right) |\Sigma^-\pi^+\rangle \tag{5.7}$$

$$- \frac{1}{\sqrt{6}} T^0_{\bar{K}\Sigma} |\Sigma^0\pi^0\rangle + T'_{\bar{K}\Lambda} |\Lambda\pi^0\rangle$$

Using this equation together with (5.2) and (5.3) the

scattering matrix for the experimentally observed

processes may be obtained. Hence by (2.27) the total

cross sections for pure S-wave scattering may be

written down as

$$\tag{5.8}$$

$$\sigma_{K^-p} = 4\pi \left| \frac{\frac{1}{2}(A_1 + A_0) - ikA_0 A_1}{(1 - ikA_0)(1 - ikA_1)} \right|^2$$

$$\sigma_{\bar{K}^0 n} = 4\pi \left| \frac{\frac{1}{2}(A_1 - A_0)}{(1 - ikA_0)(1 - ikA_1)} \right|^2$$

$$\sigma_{\Sigma^+ \pi^-} = \frac{4\pi q}{k}\varepsilon \left| \frac{1}{\sqrt{6}} \frac{M_0}{(1 - ikA_0)} + \frac{1}{2} \frac{M_1}{(1 - ikA_1)} \right|^2$$

$$\sigma_{\Sigma^- \pi^+} = \frac{4\pi q}{k}\varepsilon \left| \frac{1}{\sqrt{6}} \frac{M_0}{(1 - ikA_0)} - \frac{1}{2} \frac{M_1}{(1 - ikA_1)} \right|^2$$

$$\sigma_{\Sigma^0 \pi^0} = \frac{4\pi q}{k}\varepsilon \left| \frac{1}{\sqrt{6}} \frac{M_0}{(1 - ikA_0)} \right|^2$$

$$\sigma_{\pi^0} = \frac{4\pi q}{k}\wedge \left| \frac{1}{\sqrt{2}} \frac{N_1}{(1 - ikA_1)} \right|^2 \qquad (5.8)$$

The charge corrections may now readily be introduced by the rules of Appendix 1.

(1) The replacement of the following factors as shown:

$$\frac{1}{1-ikA_0} \longrightarrow \frac{1-ik_0A_1}{D} \quad ; \quad \frac{1}{1-ikA_1} \longrightarrow \frac{1-ik_0A_0}{D}$$

where $D = 1 - \frac{1}{2}(A_0+A_1)\left\{k_0+kC_0^2(1-i\lambda)\right\} - k_0 kC_0^2(1-i\lambda)A_0A_1$

and

$$\lambda = -\frac{2}{kBC_0^2}\left\{\ln(2kR) + Re\,\psi\left(\frac{i}{kB}\right) + 2\gamma\right\}$$

B is the Bohr radius for the K^-p system which is given in terms of the reduced mass μ for the K^-p system as

$$B = \frac{\hbar^2}{\mu e^2} = 84\,fm.$$

R is the radius at which the nuclear and Coulomb wave functions are matched and is taken here as R = 0.4 fm. The fits are in fact found to be insensitive to any interaction radius $\lesssim$ 1 fm.

γ is Euler Constant.

The S-wave Coulomb penetration factor C_0 is given by

$$C_0^2 = \frac{2\pi}{kB}\left[1-exp\left(-\frac{2\pi}{kB}\right)\right]^{-1}$$

(2) Every time the K^-p state occurs the amplitude must be multiplied by the S-wave Coulomb penetration factor C_0.

It is convenient at this stage to introduce the total absorption cross sections for the I=0 and I=1 reactions

$$\sigma_0 = \frac{4\pi q_\Sigma}{k} \left| T_{\bar{K}\Sigma}^{\circ} \right|^2 = \frac{4\pi b_0}{k} \left| \frac{1 - ik_0 A_1}{D} \right|^2$$

$$\sigma_1 = \frac{4\pi q_\Sigma}{k} \left| T_{\bar{K}\Sigma}' \right|^2 + \frac{4\pi q_\Lambda}{k} \left| T_{\bar{K}\Lambda}' \right|^2 = \frac{4\pi b_1}{k} \left| \frac{1 - ik_0 A_0}{D} \right|^2 \quad (5.9)$$

where we have written $A_I = a_I + ib_I$ with a_I and b_I

real and we have used the optical theorem to give

$$b_0 = q_\Sigma |M_0|^2$$
$$b_1 = q_\Sigma |M_1|^2 + q_\Lambda |N_1|^2$$

Finally it is convenient to define the quantity

as the ratio between Λ production and total $I=1$

hyperon production and the angle ϕ as the relative

phase between the $I=0$ and $I=1$ $\Sigma\pi$ production amplitudes.

Thus

$$\epsilon = \frac{\sigma(\Lambda\pi^0)}{\sigma^{I=1}(\text{All hyperons})} = \frac{q_\Lambda |N_1|^2}{q_\Sigma |M_1|^2 + q_\Lambda |N_1|^2}$$

And

$$\phi = \text{Arg}\left[\frac{T_{\bar{K}\Sigma}^{\circ}}{T_{\bar{K}\Sigma}'} \right] = \text{Arg}\left[\frac{M_0}{M_1} \right] + \text{Arg}\left[\frac{1 - ik_0 A_1}{1 - ik_0 A_0} \right] \quad (5.10)$$

In terms of these quantities the K^-p S-wave cross

sections, corrected for Coulomb and mass difference

effects, may be written

$$\frac{d\sigma_{\bar{K}p}}{d\Omega} = \left| \frac{\text{cosec}^2 \frac{\theta}{2}}{2Bk^2} \exp\left[\frac{2i}{kB} \ln \sin\frac{\theta}{2} \right] + \frac{C_0^2}{2} \frac{A_0 + A_1 - 2ik_0 A_0 A_1}{D} \right|^2$$

(where we have included the Coulomb scattering term,

cf. Appendix 1).

$$\sigma_{\bar{K}^0n} = \frac{\pi k_0 C_0^2}{k} \left| \frac{A_1 - A_0}{D} \right|^2$$

$$\sigma_{\Sigma^+\pi^-} = \left\{ \frac{1}{6}\sigma_0 + \frac{1}{4}(1-\epsilon)\sigma_1 - \sqrt{\frac{1}{6}\sigma_0\sigma_1(1-\epsilon)}\cos\phi \right\} C_0^2$$

$$\sigma_{\Sigma^-\pi^+} = \left\{ \frac{1}{6}\sigma_0 + \frac{1}{4}(1-\epsilon)\sigma_1 + \sqrt{\frac{1}{6}\sigma_0\sigma_1(1-\epsilon)}\cos\phi \right\} C_0^2 \qquad (5.11)$$

$$\sigma_{\Sigma^0\pi^0} = \frac{1}{6}\sigma_0 C_0^2$$

$$\sigma_{\Lambda\pi^0} = \frac{1}{2}\sigma_1\epsilon C_0^2$$

We now derive the $K_2^0 p$ scattering amplitudes and cross sections.

Using (3.49) for the $|K_2^0\rangle$ state we may write

$$|K_2^0 p\rangle = \frac{1}{\sqrt{2}} \left\{ |K^0 p\rangle - |\bar{K}^0 p\rangle \right\} \qquad (5.12)$$

Following (2.34) and (2.35) this may be decomposed into the isospin wave functions

$$|K_2^0 p\rangle = \frac{1}{\sqrt{2}} \left\{ \frac{1}{\sqrt{2}} \left[|I=1\ S=1\rangle + |I=0\ S=1\rangle \right] - |a_1\rangle \right\} \qquad (5.13)$$

Once again the state after scattering may be computed to give

$$T|K_2^0 p\rangle = \frac{1}{\sqrt{2}} \left\{ \frac{1}{\sqrt{2}} \left[T_{KK}^1 |I=1\ S=1\rangle + T_{KK}^0 |I=0\ S=1\rangle \right] \right.$$
$$\left. - T_{\bar{K}\bar{K}}^1 |a_1\rangle - T_{\bar{K}\Sigma}^1 |b_1\rangle - T_{\bar{K}\Lambda}^1 |c_1\rangle \right\}$$

where K labels the KN isospin channels.

Using (2.34), (2.35) and (3.49) this may be decomposed into the experimentally observed scattering

tates.

$$T|K_1^0 p\rangle = \frac{1}{2}\left\{\frac{1}{2}(T'_{KK}+T^0_{KK})+T'_{\bar{K}\bar{K}}\right\}|K_1^0 p\rangle$$
$$+\frac{1}{2}\left\{\frac{1}{2}(T'_{KK}+T^0_{KK})-T'_{\bar{K}\bar{K}}\right\}|K_1^0 p\rangle \qquad (5.14)$$
$$+\frac{1}{2\sqrt{2}}(T^0_{KK}-T'_{KK})|K^+ n\rangle$$
$$-\frac{1}{2}T'_{\bar{K}\Sigma}|\Sigma^0\pi^+\rangle+\frac{1}{2}T'_{\bar{K}\Sigma}|\Sigma^+\pi^0\rangle$$
$$-\frac{1}{\sqrt{2}}T'_{\bar{K}\Lambda}|\Lambda\pi^+\rangle$$

As mentioned in the previous chapter the low

energy isospin zero KN amplitude has been analysed by

Stenger et al.[28] who find that the low energy S wave

amplitude may be adequately described by a scattering

length parameterisation with scattering length $d_0 = 0.04$ fm.

They also find significant amounts of P-waves and obtain

two solutions for the P-wave scattering lengths

$d_{0_{1-}}$, $d_{0_{1+}}$ the ambiguity in these solutions

corresponding to the Fermi-Yang ambiguity. These

solutions are

$$\alpha_{0_{1-}} = 0.11 \text{ fm}. \qquad \alpha_{0_{1+}} = 0.01 \text{ fm}. \qquad \text{Yang}$$
$$\alpha_{0_{1-}} = -0.02 \text{ fm}. \qquad \alpha_{0_{1+}} = 0.08 \text{ fm} \qquad \text{Fermi}$$

and we have adopted the notation of subscripts 1-, 1+

referring to P-wave amplitudes with $J=\frac{1}{2},\frac{3}{2}$ respectively.

The isospin one KN amplitude may be described

by a pure S-wave scattering length parameterisation and

we use the Goldhaber et al. solution namely

$$d_1 = \left[-\frac{1}{0.29} + 0.25 k^2 \right]^{-1} fm.$$

where d_1 is the S wave scattering length.

Using these parameterisations for the S = +1

amplitudes and applying the optical theorem we

obtain the $K_2^0 p$ total cross section as

$$\sigma_{tot}(K_2^0 p) = \frac{4\pi}{k} \left[\frac{1}{2} \left\{ \frac{1}{2} \mathcal{I}m \left(T_{KK}' + T_{KK}^0 \right) + \mathcal{I}m T_{\bar{K}\bar{K}}' \right\} \right]$$

$$= 2\pi \left[\frac{1}{2} \left\{ \frac{d_0^2}{1+k^2 d_0^2} + \frac{d_1^2}{1+k^2 d_1^2} + \frac{2 k^4 d_0^2}{1+k^6 d^2}_H \right. \right.$$

$$\left. \left. + \frac{k^4 d_0^2}{1+k^6 d^2}_{1-} \right\} + \frac{b_1/k + a_1^2 + b_1^2}{(1+kb_1)^2 + (ka_1)^2} \right] \qquad (5.15)$$

For the remaining $K_2^0 p$ cross sections we have

$$\sigma(K_2^0 p \to K_1^0 p) = \pi \left| \frac{1}{2} \left(T_{KK}^0 + T_{KK}' \right) - T_{\bar{K}\bar{K}}' \right|^2$$

$$= \pi \left| \frac{1}{2} \left\{ \frac{d_0}{1-ikd_0} + \frac{d_1}{1-ikd_1} \right\} - \frac{A_1}{1-ikA_1} \right|^2 \qquad (5.16)$$

$$\sigma(K_2^0 p \to \Sigma^0 \pi^+) = \pi \frac{q_\Sigma}{k} \left| \frac{M_1}{1-ikA_1} \right|^2$$

$$\sigma(K_2^0 p \to \Lambda \pi^+) = \pi \frac{q_\Lambda}{k} \left| \frac{N_1}{1-ikA_1} \right|^2$$

It should be noted that for the $K_0^2 p$ interaction

there is no Coulomb force, and moreover, there is

no mass correction necessary, the momentum k here

referring to the K_2^0 centre of mass momenta.

Experimentally the $K_2^0 p$ cross sections are given in terms of the two ratios R and $\in$ which are defined

by
$$R = \frac{\sigma(K_2^0 p \rightarrow K_1^0 p)}{\sigma(K_2^0 p \rightarrow \Lambda \pi^+) + 2\sigma(K_2^0 p \rightarrow \Sigma^0 \pi^+)}$$

and
$$\in = \frac{\sigma(K_2^0 p \rightarrow \Lambda \pi^+)}{\sigma(K_2^0 p \rightarrow \Lambda \pi^+) + 2\sigma(K_2^0 p \rightarrow \Sigma^0 \pi^+)} \qquad (5.17)$$

R may be calculated using (5.16) whilst $\in$ is conveniently computed in the form

$$\in = \frac{q_\Lambda |N_1|^2}{q_\Sigma |M_1|^2 + q_\Lambda |N_1|^2} \qquad (5.18)$$

(iii) Details of the Zero range fit

The nine zero range parameters of (5.1) were used to predict the experimentally observed quantities and hence the χ^2 function was computed (cf. Appendix 3).

$$\chi^2(\kappa) = \sum_i (C_i - O_i)^2 (E_i)^{-2} \qquad (5.19)$$

where C_i is the value for measurement i predicted using the K-matrix elements of (5.1), O_i is the experimental value for i and E_i the experimental error on the measurement. Here we have assumed the experimental results statistically independent as the full error matrix E_{ij} is not generally quoted in the

experimental results. The experimental data used
consisted of all that available for the cross sections
of (5.11), (5.15), (5.16) in the momentum range
0-280 Mev/c for the K^-p and $K_2^0 p$ processes as discussed
in Chapter 2 (cf. refs.(E1-E7,E11)).

In the search of parameter space in order to
find the minima of the χ^2 function the general min-
imising program VAO4A was used. This routine requires
a starting set of values for the parameters and from
there proceeds to a minimum by a step procedure.
Care must therefore be taken to ensure that a
sufficiently complete set of starting values are
tried in order to find all the minima of the χ^2
function. This was done in the present analysis.

From the search of parameter space a unique
solution was found which gives a good fit to the data.
The values of the K-matrix elements are given in
Table (5.1) and the error matrix for this solution
is given in Table (5.2). The total number of data
points used was 194 and the corresponding value of
was 168 giving a confidence level of 91% in the fit.
In Table (5.3) we list the contributions to χ^2 from
the various data points.

From equations (5.11), (5.15) and (5.16) it
is apparent that only the six quantities a_o, b_o, a_1,
b_1, ϵ and ϕ are necessary to give the experimentally
observed data at any energy, and that it is the energy
variations of these quantities which determine the full
nine-K-matrix parameters. Accordingly, as a test
of the validity of using the full K-matrix parameterisa-
tion, a new fit the data was performed using these
parameters. It was found that a fit to the data
was obtained, which could be improved by including
effective range terms on the scattering lengths. The
fit obtained using the six zero range parameters had
a value for χ^2 of 180 for 188 degrees of freedom. In
general the fit was good but the branching ratio $\dfrac{(\sigma_{\Sigma^-} + \sigma_{\Sigma^+})}{(\sigma_{\Sigma^0} + \sigma_{\Lambda})}$
was badly predicted due to the absence of energy dependence
in the parameter ϵ. It is evident from a comparison of
the values of χ^2 that statistically the fit is improved
by going to the zero range K-matrix parameterisation
and, it is found, the prediction of the ratio $\dfrac{(\sigma_{\Sigma^-} + \sigma_{\Sigma^+})}{(\sigma_{\Sigma^0} + \sigma_{\Lambda})}$
is considerably improved due to the energy dependence
(5.10) of the quantity ϵ. Thus it may be concluded
that the data can accomodate the nine zero range K
matrix parameters. The parameterisation

was then tested against the increase in the number of
parameters by adding effective range terms to the
series expansion of (3.17). The formalism of section
(ii) may be used for this parameterisation by first
computing the nine K-matrix elements of (5.1), which
will now be energy dependent, via equation (3.17) in
which certain of the elements of the effective range
matrix are now non zero. No solution was found which
statistically improved the fit and although the
effective range terms were badly determined, no solution
was found with large effective ranges   which changed
the character of the solution. We conclude that the
zero range parameterisation is sufficient to describe
the data below 280 Mev/c. It should be noted that, as
the quantities a_o, b_o, a_1, b_1, ϵ, ϕ, which are
determined by the data via (5.11), give only the
magnitude and relative sign of M_o and M_1 and the magnitude
of N_1 there is an ambiquity in the sign of some of
the K-matrix elements. From (5.4) and (5.5) it may
be seen that these quantities, and consequently the
fit to the data, are unchanged under the replacement

$$K'_{\bar{K}\Lambda} \rightarrow -K'_{\bar{K}\Lambda} \qquad K'_{\Sigma\Lambda} \rightarrow -K'_{\Sigma\Lambda}$$

and also under the replacement

$$K_{\bar{K}\ell}^{o} \rightarrow -K_{\bar{K}\ell}^{o} \qquad K_{\bar{K}\ell}^{'} \rightarrow -K_{\bar{K}\ell}^{'} \qquad K_{\Sigma\Lambda}^{'} \rightarrow -K_{\Sigma\Lambda}^{'}$$

These ambiguities in sign will probably not be resolved until accurate$_\wedge^{\Sigma\pi}$differential cross section data becomes available to determine the sign of the Coulomb interference term.

In Figures (5.1a) - (5.1h) we show the fits, labelled ZR, to some of the data using this zero range solution. For comparison we also show the curves, labelled KK, calculated from Kim's K-matrix fit. In showing the fit to the ratio R, Fig. (5.1e), the two curves corresponding to the use of the Yang or the Fermi solution for the S = +1 P-waves are not shown as the difference between them over the energy range of interest is very small. Only the Yang solution is drawn.

It should be mentioned here that a zero range nine parameter fit, similar to the one presented here has recently been performed by Martin and Sakitt[55]. However they do not use the $K_2^{o}p$ and $K^{-}p$ data of refs. (E6, E11). We do not find that their parameters give an acceptable fit to the data. The main reason is that the value of ϵ, obtained from their parameters

is significantly larger than that found in our fit, and also that of the constant scattering length or Kim's K-matrix fits. In Figures (5.1d) to (5.1g) we show their fits, labelled MS, to the data most affected by this difference. It may be seen that their fit to these data points is very poor. Their fit to the remaining data points does not improve on the present zero range fit and we conclude that their solution is unacceptable.

The comparison of Kim's K-matrix fit and the zero range fit of this analysis shows that both give good agreement with the data involving only the KN and $\Sigma\pi$ channels over the energy range considered. However for processes involving the $\Lambda\pi$ channel there is a marked discrepancy between the fits and it may be seen that the present fit improves on the KK fit over the kaon laboratory momentum range 0-280 Mev/c.

It is of interest to compare the energy dependence of the scattering lengths predicted by the two fits and in Fig. (5.2) this is done. It is apparent from this that the present solution and that of Kim are very different. The continuation of the para-meterisation below the $\bar{K}N$ threshold may be used to

predict the imaginary part of the I=0 $\bar{K}N$ amplitude and this is drawn in Fig. (5.3). Once again the result using Kim's K-matrix parameterisation (**KK**) is drawn and also, for comparison, that using Kim's Constant scattering length fit (CSL). It may be seen that, in agreement with the previous fits, the zero range parameters predict a resonance behaviour in this amplitude. This may be associated with an I = 0 virtual bound state resonance.

The quantity $(1 + |k|K^o_{\bar{K}\bar{K}})$ is found to vanish at the resonant energy, thus satisfying criterion (**3.46**) for a virtual bound state resonance. From an analysis of the predicted $\Sigma\pi$ elastic cross section, the position and width of the resonance may be found. They are

$$E_r = 1420 \text{ Mev} \qquad \Gamma = 20 \text{ Mev}$$

It may be seen from Fig. (5.3) that the contribution to dispersion relations from the unphysical region will be smaller than that given by Kim's K-matrix parameterisation and quite close to the constant scattering length predictions. This is reflected in the application of the new fit to the subtracted dispersion relation of (4.28). In Fig. (5.4) we show the variation of the prediction of g^2_Λ against change of the subtraction

point ω. The details of the calculation were described
in Chapter 4. As mentioned there the errors between
the calculations of g_Λ^2 at adjacent values of ω are
strongly correlated. Using the estimate of this error
given by Martin et al. the best fit constant value of
g_Λ^2 is drawn together with this error in Fig. (5.4).
It may be seen that the values of g_Λ^2 obtained by
the present fit are consistent, within the estimated
error, with a constant value. This may be compared
with the inconsistency suggested for Kim's solution.
As expected the constant scattering length solution
gives similar results for g_Λ^2 as the present fit.
Finally, using the subtracted dispersion relation
(4.28) with $\omega = \omega_0 = m$ which corresponds to the
conventional dispersion relation, the coupling constants
may be evaluated and are given by [35]

$$g_\Lambda^2 = 3.40 \qquad g_\Sigma^2 = 0.88$$

From the discussion of Chapter 4 it is evident that
their prediction for g_Λ^2 is inconsistent with the SU(3)
allowed values.

A feature of the K-matrix parameterisation is
that it enables us to estimate the $\Sigma\pi$ and $\Lambda\pi$ amplitudes
once the K-matrix elements are known. Thus if we

write the complex scattering lengths for the $\Sigma\pi$ amplitude of isospin I as A_Σ^I and that for the $\Lambda\pi$ amplitude as A_Λ^1 we have

$$T_{\Sigma\Sigma}^I = \frac{A_\Sigma^I}{1 - i q_\Sigma A_\Sigma^I}$$

$$T_{\Lambda\Lambda}^1 = \frac{A_\Lambda^1}{1 - i q_\Lambda A_\Lambda^1}$$

(5.20)

By (5.15) we may express these scattering lengths in terms of the K-matrix elements as follows

$$A_\Sigma^0 = K_{\Sigma\Sigma}^0 + \frac{ik(K_{\bar{K}\Sigma}^0)^2}{1 - ik K_{\bar{K}\bar{K}}^0}$$

$$A_\Sigma^1 = K_{\Sigma\Sigma}^1 + \frac{kq_\Lambda}{\Delta_\Sigma}\left\{ \left((K_{\Sigma\Lambda}^1)^2 K_{\bar{K}\bar{K}}^1 + (K_{\bar{K}\Sigma}^1)^2 K_{\Lambda\Lambda}^1 \right.\right.$$

$$\left.\left. - 2 K_{\Sigma\Lambda}^1 K_{\bar{K}\Sigma}^1 K_{\bar{K}\Lambda}^1 \right) + i\left(q_\Lambda (K_{\Sigma\Lambda}^1)^2 + k (K_{\bar{K}\Sigma}^1)^2 \right) \right\}$$

where $\Delta_\Sigma = 1 + k q_\Lambda \left((K_{\bar{K}\Lambda}^1)^2 - K_{\Lambda\Lambda}^1 K_{\bar{K}\bar{K}}^1 \right) - i\left(q_\Lambda K_{\Lambda\Lambda}^1 + k K_{\bar{K}\bar{K}}^1 \right)$ (5.21)

$$A_\Lambda^1 = K_{\Lambda\Lambda}^1 + \frac{kq_\Sigma}{\Delta_\Lambda}\left\{ \left((K_{\bar{K}\Lambda}^1)^2 K_{\Sigma\Sigma}^1 + (K_{\Sigma\Lambda}^1)^2 K_{\bar{K}\bar{K}}^1 \right.\right.$$

$$\left.\left. - 2 K_{\bar{K}\Lambda}^1 K_{\Sigma\Lambda}^1 K_{\bar{K}\Sigma}^1 \right) + i\left(k (K_{\bar{K}\Lambda}^1)^2 + q_\Lambda (K_{\Sigma\Lambda}^1)^2 \right) \right\}$$

where $\Delta_\Lambda = 1 + k q_\Sigma \left((K_{\bar{K}\Sigma}^1)^2 - K_{\bar{K}\bar{K}}^1 K_{\Sigma\Sigma}^1 \right) - i\left(k K_{\bar{K}\bar{K}}^1 + q_\Lambda K_{\Sigma\Sigma}^1 \right)$

Using (5.4), (5.5), (5.20), (5.21) the scattering lengths for the $\bar{K}N$, $\Sigma\pi$ and $\Lambda\pi$ processes are evaluated at the relevant channel thresholds and tabulated in

Table (5.4). For comparison we also list the scattering

lengths obtained by previous analyses (E3, 10, 56).

An independent estimate of $T_{\Lambda\Lambda}{}'$ may be obtained

from the analysis of the weak decay process $\Xi^- \to \Lambda\pi^-$

The characteristics of the decay are usually specified

by the parameter[53]

$$\alpha = 2Re(B_0^* B_1), \quad \beta = 2Im(B_0^* B_1)$$

where B_L is the decay amplitude for a final $\Lambda\pi$ state

of orbital angular momentum L, normalised so that

$$|B_0|^2 + |B_1|^2 = 1.$$

It may be shown that[61], if time-reversal invariance

is assumed to hold in the decay process,

$$\tan(\delta_1 - \delta_0) = \beta/\alpha$$

where δ_0 and δ_1 are, respectively, the $S_{\frac{1}{2}}$ and $P_{\frac{1}{2}}$

scattering phase shifts at the decay energy. If we take

the value $\delta_1 \approx -1.2°$ obtained by Martin[58] using a

dynamical model of $\Lambda\pi$ scattering based on a partial-

wave dispersion relation and use the average values

for α and β obtained by ref(59) we find

$$\delta_0 = +22° \pm 20°$$

which may be compared with the present estimate of

$$\delta_0 = -4.7° \pm 25°$$

and that obtained using Kim's K-matrix fit

$$\delta_0 = 82.3°$$

It should be noted that the errors in predicting
this phase and also in predicting the $\Lambda\pi$ and $\Sigma\pi$
scattering lengths using the K-matrix are very large.
This is because these quantities are obtained
indirectly by analysing the energy dependence of the
various $\bar{K}N$ processes, there being no data for the
elastic $\Lambda\pi$ and $\Sigma\pi$ channels.

$(\text{Fermi})^{+1}$

$K^{0}_{\bar{K}\bar{K}}$	-2.40	± 0.24
$K^{0}_{\bar{K}\Sigma}$	-1.21	± 0.22
$K^{0}_{\bar{\Sigma}\Lambda}$	-1.05	± 0.39
$K^{1}_{\bar{K}\bar{K}}$	-0.014	± 0.15
$K^{1}_{\bar{K}\Sigma}$	-0.71	± 0.06
$K^{1}_{\bar{K}\Lambda}$	-0.38	± 0.06
$K^{1}_{\Sigma\Sigma}$	0.34	± 0.27
$K^{1}_{\Sigma\Lambda}$	-0.21	± 0.86
$K^{1}_{\Lambda\Lambda}$	0.17	± 0.66

Zero range S-wave solution (ZR) TABLE(5.1)

Label	$K^0_{\xi\xi}$	$K^0_{\xi\Sigma}$	$K^0_{\Sigma\Sigma}$	$K'_{\xi\xi}$	$K'_{\xi\Sigma}$	$K'_{\xi\Lambda}$	$K'_{\Sigma\Sigma}$	$K'_{\Sigma\Lambda}$	$K'_{\Lambda\Lambda}$
$K^0_{\xi\xi}$	5.4×10^{-2}								
$K^0_{\xi\Sigma}$	5.1×10^{-2}	4.7×10^{-2}							
$K^0_{\Sigma\Sigma}$	9.2×10^{-1}	8.4×10^{-2}	1.5×10^{-1}						
$K'_{\xi\xi}$	2.2×10^{-2}	2.0×10^{-2}	3.7×10^{-2}	2.2×10^{-2}					
$K'_{\xi\Sigma}$	-1.2×10^{-3}	-9.2×10^{-4}	-1.1×10^{-2}	3.8×10^{-3}	3.8×10^{-3}				
$K'_{\xi\Lambda}$	-2.4×10^{-3}	-2.4×10^{-3}	-5.4×10^{-3}	-4.2×10^{-3}	-3.3×10^{-3}	3.9×10^{-3}			
$K'_{\Sigma\Sigma}$	1.1×10^{-2}	8.9×10^{-3}	1.2×10^{-2}	1.6×10^{-2}	-5.0×10^{-3}	8.7×10^{-3}	7.1×10^{-2}		
$K'_{\Sigma\Lambda}$	4.5×10^{-2}	4.2×10^{-2}	8.0×10^{-2}	4.5×10^{-3}	5.3×10^{-3}	-2.4×10^{-2}	-7.3×10^{-2}	1.3×10^{-1}	
$K'_{\Lambda\Lambda}$	-5.0×10^{-2}	-4.6×10^{-2}	-9.1×10^{-2}	3.4×10^{-2}	8.5×10^{-3}	6.4×10^{-3}	1.4×10^{-2}	-2.1×10^{-1}	4.4×10^{-1}

Variance-Covariance Matrix for the scattering

parameters of Table (5.1)

TABLE (5.2)

Experimental Measurement	Reference	Kaon Lab. Momentum (Mev/c)	χ^2 Contribution	Number of Measurements
$\int_{0.95}^{0.965} \frac{d\sigma_{el}}{d\Omega} \, d\Omega$	E3	100-280	3.9	9
$\int_{0.90}^{0.95} \frac{d\sigma_{el}}{d\Omega} \, d\Omega$	E3	100-280	7.6	9
$\int_{0.85}^{0.90} \frac{d\sigma_{el}}{d\Omega} \, d\Omega$	E3	100-280	3.9	9
$\int_{0.80}^{0.85} \frac{d\sigma_{el}}{d\Omega} \, d\Omega$	E3	100-280	4.2	9
$\int_{0.70}^{0.80} \frac{d\sigma_{el}}{d\Omega} \, d\Omega$	E3	100-280	6.3	9
$\int_{0.60}^{0.70} \frac{d\sigma_{el}}{d\Omega} \, d\Omega$	E3	100-280	5.3	9
$\int_{-0.965}^{0.60} \frac{d\sigma_{el}}{d\Omega} \, d\Omega$	E3	100-280	5.6	9
$\sigma(K^-p \to \bar{K}^0 n)$	E1,E3,E4	100-280	11.7	23
$\sigma(K^-p \to \Sigma^+\pi^-)$	E1,E2,E3	60-280	29.1	30
$\sigma(K^-p \to \Sigma^-\pi^+)$	E1,E2,E3	60-280	49.9	32
$\sigma(K^-p \to \Sigma^0\pi^0) + \sigma(K^-p \to \Lambda\pi^0)$	E1,E3	100-260	4.0	9
$\dfrac{\sigma(K^-p \to \Lambda\pi^0)}{\sigma(K^-p \to \Sigma^0\pi^0) + \sigma(K^-p \to \Lambda\pi^0)}$	E1,E3	100-260	5.9	8
$(\Lambda / \Sigma^0 + \Lambda)$ Branching ratio	E1,E3	0	0.5	2
$(\Sigma^+ + \Sigma^- / \Sigma^0 + \Lambda)$ Branching ratio	E1	0	1.9	1
(Σ^- / Σ^+) Branching ratio	E1,E3	0	1.1	2

Experimental Measurement	Reference	Kaon Lab. Momentum (Mev/c)	Contribution	Number of Measurements
R	E6,E11	170-250	11.3	3
ϵ	E6,E11	170-250	1.9	3
$\sigma_{K^0_2 p}$ total	E7	160-280	6.0	9
$\sigma(K^0_2 p \to \Lambda\pi^+)$	E6,E11	160-280	6.0	6
$\sigma(K^- p \to \Lambda\pi^0)$	E6,E11	230-280	2.1	3
TOTAL			168.2	194

Table(5.3)

Reaction	Isospin	S-Wave Scattering Length	Reference
$\bar{K}N \to \bar{K}N$	0	$(-1.67\pm0.04)+i(0.72\pm0.04)$	E3
$\bar{K}N \to \bar{K}N$	0	$(-1.65\pm0.04)+i(0.73\pm0.02)$	56
$\bar{K}N \to \bar{K}N$	0	$(-1.74\pm0.03)+i(0.70\pm0.02)$	Present Fit
$\bar{K}N \to \bar{K}N$	1	$(0.00\pm0.06)+i(0.69\pm0.03)$	E3
$\bar{K}N \to \bar{K}N$	1	$(-0.13\pm0.02)+i(0.51\pm0.03)$	56
$\bar{K}N \to \bar{K}N$	1	$(-0.05\pm0.02)+i(0.63\pm0.03)$	Present Fit
$\Sigma\pi \to \Sigma\pi$	0	1.09 ± 0.23	56
$\Sigma\pi \to \Sigma\pi$	0	-0.14 ± 0.32	Present Fit
$\Sigma\pi \to \Sigma\pi$	1	$(0.39\pm0.07)+i(0.14\pm0.03)$	56
$\Sigma\pi \to \Sigma\pi$	1	$(-0.31\pm0.15)+i(0.24\pm0.19)$	Present Fit
$\Lambda\pi \to \Lambda\pi$	1	1.75 ± 0.06	19
$\Lambda\pi \to \Lambda\pi$	1	-0.45 ± 0.31	Present Fit

TABLE (5.4)
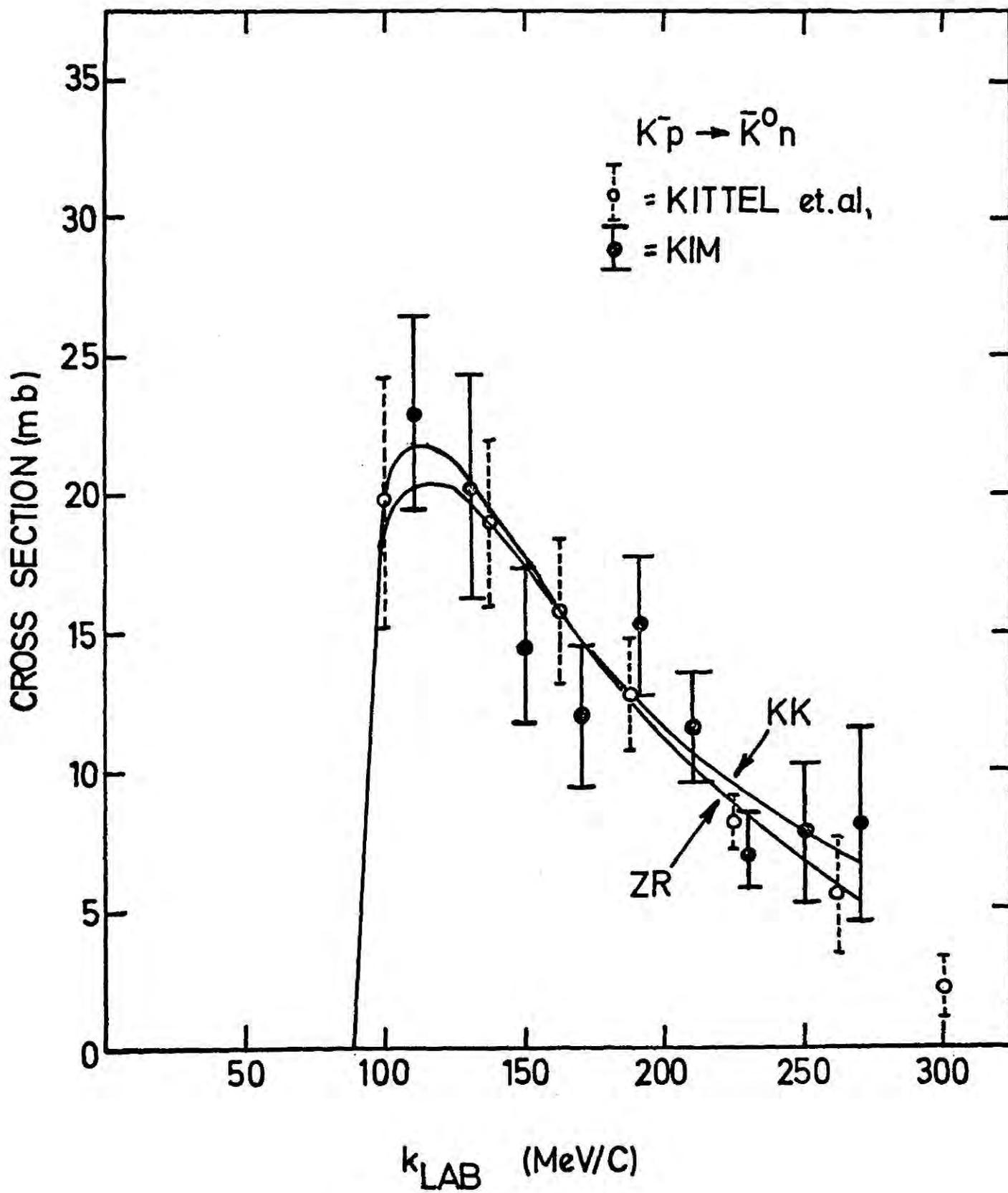
Fig.(5.1) (a)

Fig (5.1 b)

Fig(5.1c)

Fig (5.1d)

Top panel:

$$\epsilon = \frac{\sigma(\pi\Lambda)}{\sigma(\pi Y)}$$

MS

ZR

KK

$E_{c.m.}(Mev)$

Bottom panel:

$$R = \frac{\sigma(K_1^0 p)}{\sigma(\pi Y)}$$

ZR

MS

KK

$E_{c.m.}(Mev)$

Fig(5.1e)

Fig (5.1f)

$\sigma_{tot}(K_L^0 p)$
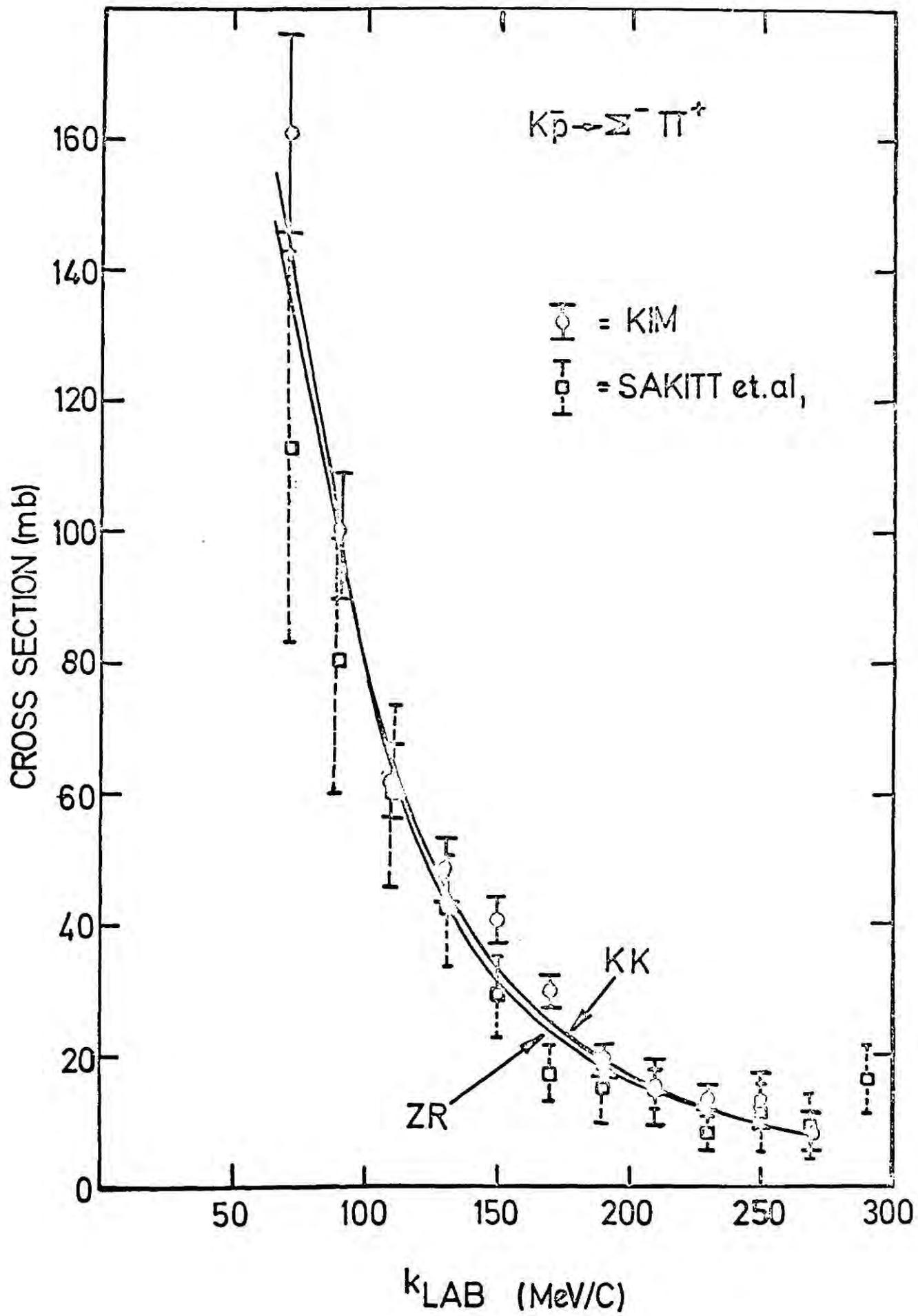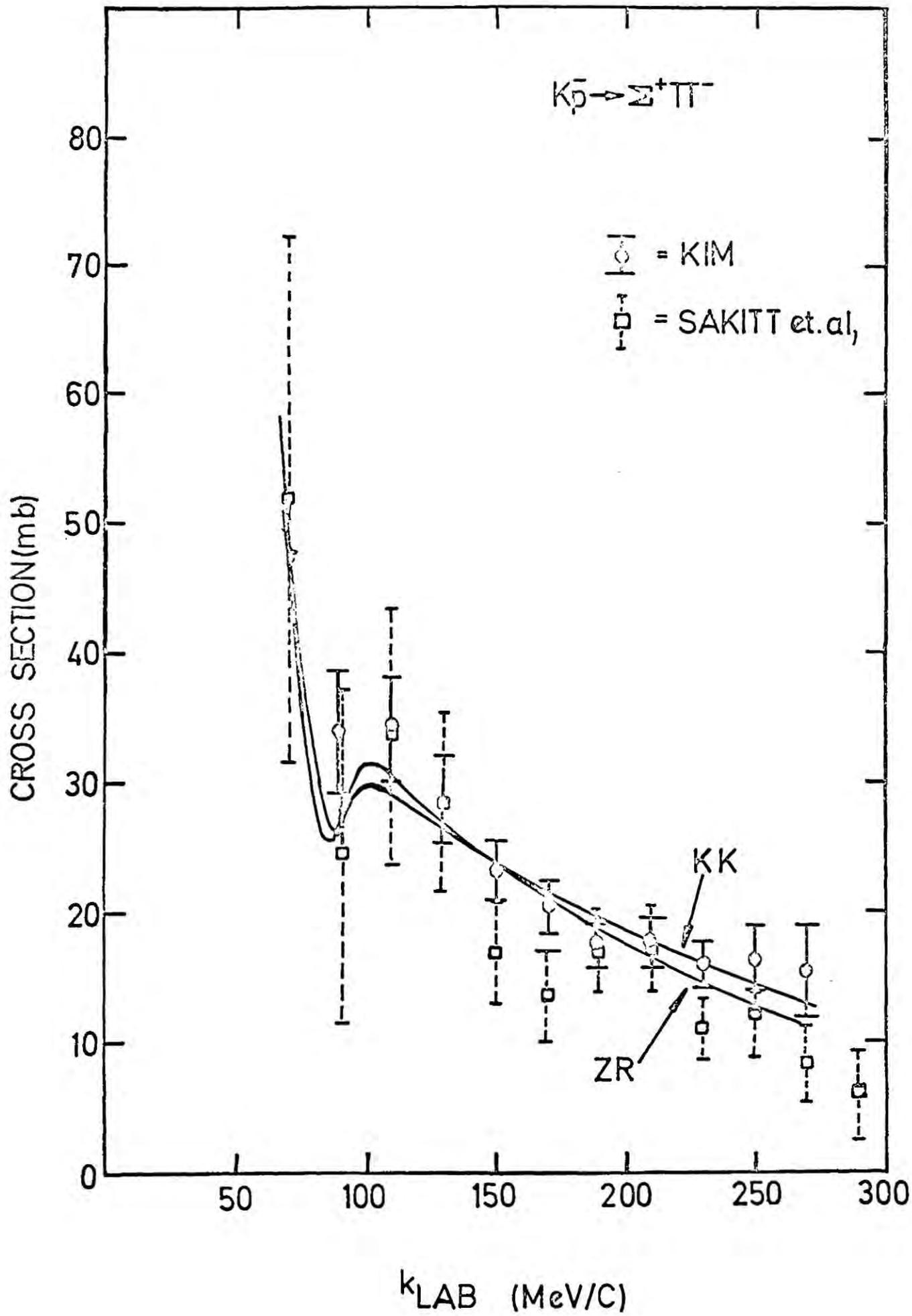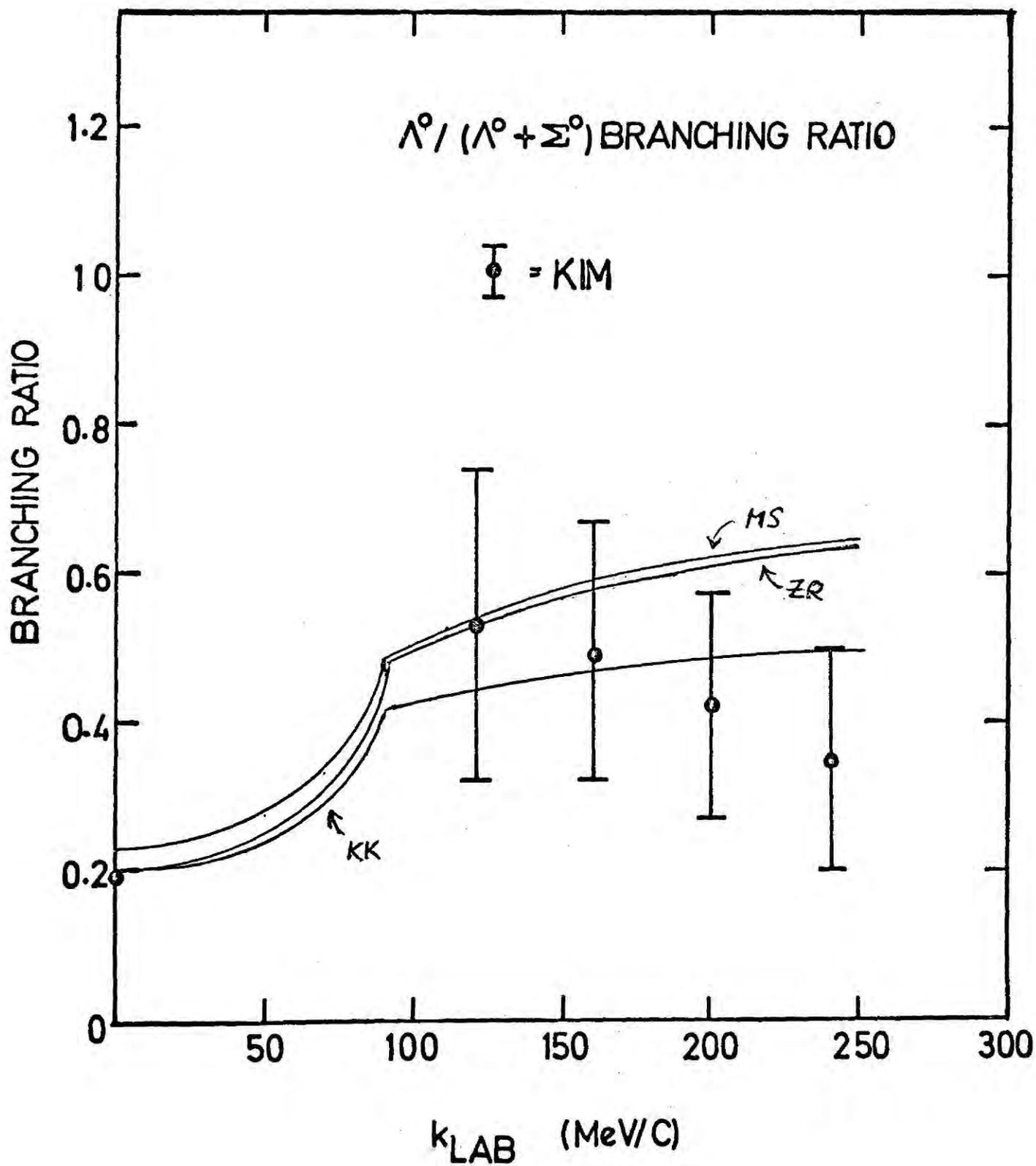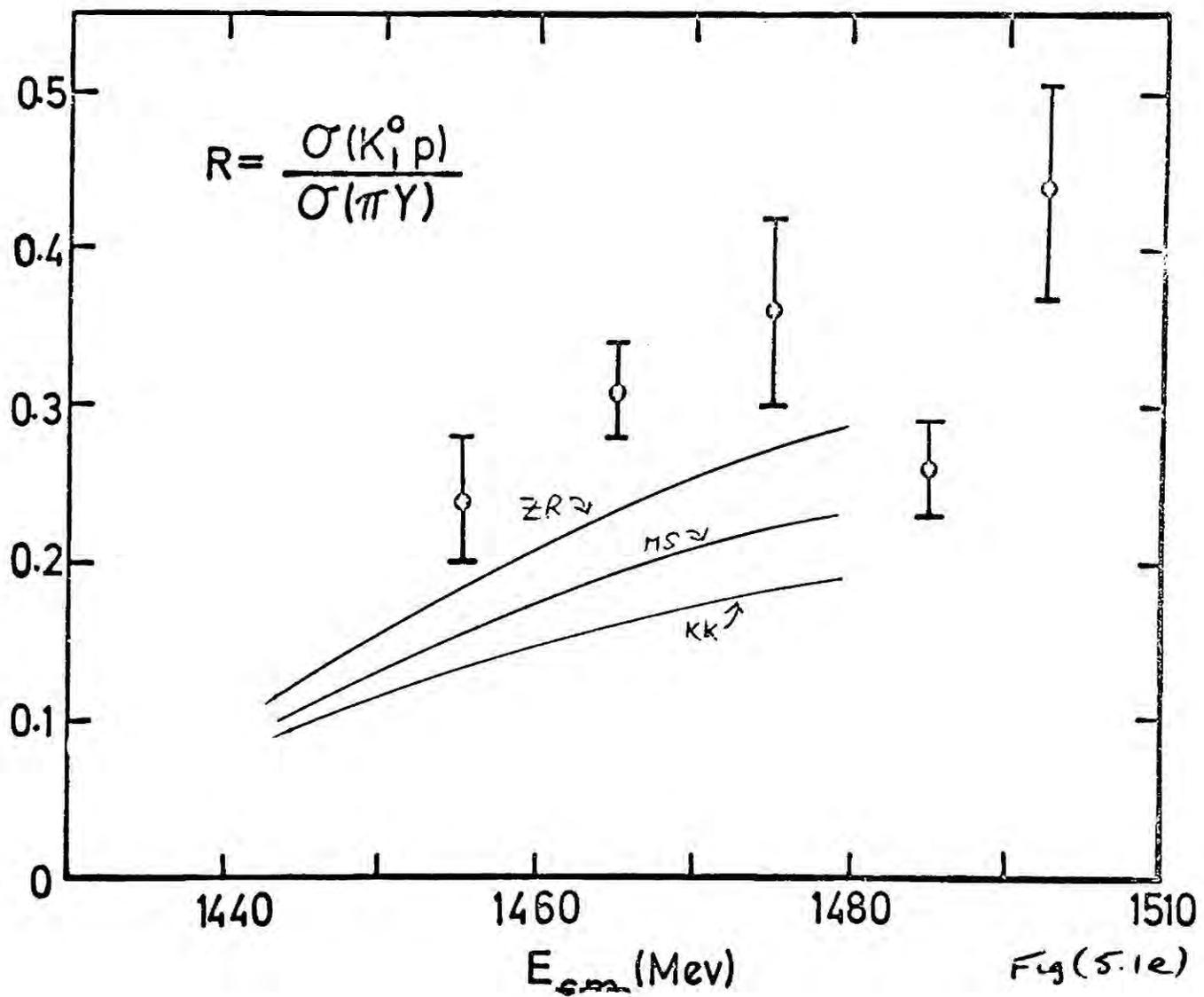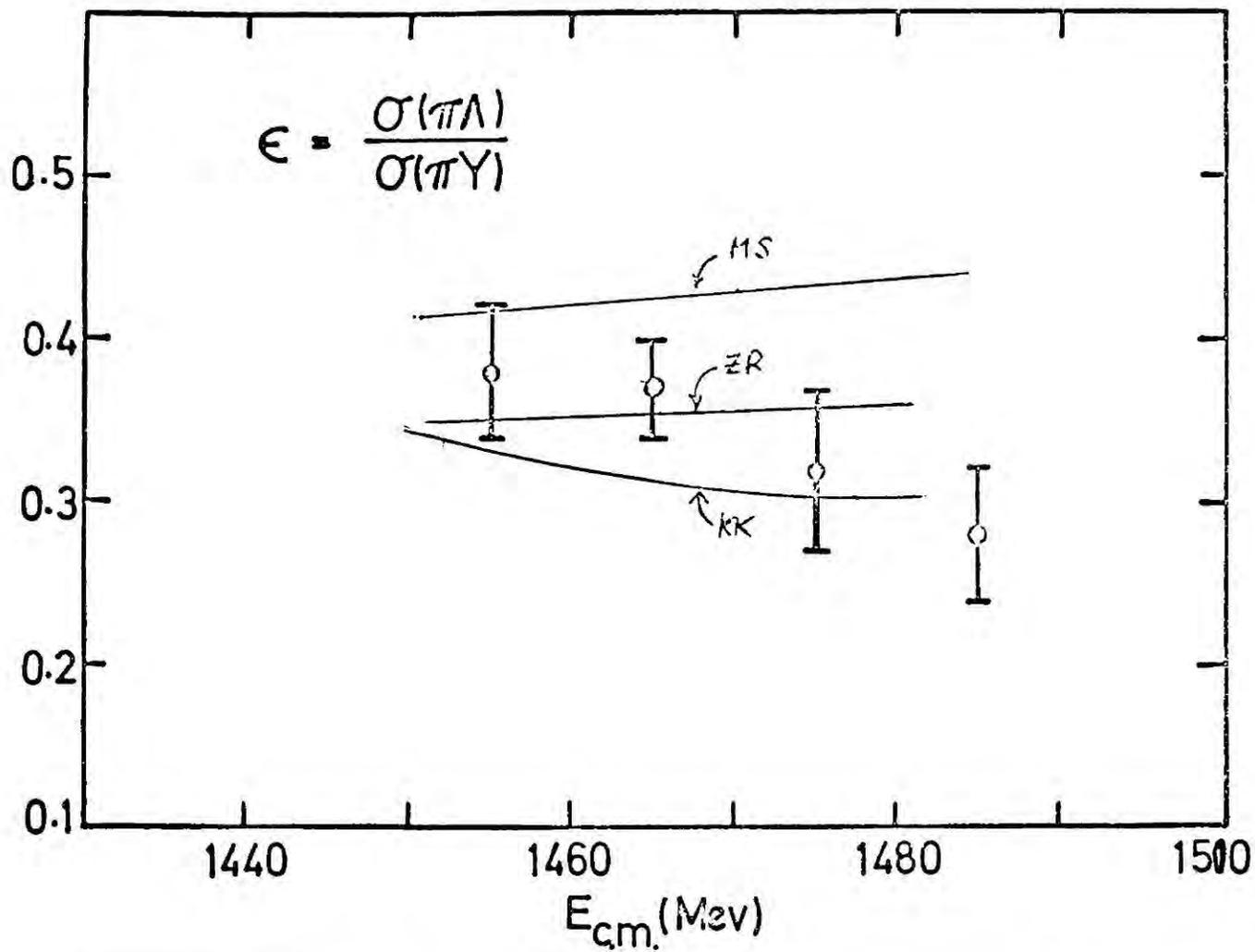
Fig (5.1 g)
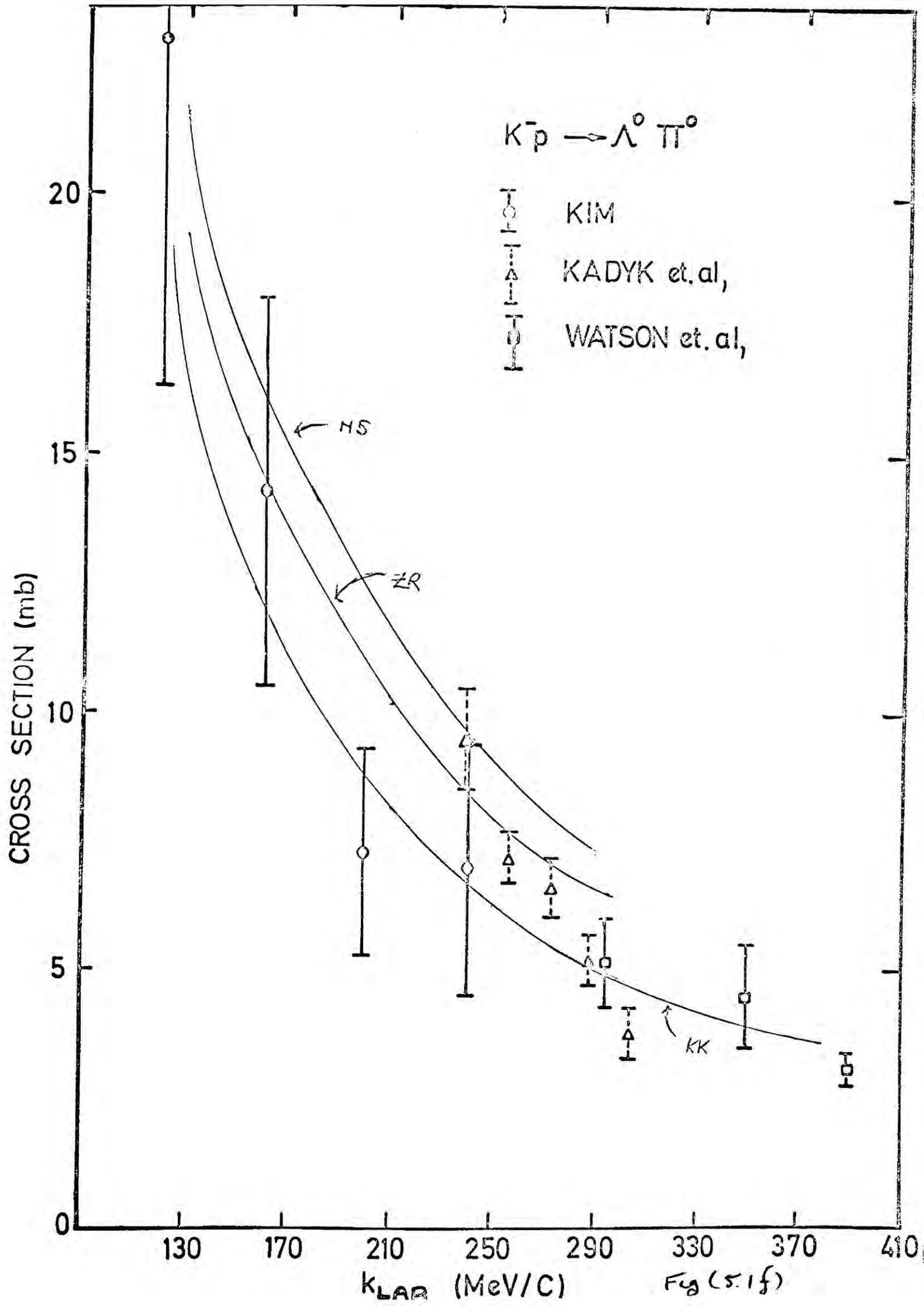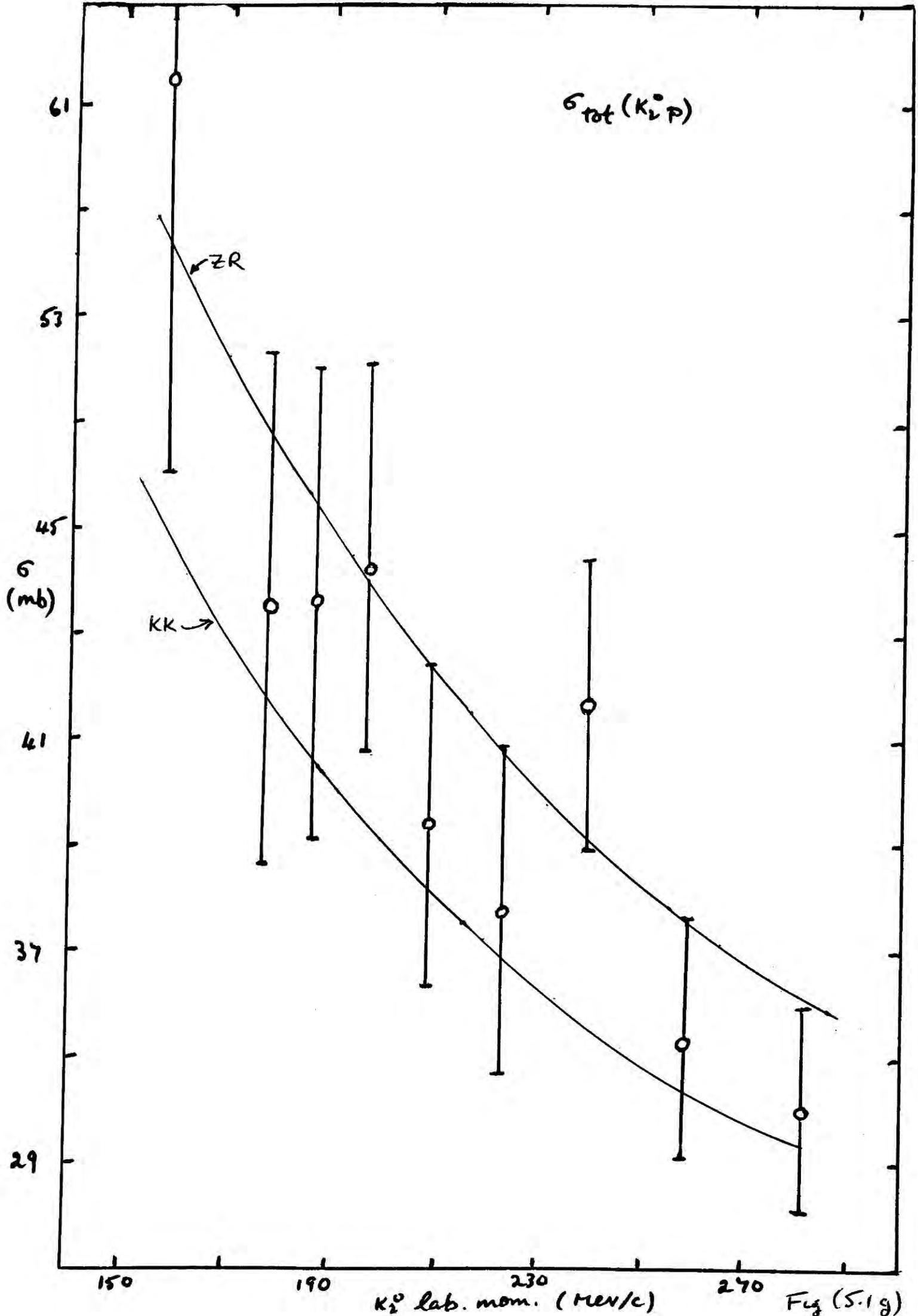
K⁻p ELASTIC DIFFERENTIAL CROSS SECTION.

Fig (5.1h)

Fig (5.2)

Fig (5.3)
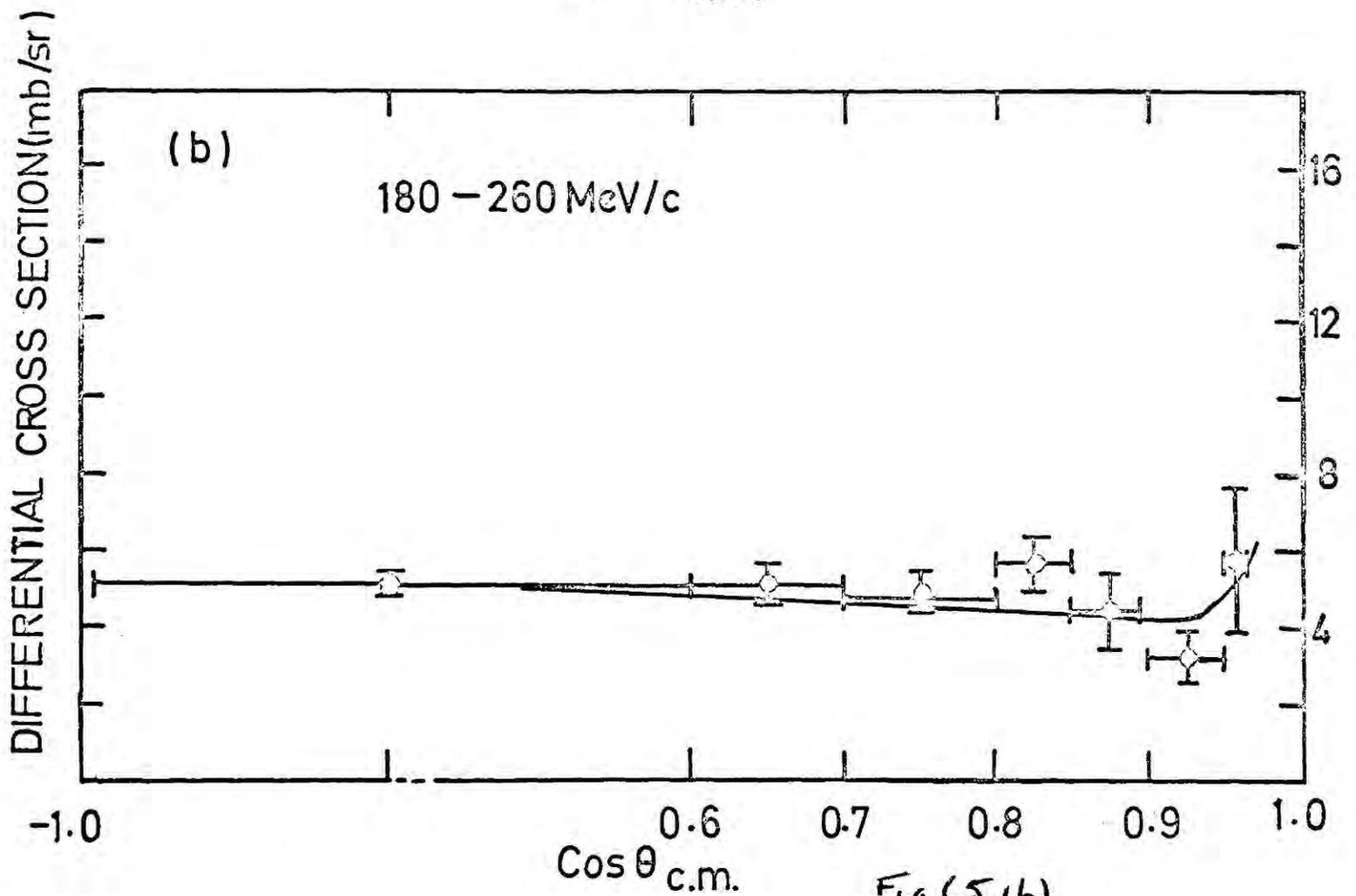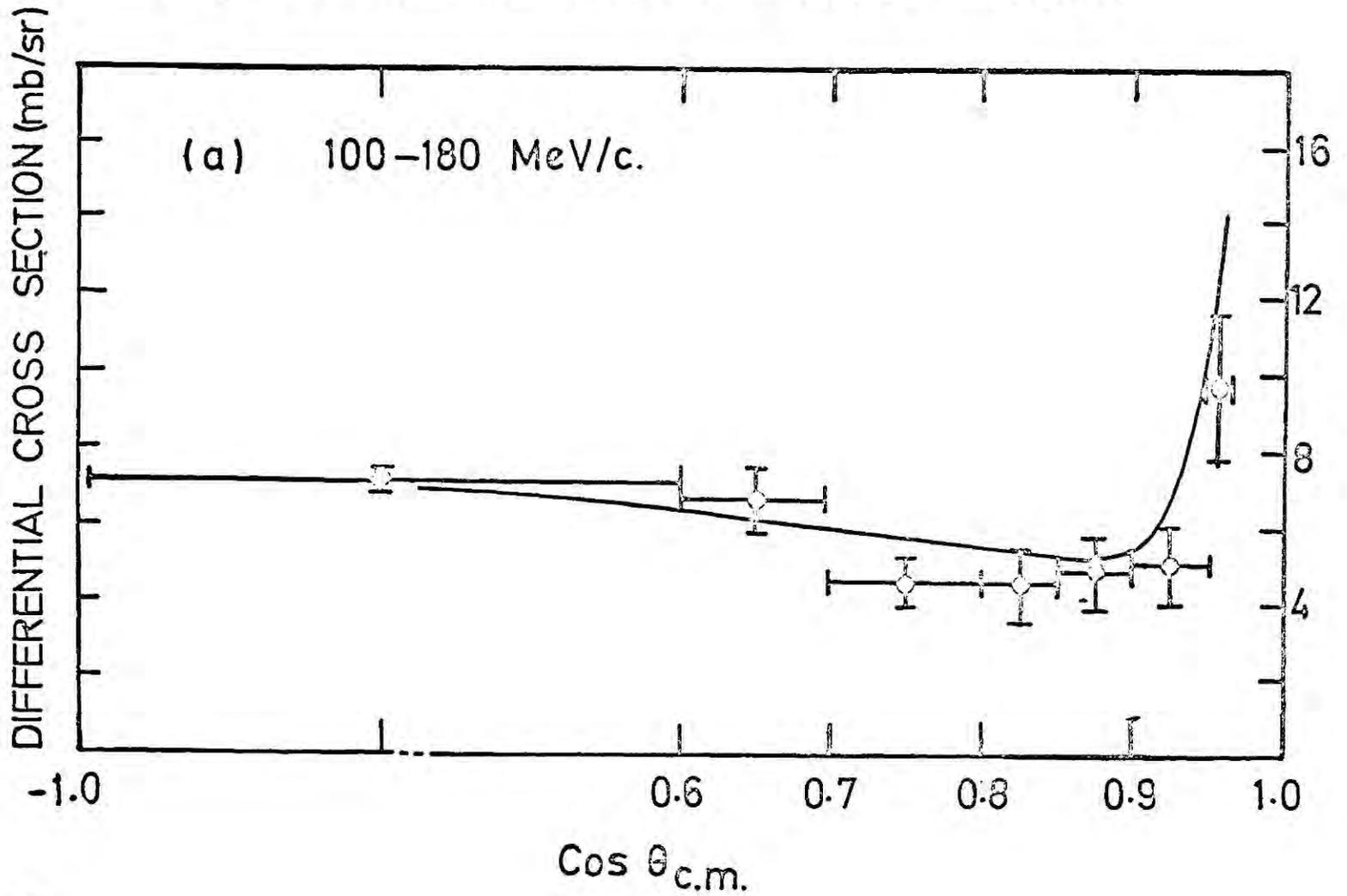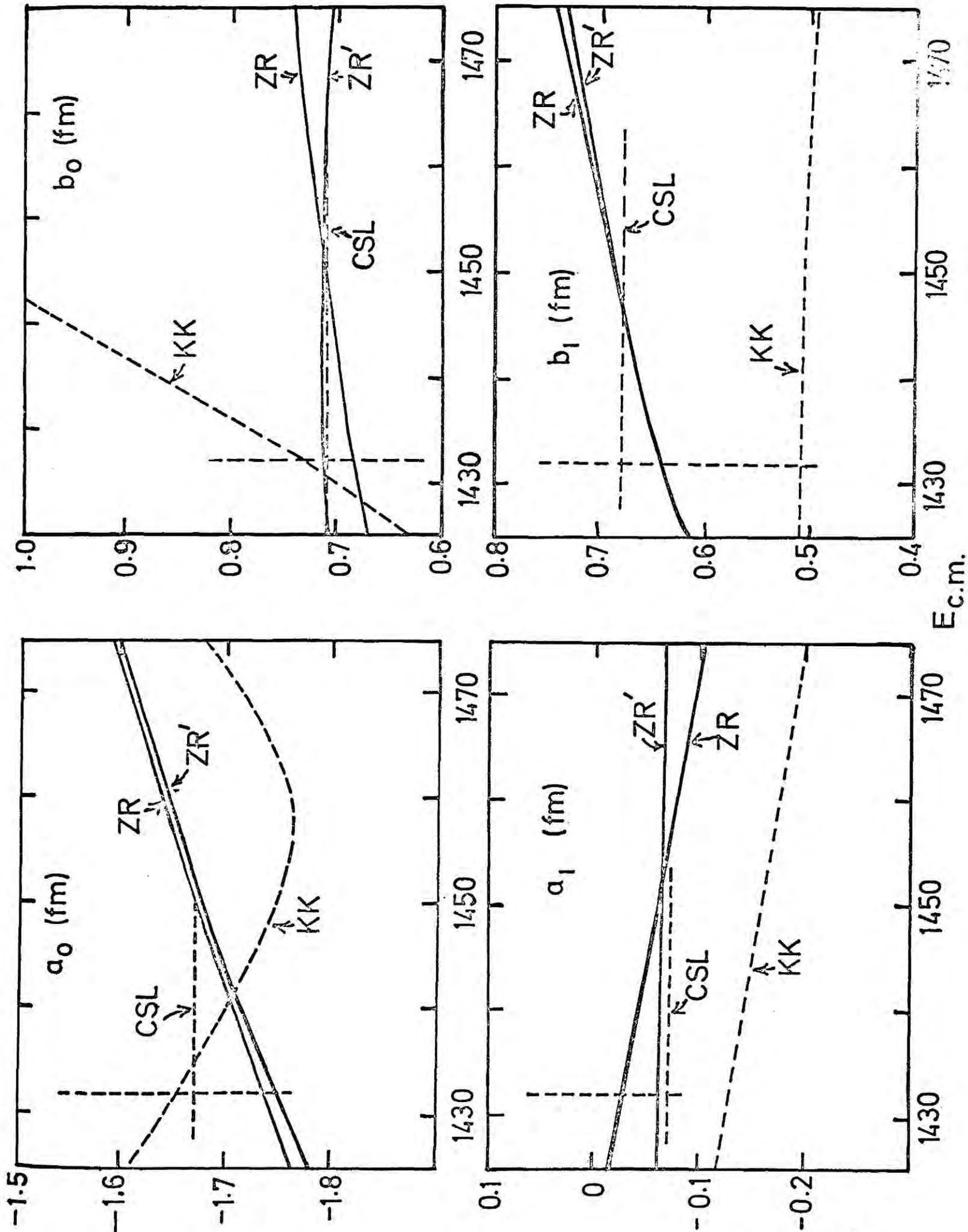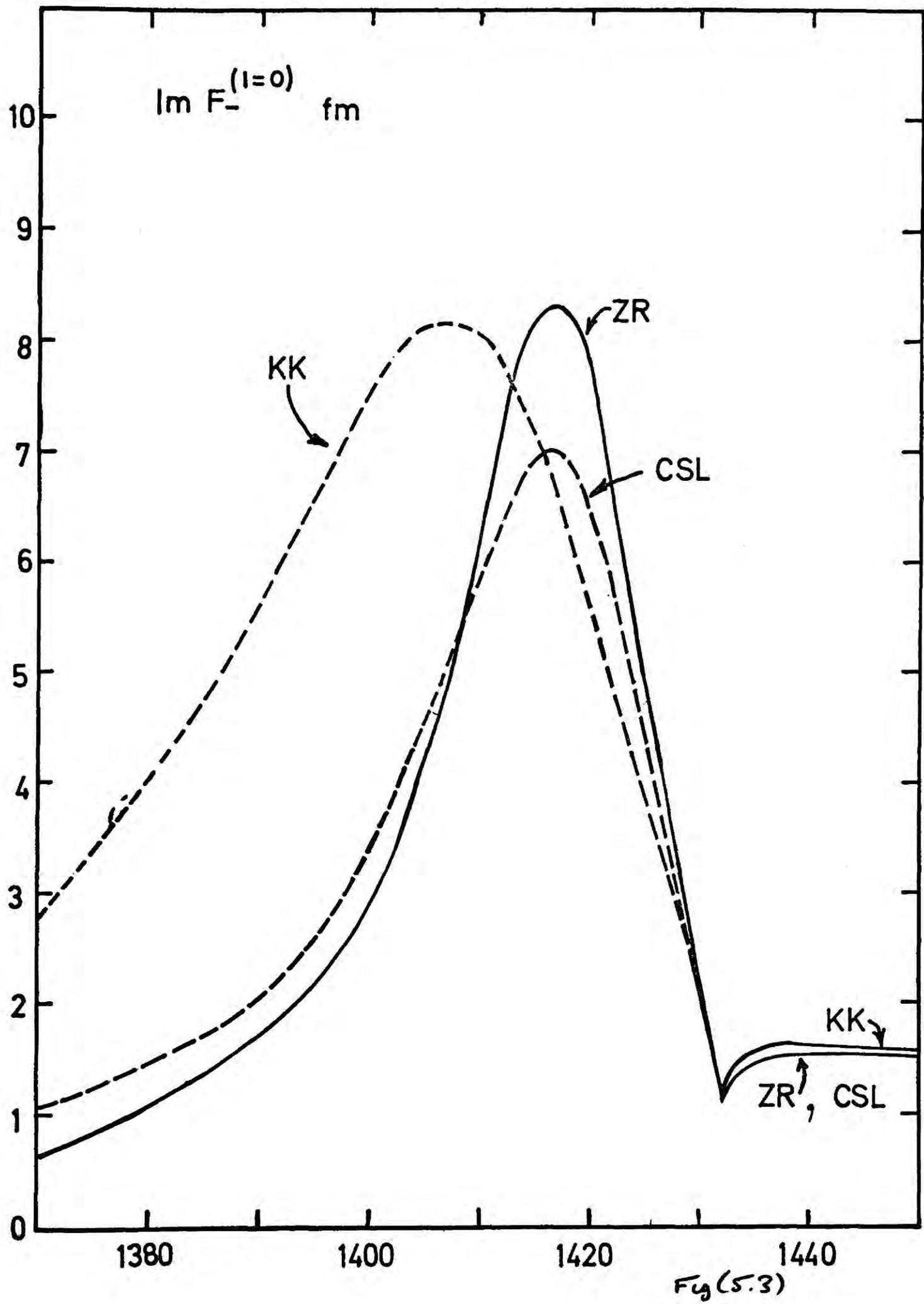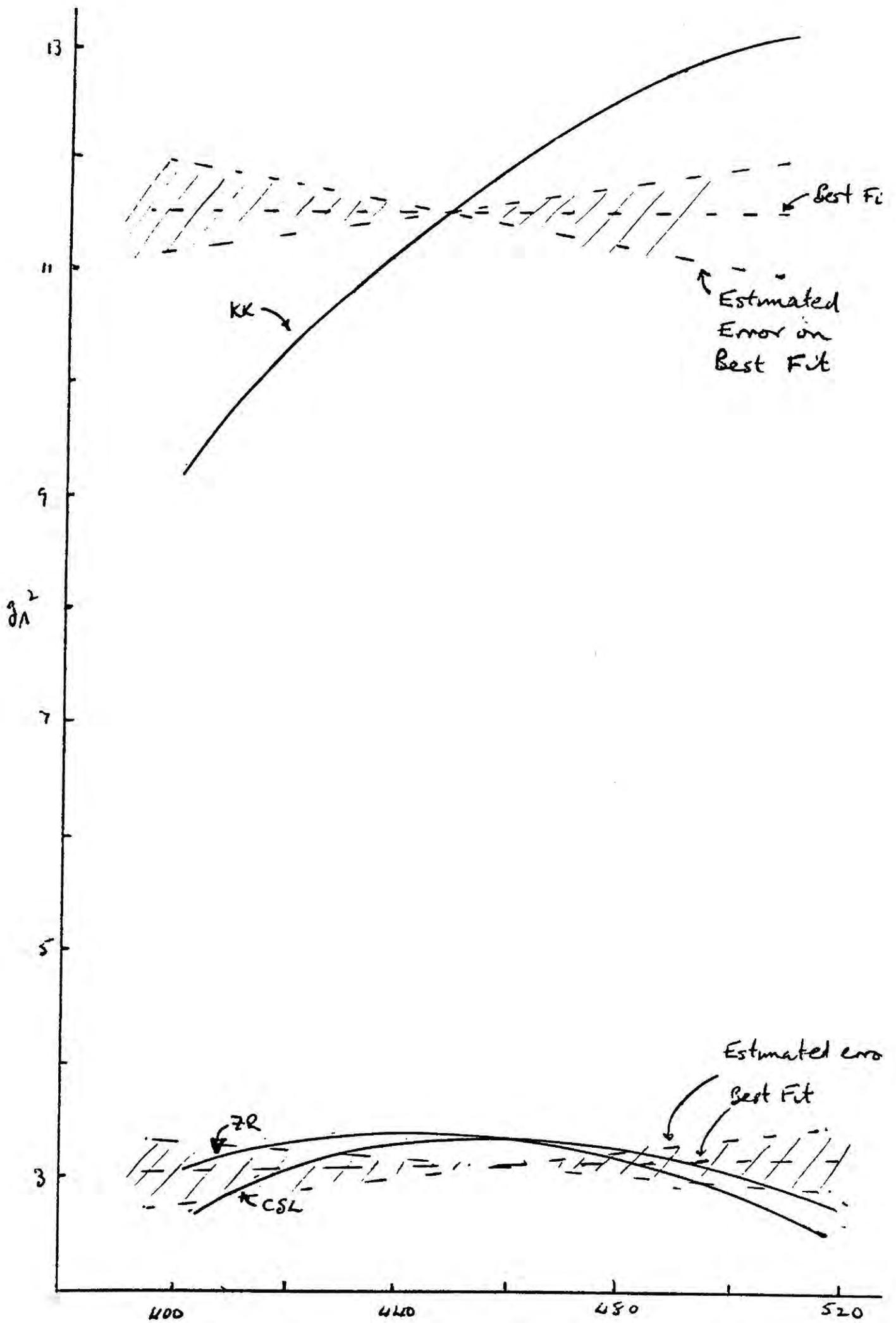
CHAPTER 6

S-wave and I=1 P wave analysis of the low energy $\bar{K}N$ data

(i) Choice of Parameterisation

The available experimental data suggest that the I=0 $\bar{K}N$ and $\Sigma\pi$ amplitudes may be described well in terms of pure S-wave interaction in the kaon momentum range 0-300 Mev/c. However, as we have remarked in Chapter 3, due to the presence of the $D_{3/2} Y_0^*(1520)$ resonance, it is difficult to apply the I=0 analysis over a larger momentum range without introducing a large number of extra parameters to describe the S, P and D waves adequately.

For the I=1 amplitudes the experimental data for $K^-p \to \Lambda\pi^0$ and $K_2^0 p \to \Lambda\pi^{-1}$ suggests the presence of a significant amount of P-wave interaction even below 300 Mev/c. This I=1 P wave seems to be coupled weakly to the $\bar{K}N$ and $\Sigma\pi$ channels and so the data affected by P-wave corrections will be mainly that involving the $\Lambda\pi$ channel. The recent experiments of Kadyk et al.[E6,E11] and Sayer[E7] together with some of the measurements of Watson[E5] provide 76 data points in the kaon momentum range 0-400 Mev/c, for the pure I=1 processes, namely those involving the $\Lambda\pi$ and $K_2^0 p$ channels. This data

includes accurate angular distribution measurements together with some polarisation data all of which involve interference terms between S and P waves and which therefore should be useful in determining the P-wave parameters and improving the accuracy with which the $I=1$ S-wave parameters are given.

In order to make use of this data to determine the $I=1$ P-waves, whilst avoiding the enormous increase in the number of parameters necessary to describe the $I=0$ channel in an extended momentum range, a new fit to the low energy $\bar{K}N$ data was proposed. This fit includes the effect of the $I=1$ P waves and extends the $I=1$ data analysed to the momentum range 0-400 Mev/c, and simultaneously S-wave analysed the $I=0$ data upto 280 Mev/c.

The $I=1$ $P_{3/2}$ wave contains the $Y_1^*(1385)$ scattering resonance and it may be a good approximation to describe the $I=1$ P-waves purely in terms of the high energy tail of the resonance. This was the approach adopted by Kadyk et al.[E6,E11] who found they could adequately fit the angular distributions for $K^-p \rightarrow \Lambda\pi^\circ$ and $K_2^0 p \rightarrow \Lambda\pi^+$ in this manner.

Accordingly in a preliminary fit to the data the $I=1$ $P_{3/2}$ wave was parameterised by a multichannel Breit

161.

Wigner form as given by (3.45)

$$f_{1+_{ij}} = \frac{k_i k_j \sqrt{\Gamma_i \Gamma_j}}{\epsilon_r - \epsilon - \frac{i}{2}(k^3 \Gamma_{\bar{K}N} + q_\Sigma^3 \Gamma_{\Sigma\pi} + q_\Lambda^3 \Gamma_{\Lambda\pi})}$$

where Γ_i is the decay width into channel i, momentum k_i. $(\epsilon_r - \frac{i}{2} k_r^3 \Gamma_{\bar{K}N})$ is taken to be 1385 Mev and from the experimentally observed decay ratio of the $Y_1^*(1385)$ into the $\Sigma\pi$ and $\Lambda\pi$ channels, together with the observed width, $\Gamma_{\Sigma\pi}$ and $\Gamma_{\Lambda\pi}$ may be determined. This leaves one free parameter, namely $\Gamma_{\bar{K}N}$, to describe the $P_{3/2}$ wave. The $P_{\frac{1}{2}}$ wave was ignored and an S-wave zero range parameterisation used. It was found in the fit to the data that, although the $\bar{K}N \rightarrow \Lambda\pi$ angular distribution could be fitted well, other P-wave dependent data were inadequately fitted. Moreover the process $\bar{K}_2^0 p \rightarrow K_1^0 p$ includes the $\bar{K}^0 p$ interaction which has large P waves from the I=0 KN amplitude, and the interference between these P waves and the P waves arising from the $\bar{K}^0 p$ interaction can have important effects. Since the Yang solution for the I=0 KN amplitude predicts large $P_{\frac{1}{2}}$ and small $P_{\frac{3}{2}}$ waves, it would appear that the $P_{\frac{1}{2}}$ wave for the I=1 KN amplitude may be important. From these considerations it is concluded that the approximation of including only the resonant $P_{\frac{3}{2}}$ wave is insufficient.

As the recent analysis of Kadyk et al.[E11] provides
very much more accurate I=1 data, it is possible to
perform an S and P-wave analysis, including both P-waves
in a scattering length parameterisation. This has
been done in a fit in which the S waves are parameterised
by means of the nine zero range K-matrix parameters.
Once again, this parameterisation is modified to include
effective range terms in order to test the validity of
the parameterisation. As the I=1 data is analysed up to
400 Mev/c the P waves have an important effect in
determining the ratio R which involves the Fermi -Yang
ambiguity in the S=+1 part of the P waves. From the
result of determining this ratio the possiblity of
resolving this ambiguity is discussed.

Details of the inclusion of the P-waves in a
scattering length parameterisation are given in section
(ii) and in section (iii) an account is given of the fit.

(ii) Inclusion of I=1 P waves in a scattering length
      formalism

The two elastic I=1 P waves may be written in terms
of the constant scattering length parameters

$$T_{K\pi}{}'_{1\pm} = \frac{k^2 A_{1\pm}}{1 - ik^3 A_{1\pm}} \qquad (6.1)$$

where $A_{1\pm} = a_{1\pm} + ib_{1\pm}$ and the subscripts $1\pm$ refer to P-wave amplitudes with $J=\frac{1}{2}$, $\frac{3}{2}$ respectively.

In order to describe the $\Sigma\pi$ and $\Lambda\pi$ production amplitudes it is necessary to introduce the P wave $\Sigma\pi$ and $\Lambda\pi$ reaction amplitudes $M_{1\pm}$ and $N_{1\pm}$. In terms of these amplitudes we have

$$T'_{R\Sigma_{1\pm}} = \frac{kq_\Sigma M_{1\pm}}{1 - \nu k^3 A_{1\pm}}$$

$$T'_{R\Lambda_{1\pm}} = \frac{kq_\Lambda N_{1\pm}}{1 - \nu k^3 A_{1\pm}} \qquad (6.2)$$

From equations (2.25) and (2.27) the differential cross section for a process involving only S and P waves may be written

$$\frac{d\sigma}{d\Omega} = \frac{Q^{(f)}}{Q^{(\omega)}} \left[|f_{0+} + (2f_{1+} + f_{1-})\cos\theta|^2 + |f_{1+} - f_{L}|^2 \sin^2\theta \right] \quad (6.3)$$

This may immediately be integrated to give the cross section for the process $i \rightarrow f$ as

$$\sigma = \frac{4\pi Q^{(f)}}{Q^{(\omega)}} \left[|f_{0+}|^2 + |f_{1-}|^2 + 2|f_{1+}|^2 \right] \qquad (6.4)$$

Using (6.2) and (6.4) we may define two parameters $\epsilon_{1\pm}$ as follows

$$\epsilon_{1\pm} = \frac{\sigma_{1\pm}(\Lambda\pi^0)}{\sigma_{1\pm}^{I=1}(\text{All hyperons})}$$

$$\approx \frac{q_\Lambda^3 |N_{1\pm}|^2}{q_\Sigma^3 |M_{1\pm}|^2 + q_\Lambda^3 |N_{1\pm}|^2} \tag{6.5}$$

Here $\sigma_{1\pm}$ stands for the cross section evaluated for the $P_{\frac{3}{2}}$ and $P_{\frac{1}{2}}$ waves respectively.

Applying the optical theorem to the elastic amplitude and identifying the various terms we obtain the relations

$$b_{1\pm} = q_\Sigma^3 |M_{1\pm}|^2 + q_\Lambda^3 |N_{1\pm}|^2 \tag{6.6}$$

Using (6.5) and (6.6) we may express the magnitude of the reaction amplitudes in terms of the parameters $b_{1\pm}$ and $\epsilon_{1\pm}$ as

$$|M_{1\pm}|^2 = \sqrt{\frac{(1-\epsilon_{1\pm})\,b_{1\pm}}{q_\Sigma^3}}$$

$$|N_{1\pm}|^2 = \sqrt{\frac{\epsilon_{1\pm}\,b_{1\pm}}{q_\Lambda^3}} \tag{6.7}$$

Finally, in order to evaluate the differential cross section and polarisation for the process $\bar{K}N \rightarrow \Lambda\pi$ it is necessary to know the relative phase of the P-wave production amplitude to the S-wave amplitude. Thus we introduce two further parameters $\phi_{1\pm}$ defined as follows

$$\phi_{1\pm} = \text{Arg}\,[N_{1\pm}] \tag{6.8}$$

and so the $\Lambda\pi$ production amplitude may be written

$$T_{\overline{K}\Lambda\,1\pm}' = \frac{k q_\Lambda |N_{1\pm}| e^{i\phi_{1\pm}}}{1 - ik^3 A_{1\pm}} \tag{6.9}$$

We may therefore parameterise the $I=1$ P waves by the eight real parameters

$$a_{1\pm}, \quad b_{1\pm}, \quad \epsilon_{1\pm}, \quad \phi_{1\pm}.$$

The inclusion of the K^-p, $\overline{K}^0n$ mass differences gives, by the method of Appendix 1, the following corrections to the P wave amplitudes

$$T_{K^-p \to K^-p\,1\pm} = \frac{1}{2}\left\{\frac{k^2 A_{1\pm}}{1 - \frac{1}{2}i(k^3 + k_0^3)A_{1\pm}}\right\}$$

$$T_{K^-p \to \overline{K}^0n\,1\pm} = \frac{1}{2}\left\{\frac{k k_0 A_{1\pm}}{1 - \frac{1}{2}i(k^3 + k_0^3)A_{1\pm}}\right\} \tag{6.10}$$

$$\left|T_{\overline{K}\Sigma\,1\pm}'\right| = \frac{k q_\Sigma |H_{1\pm}|}{\left|1 - \frac{1}{2}i(k^3 + k_0^3)A_{1\pm}\right|}$$

$$T_{\overline{K}\Lambda\,1\pm}' = \frac{k q_\Lambda |N_{1\pm}| e^{i\phi_{1\pm}}}{1 - \frac{1}{2}i(k^3 + k_0^3)A_{1\pm}}$$

The Coulomb correction is only significant for low relative velocity of the particles and, due to the threshold factors, this is the region where P waves are suppressed. Therefore Coulomb corrections to P waves are small and are neglected here.

Using (5.19), (6.3) and (6.8) the K^-p differential cross section will be given by

$$\frac{d\sigma_{Kp}}{d\Omega} = \left| \frac{cosec^2\frac{\theta}{2}}{2\beta k^2} exp\left[\frac{2i}{k\beta} \ln \sin^2\frac{\theta}{2} \right] + \frac{\sigma^2}{2} \frac{A_0 + A_1 - 2ik_0 A_0 A_1}{D} \right.$$

$$\left. + \left(2T_{K^-p \to K^-p_{1+}} + T_{K^-p \to K^-p_{1-}} \right) \cos\theta \right|^2 \qquad (6.11)$$

$$+ \left| T_{K^-p \to K^-p_{1+}} - T_{K^-p \to K^-p_{1-}} \right|^2 \sin^2\theta$$

The P wave hyperon production cross section $\sigma_{1t}^{I=1}$ may be defined by

$$\sigma'_{1t} = \frac{4\pi q_\Sigma}{k} \left| T'_{K\Sigma_{1t}} \right|^2 + \frac{4\pi q_\Lambda}{k} \left| T'_{K_{\Lambda_{1t}}} \right|^2 \qquad (6.12)$$

$$= \frac{4\pi b_{1t}}{k} \left| \frac{1}{1 - \frac{1}{2}i(k^3 + k_0^3)A_{1t}} \right|^2$$

Using this together with (6.4) and the decomposition of (5.14) we may obtain the modified cross sections of (5.19) as

$$\sigma_{\bar{K}^0\Lambda} = \sigma_{\bar{K}^0n}^s + \frac{4\pi k_0}{k} \left\{ 2\left| T_{K^-p \to \bar{K}^0 n_{1+}} \right|^2 + \left| T_{K^-p \to \bar{K}^0 n_{1-}} \right|^2 \right\}$$

$$\sigma_{\Sigma^+\pi^-} = \sigma_{\Sigma^+\pi^-}^s + \frac{1}{2}(1 - \epsilon_{1+})\sigma'_{1+} + \frac{1}{2}(1 - \epsilon_{1-})\sigma'_{1-}$$

$$\sigma_{\Sigma^-\pi^+} = \sigma_{\Sigma^-\pi^+}^s + \frac{1}{2}(1 - \epsilon_{1+})\sigma'_{1+} + \frac{1}{4}(1 - \epsilon_{1-})\sigma'_{1-} \qquad (6.13)$$

$$\sigma_{\Sigma^0\pi^0} = \sigma_{\Sigma^0\pi^0}^s$$

$$\sigma_{\Lambda\pi^0} = \sigma_{\Lambda\pi^0}^s + \epsilon_{1+}' + \frac{1}{2}\epsilon_{1-}\sigma'_{1-}$$

where σ^s is the S-wave cross section as given by (5.19).

We now obtain expressions for the angular distribution measurements of Kadyk et al. From (6.3) we obtain the differential cross section in the form

$$\frac{d\sigma}{d\Omega} = \frac{Q^{(f)}}{Q^{(i)}} \left[|f_{0+}|^2 + 2|f_{1+}|^2 + |f_{1-}|^2 + 2 Re\left[f_{0+}^* (2f_{1+} + f_{1-}) \right] \cos\theta \right.$$
$$\left. + \frac{2}{3} \left\{ (2f_{1+} + f_{1-})^2 + (f_{1+} - f_{1-})^2 \right\} \left(\frac{3\cos^2\theta - 1}{2} \right) \right]$$

Thus if $\frac{d\sigma}{d\Omega}$ is written in a Legendre expansion

$$\frac{d\sigma}{d\Omega}(\theta) = \sum_{n=0}^{\infty} B_n' P_n(\cos\theta) = \sigma_0' \sum_{n=0}^{\infty} B_n P_n(\cos\theta)$$

we may make the identification

$$\beta_0 = 1$$
$$\beta_1 = \frac{2 Re\left[f_{0+}^* (2f_{1+} + f_{1-}) \right]}{|f_{0+}|^2 + 2|f_{1+}|^2 + |f_{1-}|^2} \qquad (6.14)$$

The higher terms b_2 ...... will also have interference terms contributing involving higher partial waves and consequently are not to be used in this analysis.

For the reaction $K_2^0 p \rightarrow K_1^0 p$ using (5.22) we define the partial wave amplitudes for this process as $F_{\ell t}$ where

$$F_{0+} = \frac{1}{2} \left\{ \frac{1}{2} \left(\frac{d_0}{1 - ikd_0} + \frac{d_1}{1 - ikd_1} - \frac{a_1 + ib_1}{1 - ik(a_1 + ib_1)} \right) \right\}$$

$$(6.15)$$

$$F_{1\pm} = \frac{1}{2} \left\{ \frac{1}{2} \left(\frac{k^2 d_{0,1\pm}}{1 - ik^3 d_{0,1\pm}} \right) - \frac{k^2 A_{1\pm}}{1 - ik^3 A_{1\pm}} \right\}$$

where $d_{0,1}$ and $d_{\theta,1\pm}$ are as defined in (5.15).

Using these amplitudes we may write

$$\sigma_{K_2^0 p \to K_1^0 p} = 4\pi \left\{ |F_{0+}|^2 + 2|F_{1+}|^2 + |F_{1-}|^2 \right\}$$

and

$$\beta_{1\ K_2^0 p \to K_1^0 p} = \frac{2\,Re\left[F_{0+}^* \left(2F_{1+} + F_{1-} \right) \right]}{|F_{0+}|^2 + 2|F_{1+}|^2 + |F_{1-}|^2} \qquad (6.16)$$

The total $K_2^0 p$ cross section may be obtained using (5.15) and the optical theorem to give

$$\sigma_{tot}(K_2^0 p) = \sigma_{tot}^s(K_2^0 p) + \frac{2\pi}{k}\left[2\,Im\left(\frac{k^2 A_{1+}}{1 - i k^3 A_{1+}} \right) \right. \qquad (6.17)$$
$$\left. + Im\left(\frac{k^2 A_{1-}}{1 - i k^3 A_{1-}} \right) \right]$$

The cross sections for the process $K_2^0 p \to \Lambda \pi^+$ may be obtained in a similar manner to that for the process $K^- p \to \Lambda \pi$ except that there is now no mass difference correction. Thus we define P wave hyperon production cross sections $\sigma'_{1\pm}(K_2^0 p \to y\pi)$ which may be written as

$$\sigma'_{1\pm}(K_2^0 p \to y\pi) = \frac{4\pi b_{1\pm}}{k} \left| \frac{1}{1 - i k^3 A_{1\pm}} \right|^2 \qquad (6.18)$$

and the $K_2^0 p \to \Lambda \pi^+$ cross sections will then be

$$\sigma(K_2^0 p \to \Lambda \pi^1) = \sigma^s(K_2^0 p \to \Lambda \pi^1) + \epsilon_{1+}\sigma'_{1+}(K_2^0 p \to y\pi) \qquad (6.19)$$
$$+ \frac{1}{2}\epsilon_{1-}\sigma'_{1-}(K_2^0 p \to y\pi)$$

From (5.3) and (5.5) the S wave $K_2^0 p \rightarrow \Lambda \pi^+$ amplitude $T_{\bar{K}\Lambda}'$ may be computed and similarly from (6.9) and (6.7) the P wave $K_2^0 p \rightarrow \Lambda \pi^+$ amplitudes $T_{\bar{K}\Lambda, t}'$ may also be evaluated. In terms of these amplitudes the first Legendre coefficient $B_{1 \ K_L^0 p \rightarrow \Lambda \pi^+}$ may be written as

$$B_{1 \ K_2^0 p \rightarrow \Lambda \pi^+} = \frac{2 \, Re \left[T_{\bar{K}\Lambda}' \left(2 T_{\bar{K}\Lambda, 1+}' + T_{\bar{K}\Lambda, 1-}' \right) \right]}{|T_{\bar{K}\Lambda}'|^2 + 2 |T_{\bar{K}\Lambda, 1+}'|^2 + |T_{\bar{K}\Lambda, 1-}'|^2} \quad (6.20)$$

The coefficient $B_{1 \ K^- p \rightarrow \Lambda \pi^0}$ is also given by (6.20) if $T_{\bar{K}N}$ is taken as the $\bar{K}N \rightarrow \Lambda \pi$ S wave amplitude corrected for Coulomb and mass difference effects as in Appendix I

$$T_{\bar{K}\Lambda}' = \frac{C_0 N_1}{D} (1 - \iota k_0 A_0)$$

and similarly $T_{\bar{K}\Lambda, t}'$ are taken as the corrected amplitudes of (6.10).

Finally it is necessary to compute the Λ^0 asymmetry in $K^- p \rightarrow \Lambda \pi^0$. From (2.28) we see that the Λ is polarised along the normal $\hat{\underline{n}}$ to the production plane i.e. $\hat{\underline{n}} = \hat{q} \times \hat{q}'$ where $\hat{q}$ and $\hat{q}'$ are as shown in Fig. (6.1)
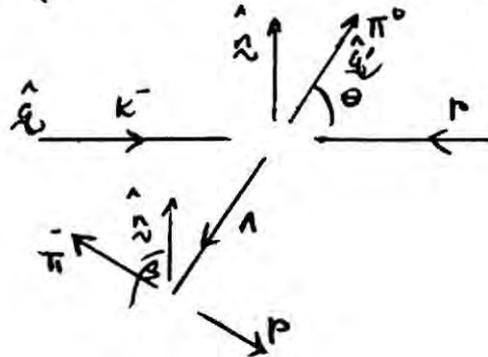
Fig. (6.1)

The polarisation $P(\theta)$ is given by

$$P(\theta) \frac{d\sigma}{d\Omega} = -2 \sin\theta \, \text{Im}\left[T_{\bar{K}\Lambda}'^{*} \left(T_{\bar{K}\Lambda \, 1+} - T_{\bar{K}\Lambda \, 1-} \right) \right]$$

If, in agreement with the convention of Kadyk et al., we define the angle β as the angle between $\hat{n}$ and the direction of the decay pion in the final decay $\Lambda \rightarrow \pi^{-} p$ the distribution of events versus β is given by $W(\beta)$ where

$$W(\beta) \sim \left(1 + \alpha_{\Lambda} P(\theta) \cos\beta \right)$$

and α_{Λ} has been obtained as

$$\alpha_{\Lambda} = 0.646 \pm 0.016$$

The coefficient A_{1} of Kadyk et al. is $\alpha_{\Lambda} P(\theta)$ averaged over θ

$$A_{1} = \frac{\int_{-1}^{1} \alpha_{\Lambda} P(\theta) \frac{d\sigma}{d\Omega} d(\cos\theta)}{\int_{-1}^{1} \frac{d\sigma}{d\Omega} d(\cos\theta)}$$

i.e.

$$A_{1} = \frac{\pi \alpha_{\Lambda}}{2} \frac{\text{Im}\left[T_{\bar{K}\Lambda}'^{*} \left(T_{\bar{K}\Lambda \, 1+}' - T_{\bar{K}\Lambda \, 1-}' \right) \right]}{|T_{\bar{K}\Lambda}'|^2 + 2|T_{\bar{K}\Lambda \, 1+}|^2 + |T_{\bar{K}\Lambda \, 1-}|^2}$$

(iii) Details of the S and P wave fits

Using the nine zero range S wave parameters of
(5.1) together with the eight I=1 P wave parameters
$a_{1\pm}$, $b_{1\pm}$, $\epsilon_{1\pm}$, $\phi_{1\pm}$ the experimentally observed
quantities were predicted by the formulae of the
previous section and the χ^2 function was formed as
in (5.19). In this case the experimental data used
consisted of all that analysed in Chapter 5 together
with the pure I=1 quantities of refs. (E5,E11) in
the kaon lab. momentum range 0-400 Mev/c. Explicitly
the latter are the total cross sections and angular
distributions E_1 for the processes $K^-p \to \Lambda\pi^\circ$, $K_2^\circ p \to K_1^\circ p$,
the angular distribution, B_1, for the process $K_2^\circ p \to K_1^\circ p$
and the Λ° decay assymetry, A_1, for the processes
$K^-p \to \Lambda\pi^\circ \to \pi^-p\pi^\circ$ and $K_2^\circ p \to \Lambda\pi^+ \to \pi^-p\pi^+$. It should be
noted that the experimental errors quoted by Watson
et al. for the angular distribution E_1 for the process
$K^-p \to \Lambda\pi^\circ$ are considerably smaller than the errors of
Kadyk et al. for the same quantity even though the
number of events analysed by Watson et al. are
considerably fewer than that of Kadyk et al. Moreover
the angular resolution of Watson's experiment is
inferior to that of Kadyk. For this reason the errors
of Watson's experiment were adjusted to correspond to

the errors of Kadyk for similar statistics.

Once again the general minimising routine VA04A was used to search parameter space for the minima of the χ^2 function. A unique solution was found and in Table (6.1) the values of the parameters at this minimum are given. The errors quoted correspond to the inverse square root of the diagonal elements of the error matrix. The full error matrix is given in Table (6.2). The total number of data points used was 246 and the value of χ^2 at the minimum was 249.8 giving a confidence level of 84% in the fit. In Table (6.3) we list the contribution to χ^2 from the various data points.

The parameterisation was again tested for stability against addition of effective range terms to the S-wave parameters and once again no significant improvement in χ^2 was obtained with the addition of these terms. Moreover no solution was obtained which altered the basic features of the zero range fit. From an examination of Table (6.1) it may be seen that the P wave parameters are not determined very exactly, and it may be concluded that the data will not accommodate any further parameters. In fact it is possible to vary

the values of ϕ_{1+} and ϕ_{1-} slightly from their best

fit positions, minimise using the other parameters,

and obtain a fit which is statistically only slightly

less probable than the one quoted. However under

their procedure the S-wave parameters are not

significantly altered and thus the accuracy with which

we know the S-wave parameters is not affected by the

uncertainty in the P-wave parameters. It may be seen

from Table (6.1) that the errors on the S-wave K

matrix elements are less than those quoted for the pure

S wave fit of Table (5.1). The addition of the new

data and the allowance for P wave effects has therefore,

as hoped, improved the determination of the S wave

parameters. It should be noted that the most significant

changes in the S wave parameters are in the zero

range elements $K'_{\Sigma\Lambda}$, $K'_{\Sigma\Sigma}$, $K'_{\Sigma\Lambda}$ and $K'_{\Lambda\Lambda}$. The

determination of these elements depends on the energy

dependence of the observed quantities and the addition

of the new data over the extended momentum range will

therefore particularly help their determination. A

thorough search of parameter space was carried out to

find any further solutions which may exist and may

not be perturbations on the S-wave solution of Chapter

5. No such solution was found and it may therefore

be concluded that we have found a unique fit to the

data with well determined S-wave parameters and slightly less well determined P-wave parameters.

It is found that the fit to the quantities not involving the 4π channel and to which no new data points have been added is not changed perceptibly from that shown in Fig. (5.1a-5.1c,5.1h). The fits, (ZRP), to the pure I=1 quantities over the extended momentum range 0-400 Mev/c are shown in Figs. (6.1a-6.1f).

In Fig. (6.1a) the fit to the quantity R, using both the Yang and Fermi solutions for the I=0 s=+1 P waves are shown. From (6.15) it may be seen that the interference between the s=+1 and s=-1 P waves produces the final P wave effect in the quantity $6(K_2^0 p \rightarrow K_1^0 p)$ and hence in R. This P wave term is proportional to

$$\frac{1}{2}\left\{ \frac{2k^2 d_{1+}}{1-ik^3 d_{1+}} + \frac{k^2 d_{1-}}{1-ik^3 d_{1-}} \right\} - \frac{2k^2 A_{1+}}{1-ik^3 A_{1+}} - \frac{k^2 A_{1-}}{1-ik^3 A_{1-}}$$

Since the imaginary parts of the I=1 s=-1 P waves are small compared to the real parts it is apparent that R will be increased and that the Fermi solution will be favoured if, roughly, a_{1+} is of greater magnitude than a_{1-} and negative whilst the Yang solution will be favoured if a_{1-} is of greater magnitude than a_{1+} and negative. From the solution of Table (6.1) it is apparent that both a_{1+} and a_{1-} are negative and of the

same order of magnitude. Thus although the Yang

solution is favoured (Fig.(6.1a)) the distinction

between them is small and, due to the errors in

determining $a_{1\pm}$, the choice between the Fermi and Yang

solutions cannot be made with any certainty.

From Table (6.3) it may be seen that the contribu-

tions to χ from the angular distributions for the

processes $K^0_2 p \to \Lambda \pi^+$ and $K^- p \to \Lambda \pi^0$ is large. However it

may be seen in Fig. (6.1d) that the fit to the data is

satisfactory and that the experimental errors are

probably underestimated. When the P waves predicted

by Kim's fit are used, together with his S wave K

matrix parameters to predict $B_{1 K^0_2 p \to \Lambda \pi^+}$ and $B_{1 K^- p \to \Lambda \pi^0}$

values between $0.26 < B_1 < 1.1$ are obtained. From Fig.(6.1d)

it may be seen that this gives an acceptable fit to the data.

The remaining fits to the I=1 data may be seen

to be good within the experimental errors.

Using the new S-wave I=0 parameters the position

and width of the virtual bound state resonance the

may be calculated. These are

$$E_r = 1421 \, Mev. \qquad \Gamma = 21 \, Mev$$

It may be seen that the position and width are somewhat larger than that predicted by the pure S-wave fit and thus the values of the coupling constants predicted using the standard dispersion relation may be expected to be larger than the previous estimate. This is found to be the case and we obtain

$$g_\Lambda^2 = 3.58 \qquad g_\Sigma^2 = 0.80$$

The energy variation of the prediction for the coupling constant using the subtracted dispersion relation was again calculated and a similar curve to that shown in Fig.(5.4) but raised by 0.15 was obtained. Thus it may be concluded that the values of g_Λ^2 found using this fit are consistent with a constant value.

Finally the scattering lengths for the $\bar{K}N$, $\Sigma\pi$ and $\Lambda\pi$ amplitudes were computed as in Chapter 5 and are listed in Table (6.4) together with the $\Lambda\pi$ phase, δ, evaluated at the $\Xi^*(1315)$ position. These may be compared with those given in Table (5.4).

In conclusion it may be stated that we have obtained good fits to the data in the low energy region using both S and S+P wave fits. The addition of P waves allows for the observed non-negligible P-waves

in the $\Lambda\pi$ channel and fits the angular distribution
measurements in the momentum region 0-400 Mev/c. More-
over the S-wave parameters are determined more precisely
in the S + P wave fit and in neither fit did effective
range terms statistically improve the fit, nor were
any solutions found which changed the nature of the
zero range parameters. Thus it may be concluded that
the zero range parameters are determined uniquely and
with the accuracy shown in Table (6.1).

The coupling constants predicted using the I=0
zero range parameters are not in agreement with the
SU(3) symmetry predictions but, as discussed in
Chapter 5, the dispersion predictions are very sensitive
to effective range terms. However the existence of
a good zero range fit to the data in the low energy
range shows that the effective ranges will have to be
determined by a fit to the data over an extended energy
range. As has been pointed out, this leads to an
unmanageable number of parameters. It is concluded
therefore that the prediction of the strange particle
coupling constants by means of a standard dispersion
relation which requires the knowledge of the effective
ranges is unsatisfactory and that a relation, such as

the subtracted sum rule introduced in Chapter 4
will have to be used to obtain accurate predictions
of the coupling constants. This will be possible when
accurate measurements of the real part of the $K^{\pm}p$
amplitudes are available.

	$(\text{Fermi})^{+1}$			$(\text{Fermi})^{3}$	
$K^{0}_{\bar{K}\bar{K}}$	-2.34	± 0.24	a_{1+}	-0.060	± 0.037
$K^{0}_{\bar{K}\Sigma}$	-1.16	± 0.20	b_{1+}	0.0037	± 0.012
$K^{0}_{\Sigma\Sigma}$	-0.96	± 0.40	a_{1-}	-0.067	± 0.037
$K'_{\bar{K}\Sigma}$	-0.21	± 0.09	b_{1-}	0.0024	± 0.002
$K'_{\bar{K}\Sigma}$	-0.70	± 0.03			
$K'_{\bar{K}\Lambda}$	-0.57	± 0.13	ϵ_{1+}	1.00	$\pm^{0}_{0.011}$
$K'_{\Sigma\Sigma}$	0.23	± 0.21	ϕ_{1+}	2.71	± 0.37
$K'_{\Sigma\Lambda}$	-0.04	± 0.05	ϵ_{1-}	1.00	$\pm^{0}_{0.011}$
$K'_{\Lambda\Lambda}$	-0.78	± 0.31	ϕ_{1-}	2.71	± 0.40

S+P-wave solution (ZRP)

TABLE (6.1)

TABLE (6.2)

Label	$K^0_{\xi\xi}$	$K^0_{\xi\zeta}$	$K^0_{\Sigma\zeta}$	$K^1_{\xi\xi}$	$K^1_{\xi\zeta}$	$K_{E\tau}$	$K^1_{K\Lambda}$	$K^1_{\Sigma\zeta}$	$K^1_{\Sigma\Lambda}$	$K^1_{\Lambda\Lambda}$	a_{1+}	b_{1+}	ϵ_{1+}	ϕ_{1+}	a_{1-}	b_{1-}	ϵ_{1-}	ϕ_{1-}
$K^0_{\xi\xi}$	5.9×10^{-2}																	
$K^0_{\xi\zeta}$	4.9×10^{-2}	4.1×10^{-2}																
$K^0_{\Sigma\zeta}$	9.5×10^{-2}	8.0×10^{-2}	1.6×10^{-1}															
$K^1_{\xi\xi}$	1.4×10^{-2}	1.1×10^{-2}	2.2×10^{-2}	5.1×10^{-3}														
$K^1_{\xi\zeta}$	-3.4×10^{-3}	-2.9×10^{-3}	-5.5×10^{-3}	-1.8×10^{-3}	8.0×10^{-4}													
$K^1_{\tau K\Lambda}$	-1.8×10^{-2}	-1.6×10^{-2}	-3.2×10^{-2}	2.1×10^{-3}	-3.8×10^{-4}	1.8×10^{-2}												
$K^1_{\Sigma\zeta}$	4.9×10^{-2}	4.1×10^{-2}	8.0×10^{-2}	1.3×10^{-3}	3.4×10^{-4}	-1.4×10^{-2}	4.2×10^{-2}											
$K^1_{\Sigma\Lambda}$	7.7×10^{-3}	6.5×10^{-3}	1.3×10^{-2}	-1.2×10^{-3}	3.3×10^{-4}	-5.5×10^{-4}	-5.8×10^{-3}	5.9×10^{-3}	2.5×10^{-3}									
$K^1_{\Lambda\Lambda}$	-4.7×10^{-2}	-4.0×10^{-2}	-8.0×10^{-2}	3.5×10^{-3}	-3.4×10^{-4}	4.2×10^{-2}	-1.4×10^{-2}	-3.5×10^{-3}	-1.4×10^{-2}	9.8×10^{-2}								
a_+	-2.5×10^{-3}	-2.0×10^{-3}	-3.8×10^{-3}	9.4×10^{-4}	-1.7×10^{-4}	3.2×10^{-4}	-7.4×10^{-4}	-1.8×10^{-3}	-7.4×10^{-4}	7.1×10^{-4}	1.4×10^{-3}							
b_+	6.5×10^{-4}	3.5×10^{-4}	6.7×10^{-5}	9.9×10^{-4}	3.2×10^{-6}	-1.6×10^{-6}	3.0×10^{-6}	1.6×10^{-6}	-4.2×10^{-5}	1.4×10^{-5}	1.5×10^{-4}							
ϵ_{1+}	-1.4×10^{-6}	-1.1×10^{-6}	-2.0×10^{-6}	-5.6×10^{-5}	3.2×10^{-7}	3.1×10^{-7}	-6.9×10^{-7}	-8.5×10^{-7}	6.0×10^{-5}	-1.8×10^{-5}	4.0×10^{-8}	1.1×10^{-4}						
ϕ_{1+}	-2.0×10^{-3}	-1.6×10^{-3}	-3.3×10^{-3}	-2.1×10^{-3}	8.9×10^{-2}	1.3×10^{-2}	-1.6×10^{-2}	-3.6×10^{-3}	2.8×10^{-3}	2.1×10^{-4}	-1.7×10^{-3}	-2.3×10^{-7}	1.4×10^{-1}					
a_{1-}	-2.3×10^{-4}	-1.7×10^{-3}	-3.5×10^{-3}	-7.2×10^{-3}	-2.2×10^{-6}	5.0×10^{-4}	-1.7×10^{-6}	-4.1×10^{-3}	1.3×10^{-4}	-3.5×10^{-4}	-3.1×10^{-4}	7.7×10^{-7}	2.7×10^{-3}	1.4×10^{-3}				
b_{1-}	-1.0×10^{-4}	-7.7×10^{-3}	-1.5×10^{-4}	-3.6×10^{-5}	-1.6×10^{-6}	1.1×10^{-6}	-7.6×10^{-5}	-1.8×10^{-5}	3.3×10^{-5}	-2.2×10^{-5}	-2.1×10^{-6}	-1.0×10^{-7}	-4.2×10^{-7}	7.6×10^{-6}	4.4×10^{-6}			
ϵ_{1-}	-2.3×10^{-2}	-2.0×10^{-2}	-3.7×10^{-2}	-2.1×10^{-3}	-6.6×10^{-6}	-1.1×10^{-6}	-1.2×10^{-2}	-1.9×10^{-6}	-3.6×10^{-2}	2.5×10^{-7}	-4.3×10^{-8}	-1.3×10^{-6}	-2.0×10^{-6}	-7.3×10^{-7}	1.1×10^{-6}	1.2×10^{-4}		
ϕ_{1-}	-2.3×10^{-2}	-1.8×10^{-2}	-3.6×10^{-1}	-1.5×10^{-3}	-1.4×10^{-2}	1.6×10^{-2}	-1.5×10^{-2}	-7.3×10^{-3}	3.5×10^{-3}	1.9×10^{-3}	8.3×10^{-5}	-3.1×10^{-6}	1.2×10^{-3}	3.1×10^{-5}	1.2×10^{-6}	-8.2×10^{-5}	1.6×10^{-1}	

Experimental Measurement	Reference	Kaon Lab. Momentum (Mev/c)	$\sqrt{\tilde{\ }}$ Contribution	Number of Measurements
$\int_{0.95}^{0.965} \frac{d\sigma_{el}}{d\Omega} d\Omega$	E3	100-280	3.7	9
$\int_{0.90}^{0.95} \frac{d\sigma_{el}}{d\Omega} d\Omega$	E3	100-280	6.1	9
$\int_{0.85}^{0.90} \frac{d\sigma_{el}}{d\Omega} d\Omega$	E3	100-280	3.6	9
$\int_{0.80}^{0.85} \frac{d\sigma_{el}}{d\Omega} d\Omega$	E3	100-280	3.6	9
$\int_{0.70}^{0.80} \frac{d\sigma_{el}}{d\Omega} d\Omega$	E3	100-280	6.7	9
$\int_{0.60}^{0.70} \frac{d\sigma_{el}}{d\Omega} d\Omega$	E3	100-280	4.6	9
$\int_{-0.965}^{0.60} \frac{d\sigma_{el}}{d\Omega} d\Omega$	E3	100-280	7.8	9
$\sigma(K^-p \to \bar{K}^0 n)$	E1,E3,E4	100-280	12.9	23
$\sigma(K^-p \to \Sigma^+\pi^-)$	E1,E2,E3	60-280	29.5	30
$\sigma(K^-p \to \Sigma^-\pi^+)$	E1,E2,E3	60-280	50.4	32
$\sigma(K^-p \to \Sigma^0\pi^0) + \sigma(K^-p \to \Lambda\pi^0)$	E1,E3	100-260	4.6	9
$\dfrac{\sigma(K^-p \to \Lambda\pi^0)}{\sigma(K^-p \to \Sigma^0\pi^0) + \sigma(K^-p \to \Lambda\pi^0)}$	E1,E3	100-260	5.0	8
$(\Lambda / \Sigma^0 + \Lambda)$ Branching ratio	E1,E3	0	0.6	2
$(\Sigma^+ + \Sigma^- / \Sigma^0 + \Lambda)$ Branching ratio	E1	0	1.7	1
(Σ^- / Σ^+) Branching ratio	E1,E3	0	1.0	2

Experimental Measurement	Reference	Kaon Lab. Momentum (Mev/c)	χ^2 Contribution	Number of Measureme
R	E11	170-400	18.9	5
ϵ	E5,E11	170-400	8.8	8
$\sigma_{K_2^0 p}$ total	E7	170-400	6.2	11
$\sigma(K_2^0 p \to \Lambda \pi^+)$	E11	170-400	18.0	11
$\sigma(K^- p \to \Lambda \pi^0)$	E5,E11	170-400	13.1	12
$B_{1\ K_2^0 p \to \Lambda \pi^+}$	E11	170-400	15.4	5
$B_{1\ K^- p \to \Lambda \pi^0}$	E5,E11	170-400	6.9	7
$B_{1\ K_2^0 p \to K_2^0 p}$	E11	170-400	6.1	5
$A_{1\ \Lambda\ Assymmetry}$	E11	170-400	14.6	12

TOTAL			249.8	246

TABLE (6.3)

Reaction	Isospin	S-wave scattering length
$\bar{K}N \to \bar{K}N$	0	$(-1.74 \pm 0.03) + i(0.70 \pm 0.02)$
$\bar{K}N \to \bar{K}N$	1	$(-0.07 \pm 0.02) + i(0.62 \pm 0.03)$
$\Sigma\pi \to \Sigma\pi$	0	-0.09 ± 0.20
$\Sigma\pi \to \Sigma\pi$	1	$(-0.41 \pm 0.15) + i(0.19 \pm 0.19)$
$\Lambda\pi \to \Lambda\pi$	1	-3.24 ± 0.40
$\Lambda\pi \to \Lambda\pi$	1	$\delta(1315.) = -47.6° \pm 15°$

TABLE (6.4)

Fig (6.1a)

$\Lambda^{\circ} / (\Lambda^{\circ} + \Sigma^{\circ})$ BRANCHING RATIO

$\bar{\underset{\perp}{\Phi}}$ = KIM

ZRP

KK

k_{LAB} (MeV/C)

Fig (6.16)

Fig (6.1c)

Top panel labels:
$-B_1$ $K^-p \rightarrow \Lambda\pi^0$
○ Kadyk et.al.
△ Watson et al.

Curve label: ← ZRP

Axis: $E_{c.m.}$ (MeV)

Bottom panel labels:
$-B_1$ $K_2^0 p \rightarrow \Lambda\pi^+$
○ Kadyk et al.

Curve labels: ← KK, ← ZRP

Axis: $E_{c.m.}$ (MeV)

Fig (6.1d)

Fit to Λ^0 decay assymetry A_1

Φ Kadyk et al $K_s^0 p \to \Lambda \pi^+ \to \pi p \pi^+$

ZRP

KK

E_{cm} (MeV)

KK
ZRP

$B_1\ K_2^0 p \to K_1^0 p.$

Φ Kadyk et. al

$E_{cm.}$ (MeV)

Fig (6.1e)

$\sigma_{tot}(K_L^0 p)$

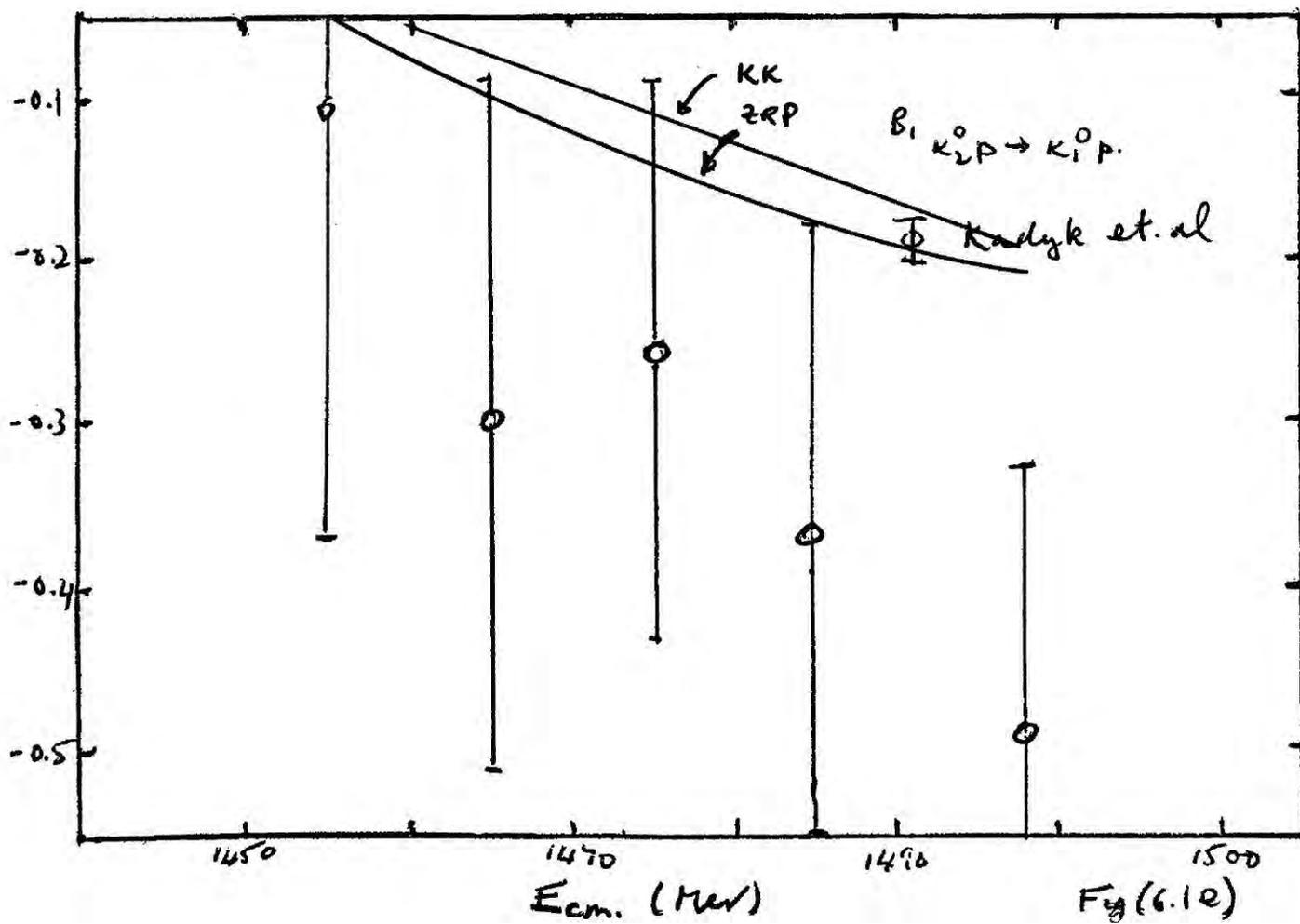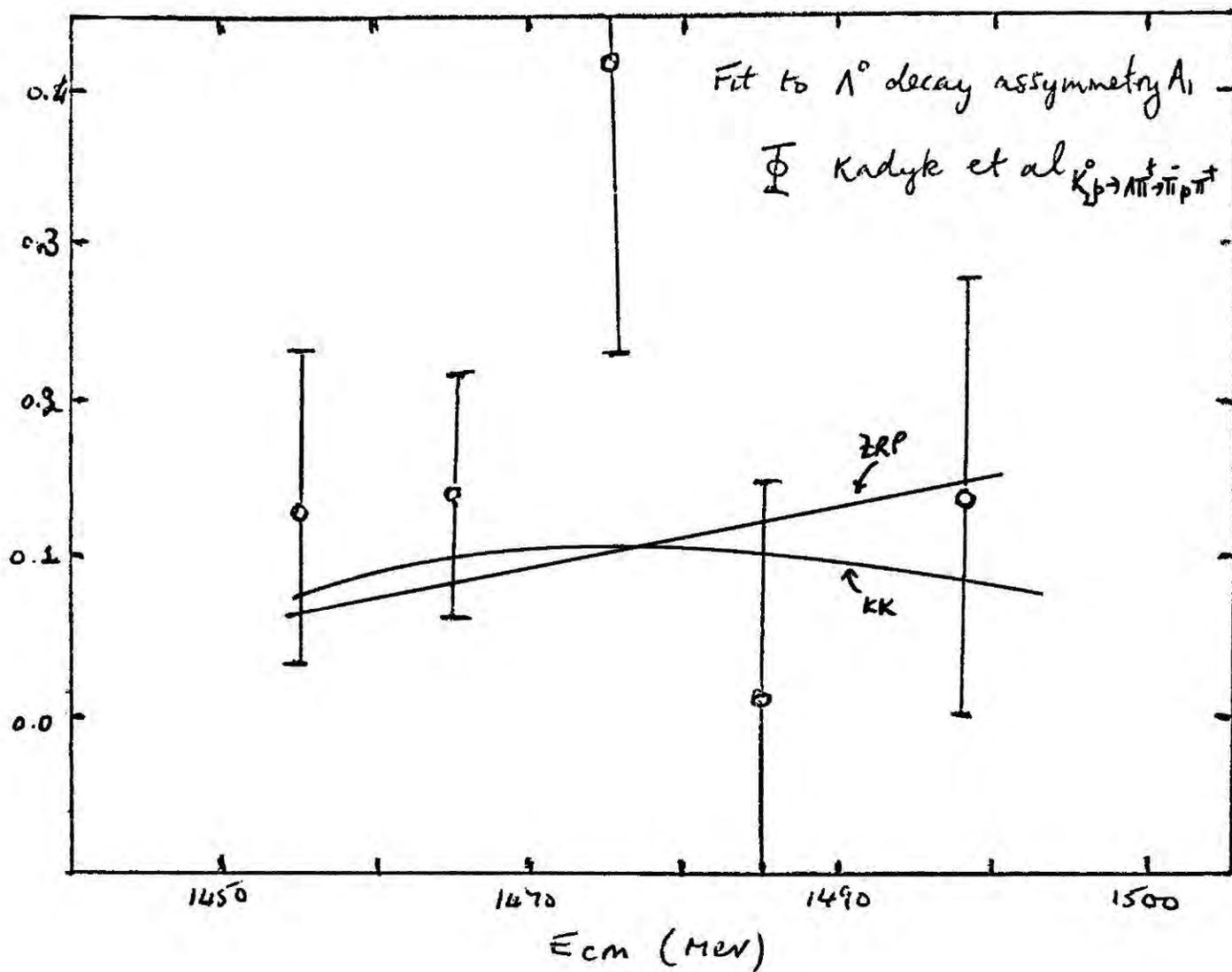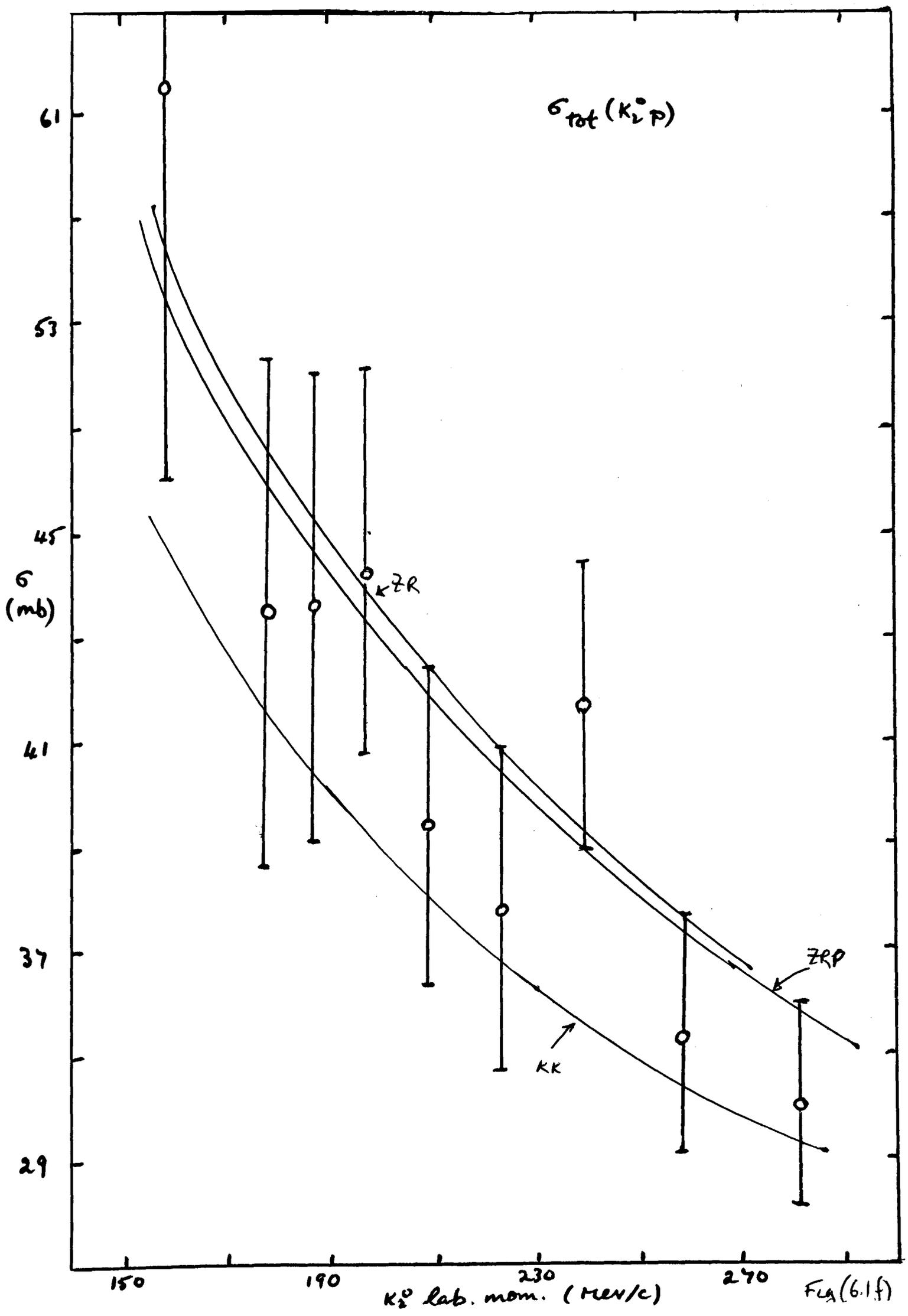σ (mb)

K_L^0 lab. mom. (Mev/c)

ZRP

KK
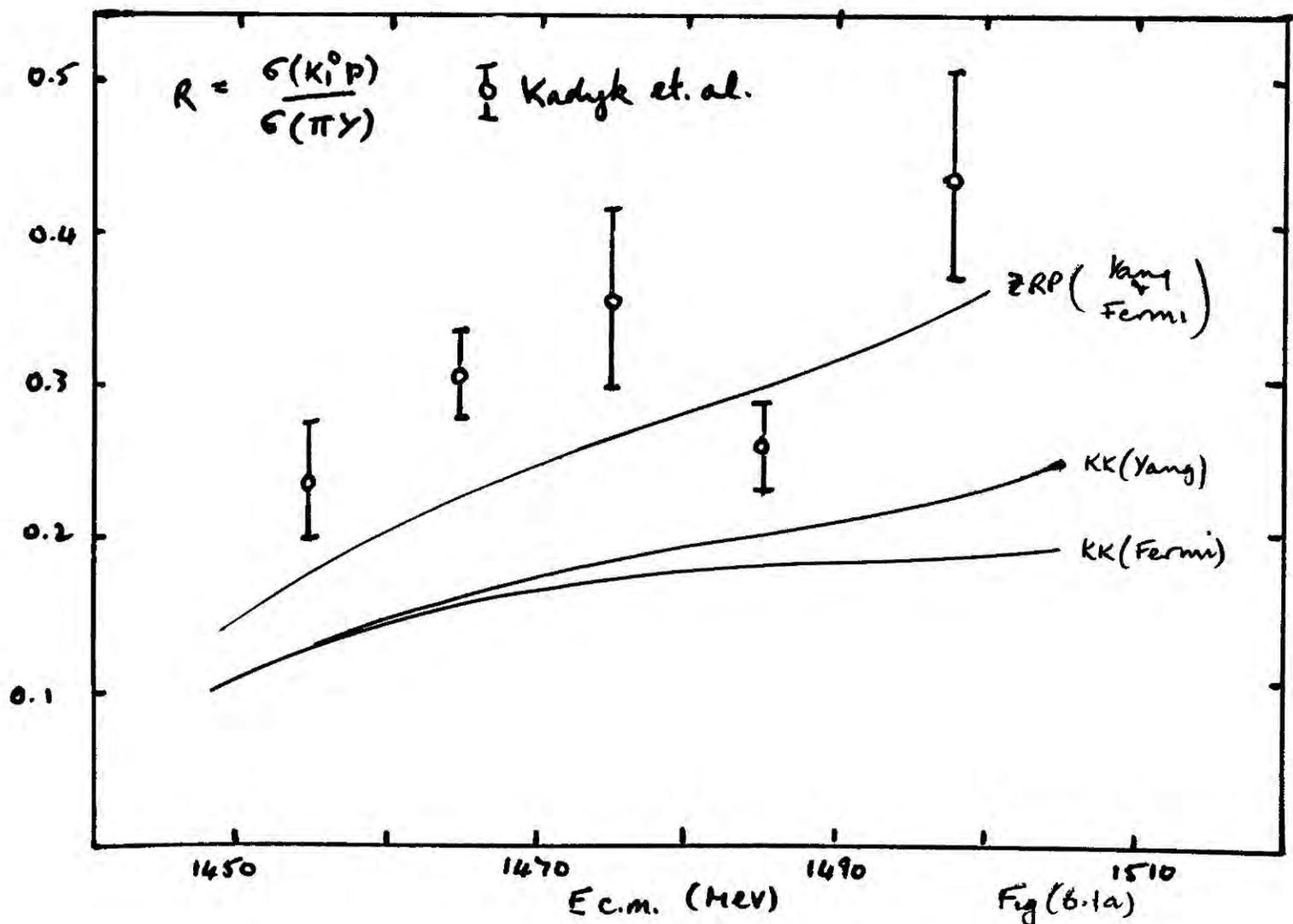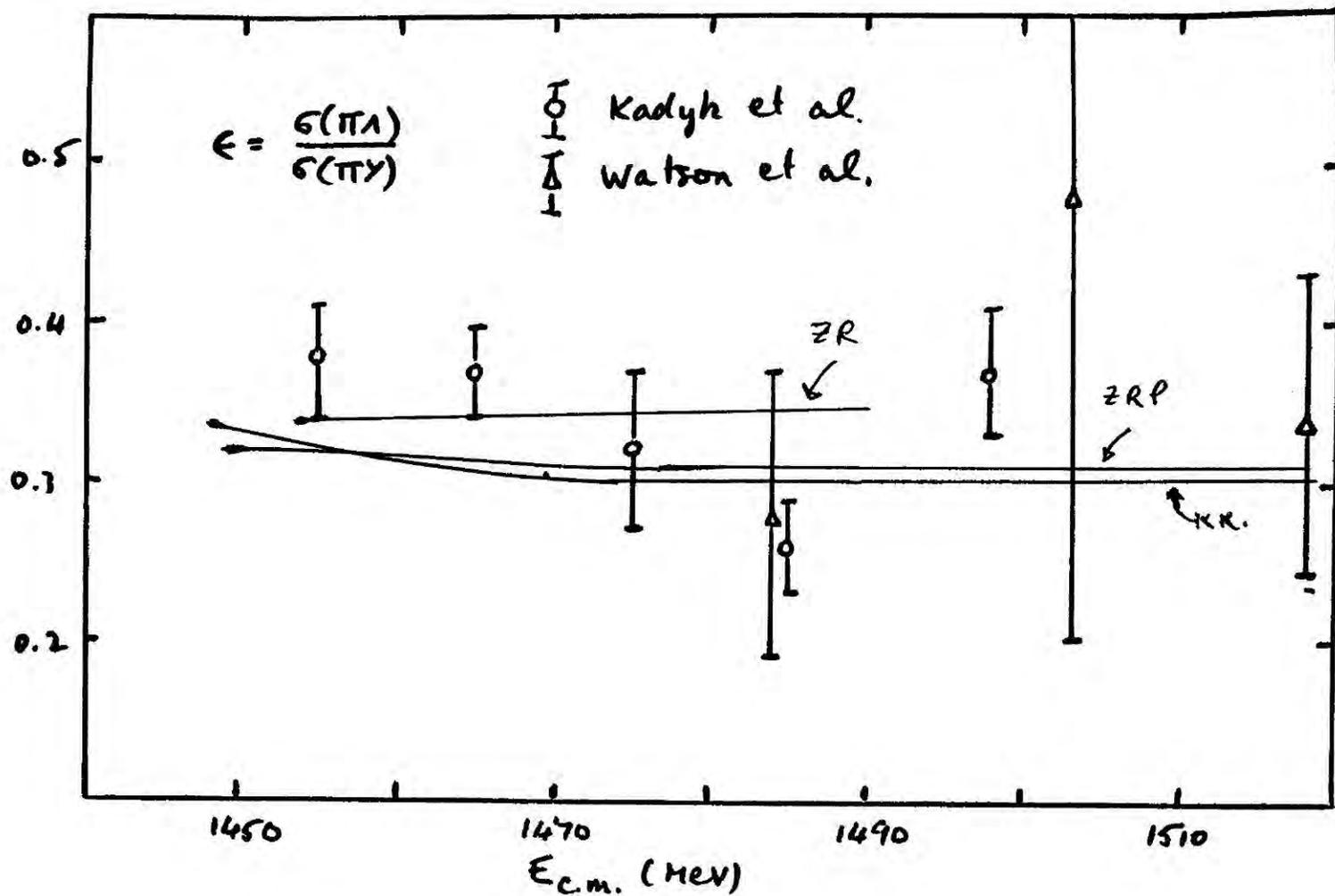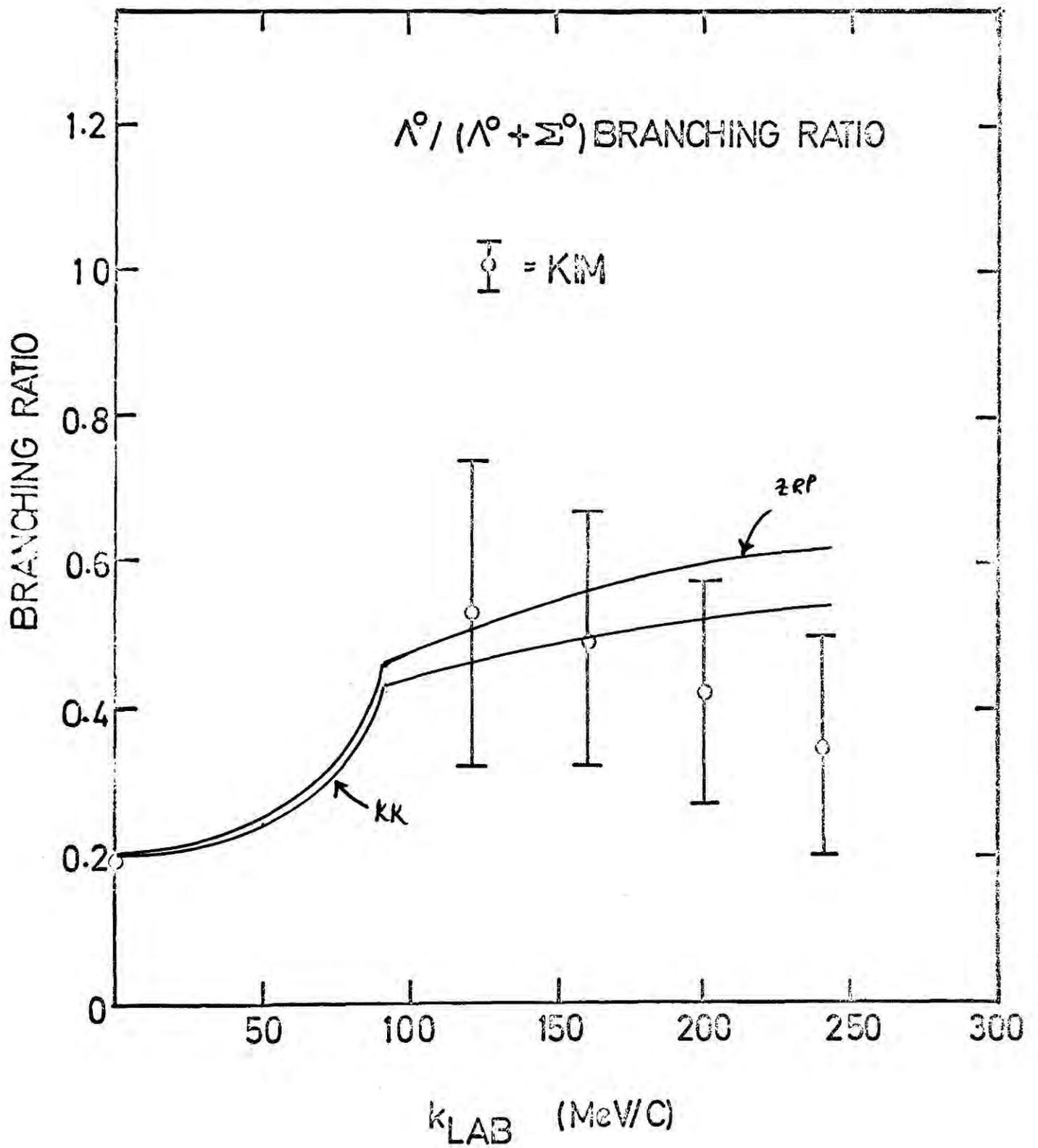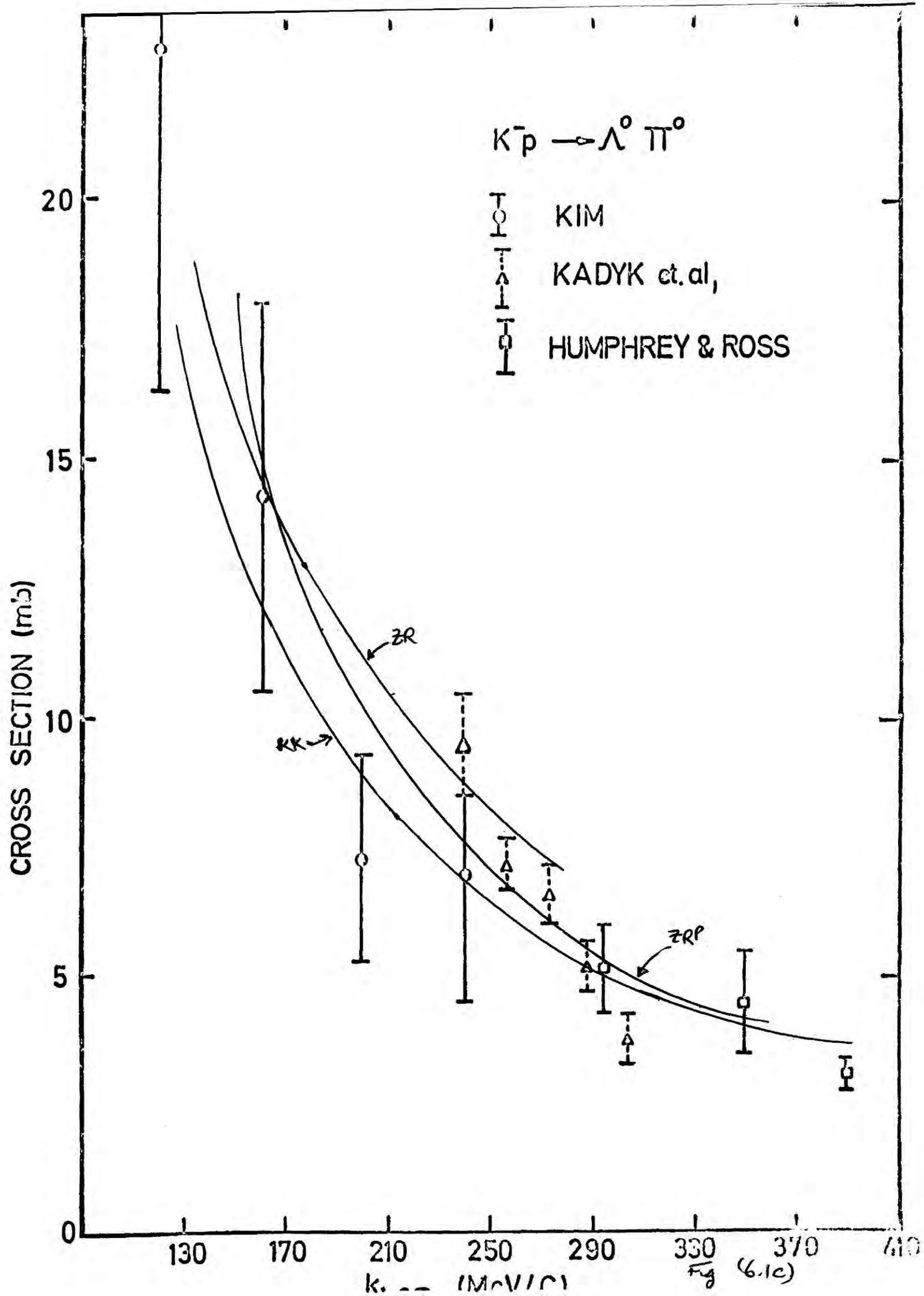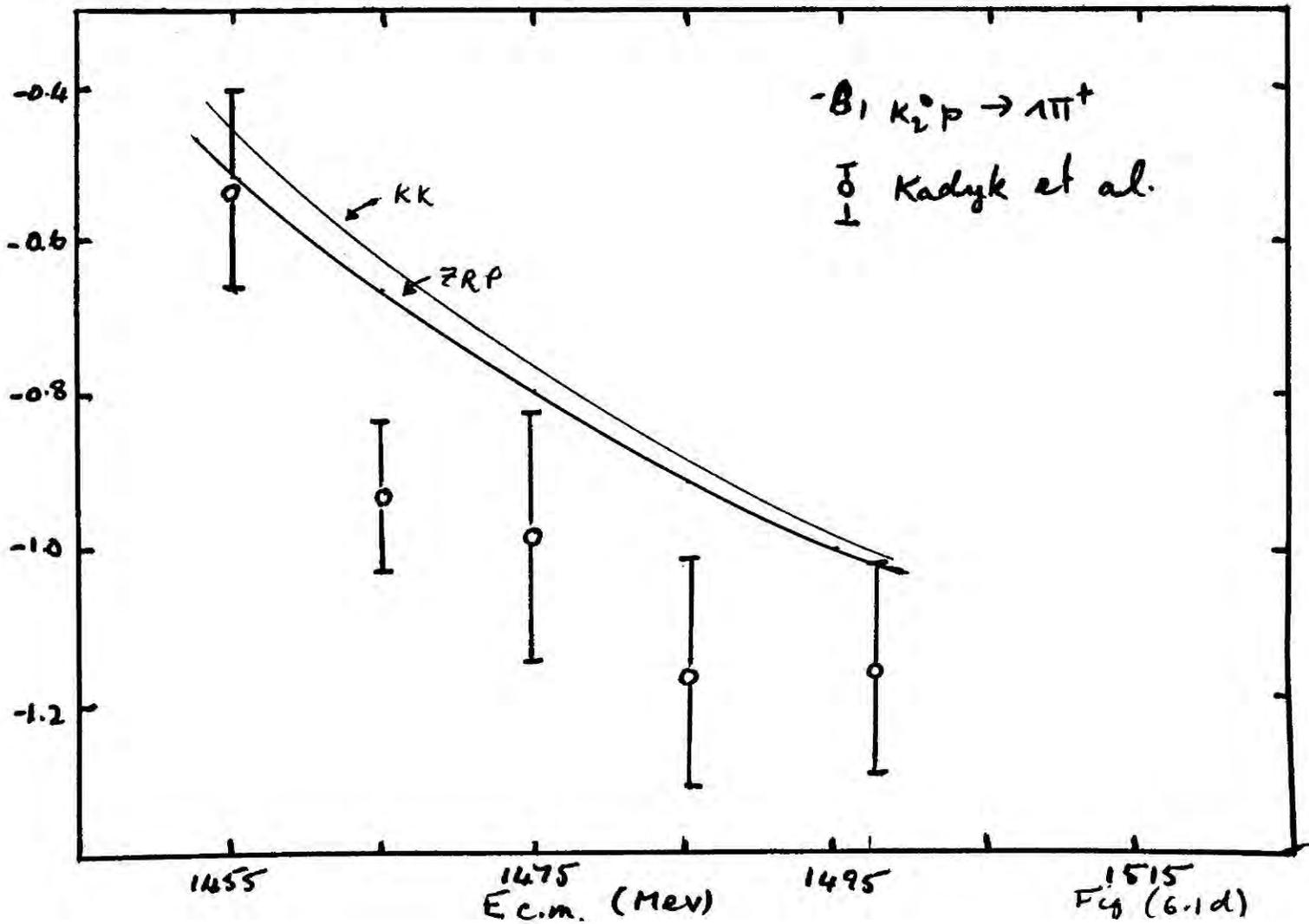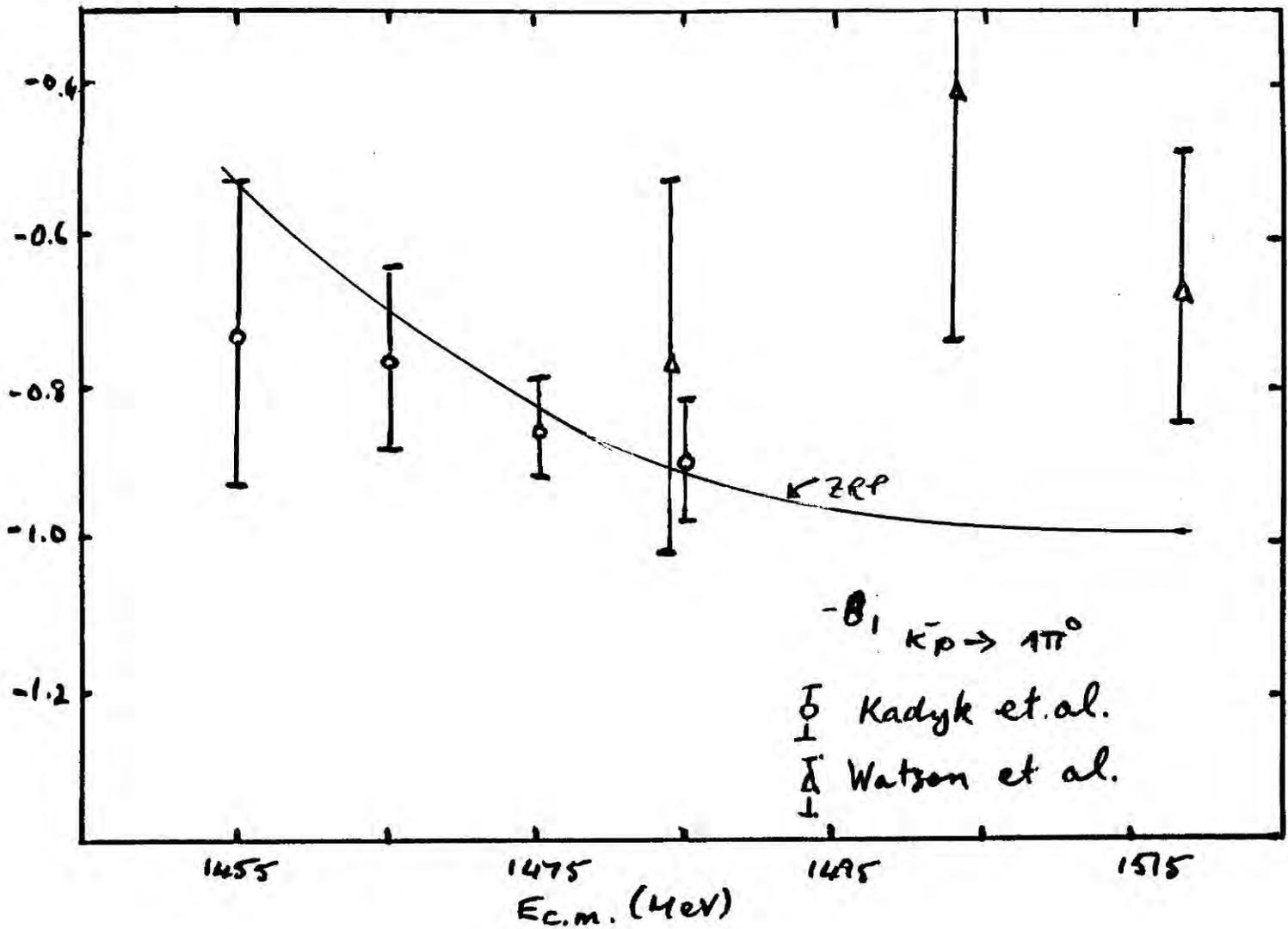
Fig (6.1.f)

APPENDIX 1

Corrections arising from charge dependent effects

The charge independence assumed for the strong interactions is violated in several ways be the effects of electromagnetic processes. Firstly, due to the mass differences generated within Isospin multiplets by the electromagnetic interactions, the channel momentum matrix may no longer be considered diagonal. The most important of these mass differences, and the only one considered here, is the K^-p, $\bar{K}^0n$ mass difference. Secondly the elements of the K matrix are modified from their values for the nuclear reactions alone by corrections which may be separated into two parts. The most important is due to the K^-p Coulomb interaction whose long range leads to appreciable corrections at low relative velocity. The significant parameter for this interaction is where B is the Bohr radius ($\frac{\hbar^2}{\mu e^2} \simeq$ 84 fm) for the K^-p system. The other corrections are those due to the electromagnetic modifications of the nuclear interactions and, being of relative order $\frac{e^2}{\hbar c} \sim \frac{1}{137}$, are neglected.

The correction due to the K^-p, $\bar{K}^0n$ mass differences was first discussed by Jackson and Wyld[57]. They noted

that the channel momenta matrix k is really diagonal
only for the basis given by the states

$$|K^-p>, \quad |\bar{K}^0n>, \quad |b_0>, \quad |b_1>, \quad |c_1>$$

where $|b_0>$, $|b_1>$ and $|c_1>$ are defined in (2.35).
In this basis, known as basis I,

$$k_{(I)} = \begin{pmatrix} k & 0 & 0 & 0 & 0 \\ 0 & k_0 & 0 & 0 & 0 \\ 0 & 0 & q_\Sigma & 0 & 0 \\ 0 & 0 & 0 & q_\Sigma & 0 \\ 0 & 0 & 0 & 0 & q_\Lambda \end{pmatrix}$$

where k and k_0 denote the K^-p and $\bar{K}^0n$ momenta respectively.

However the K matrix, with threshold factors removed,
may be written in block diagonal form for the basis,
basis II,

$$|a_0>, \quad |b_0>, \quad |a_1>, \quad |b_1>, \quad |c_1>$$

as

$$K^{-1}_{\ell t} = \begin{pmatrix} M_1 & M_2 & 0 & 0 & 0 \\ M_2 & M_3 & 0 & 0 & 0 \\ 0 & 0 & M_4 & M_5 & M_6 \\ 0 & 0 & M_5 & M_7 & M_8 \\ 0 & 0 & M_6 & M_8 & M_9 \end{pmatrix}$$

(II)

If this is now written, using (2.35), in basis I we
find

$$
K_{\ell \pm \atop (I)}^{-1} = \begin{pmatrix}
\frac{1}{2}(M_4+M_1) & \frac{1}{2}(M_4-M_1) & \frac{1}{\sqrt{2}}M_2 & \frac{1}{\sqrt{2}}M_5 & \frac{1}{\sqrt{2}}M_6 \\
\frac{1}{2}(M_4-M_1) & \frac{1}{2}(M_4+M_1) & -\frac{1}{\sqrt{2}}M_2 & \frac{1}{\sqrt{2}}M_5 & \frac{1}{\sqrt{2}}M_6 \\
\frac{1}{\sqrt{2}}M_2 & -\frac{1}{\sqrt{2}}M_2 & M_3 & 0 & 0 \\
\frac{1}{\sqrt{2}}M_5 & \frac{1}{\sqrt{2}}M_5 & 0 & M_7 & M_8 \\
\frac{1}{\sqrt{2}}M_6 & \frac{1}{\sqrt{2}}M_6 & 0 & M_8 & M_9
\end{pmatrix}
$$

If the T matrix given by

$$
T_{\ell \pm (I)}^{-1} = K_{\ell \pm (I)}^{-1} - ik^{2\ell+1}_{(I)}
$$

is now worked out in basis I it is found that the corrections due to the K^-p, $\bar{K}^0n$ mass differences may conveniently be expressed in terms of the scattering lengths by the rules:

The factor $\dfrac{1}{1-ik^{2\ell+1}A_0}$ is replaced by $\dfrac{1-ik_0^{2\ell+1}A_1}{D}$

and $\dfrac{1}{1-ik^{2\ell+1}A_1}$ is replaced by $\dfrac{1-ik_0^{2\ell+1}A_0}{D}$

where

$$
D = 1 - \tfrac{1}{2}(A_0+A_1)(k_0+k) - k\,k_0\,A_0\,A_1 \tag{A1.1}
$$

Finally the T matrix elements are obtained by the formula

$$
T_{\ell \pm} = k_{(I)}^{-\ell}\, T_{\ell \pm (I)}\, k_{(I)}^{-\ell}
$$

The S wave Coulomb corrections, together with these mass difference corrections, have been considered in detail by Dalitz and Tuan[12]. These authors assume that there is a radius R beyond which the K^-p Coulomb

interaction may be neglected.

It is well known that the K matrix element $\langle i|K|j\rangle$ denotes the amplitude of the asymptotic wave in the jth channel when the boundary conditions are standing spherical waves in all channels, together with an incident plane wave of unit amplitude in channel i. Then just within r = R the inside wave function has the form, for the case of an incident K^-p channel (channel 1).

$$\langle K^-p|\psi(r)\rangle = \angle\left(\frac{\sin kr}{kr} + K_{11}\cos kr/r\right)$$
$$\langle i|\psi(r)\rangle = \angle\, k_{1i}\cos kr/r$$

where $\angle$ is a normalisation factor and K_{11}, K_{1i} denote the nuclear K-matrix elements. The wave functions outside r = R are given by the solutions of the s-wave Coulomb equation and thus the K-matrix K_c corrected for Coulomb effects is defined by the corresponding outside wave functions

$$\langle K^-p|\psi(r)\rangle = F_0(kr)/kr + K_{c11}\, G_0(kr)/r$$
$$\langle i|\psi(r)\rangle = K_{c1i}\, 1.(\cos kr)/r$$

Here $F_0(kr)$ and $G_0(kr)$ are the regular and irregular independent solutions of the Coulomb s-wave equation.

The inside and outside wave functions may similarly be written down for incident waves in all channels, and, be demanding smooth matching between them at r = R, the corrected K matrix K_c may be obtained. Once again it is found that these corrections may be

conveniently expressed in terms of the unperturbed scattering lengths as follows.

(i) Factor $\frac{1}{1-ikA_0}$ is replaced by $\frac{1-ik_0A_1}{D}$ and $\frac{1}{1-ikA_1}$ is replaced by $\frac{1-ik_0A_0}{D}$ where D is modified from equation (A1.1) as given below.

(ii) The Coulomb penetration factor C_0 has to be multiplied every time the $\bar{K}p$ state enters.

D and C_0 are defined as follows.

$$D = 1 - \frac{1}{2}(A_0 + A_1)\left\{k_0 + kC_0^2(1-\lambda)\right\} - k_0kC_0^2(1-\lambda)A_0A_1$$

where

$$\lambda = -\frac{2}{kBC_0^2}\left\{\ln(2kR) + \ell_e\,\Psi\left(\frac{i}{kB}\right) + 2\gamma\right\}$$

$$\Psi(z) = d\left[\ln\Gamma(z)\right]/dz, \qquad \gamma \text{ is the Euler constant,}$$

B the $\bar{K}p$ Bohr radius.

$$C_0^2 = \frac{2\pi}{kB}\left[1 - \exp\left(-\frac{2\pi}{kB}\right)\right]^{-1}$$

The $\bar{K}p$ differential cross section must also be modified to take Coulomb scattering into account. This is done as follows

$$\frac{d\sigma_{\bar{K}p}}{d\Omega} = \left|\frac{\csc^2\theta/2}{2Bk^2}\exp\left[\frac{2i}{kB}\ln\sin\frac{\theta}{2}\right] + T_{\bar{K}p\to\bar{K}p}\right|^2$$

Appendix 2

Numerical evaluation of Principle value integrals

We consider the evaluation of integrals of the
type

$$I(\omega) = P\int_{\omega_1}^{\omega_2} \frac{f(\omega')}{(\omega'-\omega)} d\omega'$$

where $\omega_1 \leq \omega \leq \omega_2$. These may immediately be re-written
in the form

$$I(\omega) = \int_{\omega_1}^{\omega_2} \frac{f(\omega')-f(\omega)}{(\omega'-\omega)} d\omega' + f(\omega)\int_{\omega_1}^{\omega_2} \frac{1}{(\omega'-\omega)} d\omega'$$

The first integral may be readily evaluated by the
usual numerical methods provided that $\frac{\partial}{\partial\omega'} f(\omega')\big|_{\omega'=\omega}$
exists. The second integral may be evaluated analytically.
The result is

$$I(\omega) = \int_{\omega_1}^{\omega_2} \frac{f(\omega')-f(\omega)}{(\omega'-\omega)} d\omega' + f(\omega)\ln\left|\frac{\omega_2-\omega}{\omega-\omega_1}\right|$$

$$\simeq \int_{\omega_1}^{\omega-\epsilon} \frac{f(\omega')-f(\omega)}{(\omega'-\omega)} d\omega' + 2\epsilon f'(\omega) + \int_{\omega+\epsilon}^{\omega_2} \frac{f(\omega')-f(\omega)}{(\omega'-\omega)} d\omega'$$

$$+ f(\omega)\ln\left|\frac{\omega_2-\omega}{\omega-\omega_1}\right|$$

APPENDIX 3

Fitting of Experimental Data

In an experimental measurement of a quantity a there will, in general, be a probability distribution $P(x)$ of measuring a value x for this quantity in any single determination. This distribution will be peaked about the most likely value x* and a good approximation to this distribution is usually given by the Gaussian distribution

$$P(x) = \frac{1}{\sqrt{2\pi}\,\sigma} \exp\left[-\frac{(x-x^*)^2}{2\sigma^2}\right] \qquad (A3.1)$$

where σ is the standard error. If now N quantities are a measured to give experimental values x_i with standard errors σ_i and we suppose that we have theoretical expressions for these quantities depending on a set of n parameters a_m we may form a likelihood function given by

$$L(a_1, a_2 \cdots a_n) = \frac{1}{(2\pi)^{N/2}\,\sigma_1 \sigma_2 \cdots} \exp\left[-\sum_{i=1}^{N} \frac{(x_i - \xi_i)^2}{2\sigma_i^2}\right] \qquad (A3.2)$$

where $\xi_i = \xi_i(a_1 \cdots a_n)$ are the theoretical expressions for x_i.

We may now define the values of the parameters a_i giving a "best fit" to the data as those maximising

the likelihood function (a_m), a criterion which is obviously equivalent to minimising the exponent

$$\sum_{i=1}^{N} \frac{(x_i - \xi_i)^2}{2\sigma_i^2} = \frac{1}{2} \chi^2(a) \qquad (A3.3)$$

This defines the Chi-squared function $\chi^2(a)$ which is generally used in performing the "least-squares" fit to the data. This fit is found by the condition

$$\frac{\partial \chi^2(a)}{\partial a_i} = 0 \qquad \text{for all i} \qquad (A3.4)$$

together with the condition for a minimum

$$\frac{\partial^2 \chi^2(a)}{\partial^2 a_i} \geqslant 0 \qquad \text{for all i} \qquad (A3.5)$$

The errors associated with the parameters a_n^* which satisfy the best fit conditions (A3.4) and (A3.5) may be determined using the likelihood function of (A3.2) to compute the mean deviations $(a_m - a_m^*)(a - a^*)$. To do this we note that the Chi-square function may be expanded in a Taylor series about the best fit position a^*

$$\chi^2(a) = \chi^2(a^*) + \sum_{i=1}^{n} (a_i - a_i^*) \frac{\partial^2 \chi^2(a)}{\partial a_i} \bigg|_{a_i = a_i^*} (A3.6)$$

$$+ \frac{1}{2} \sum_{i,j=1}^{n} (a_i - a_i^*)(a_j - a_j^*) \frac{\partial^2 \chi^2(a)}{\partial a_i \partial a_j} \bigg|_{\substack{a_i = a_i^* \\ a_j = a_j^*}} + \cdots$$

Since the first derivatives vanish by condition (A3.4)

we have, from (A3.2), and neglecting third order terms and above

$$u(a) = C \exp\left[-\frac{1}{2} \sum_{i=1}^{n} \sum_{j=1}^{n} E_{ij} \beta_i \beta_j\right] \qquad \text{(A3.7)}$$

where
$$C = \frac{1}{(2\pi)^{N/2} \, e_1 e_2 \ldots} \exp\left[-\frac{1}{2} \chi^2(a^*)\right]$$

and
$$E_{ij} = \frac{1}{2} \frac{\partial^2 \chi^2(a)}{\partial a_i \partial a_j}\Bigg|_{\substack{a_i = a_i^* \\ a_j = a_j^*}}$$

with
$$\beta_i = (a_i - a_i^*)$$

E is a symmetric matrix and we suppose u is the unitary matrix that diagonalises E

$$u E u^{-1} = \begin{pmatrix} e_1 & & & 0 \\ & e_2 & \ddots & \\ 0 & & & e_n \end{pmatrix} \equiv e$$

Defining $\beta = (\beta_1 \beta_2 \cdots \beta_n)$ and $\gamma = \beta u^{-1}$ we may write the element of probability in β space as

$$dP = C \exp\left[-\frac{1}{2} \gamma e \gamma\right] d\beta$$

Since $|u| = 1$ is the Jacobean relating $d\beta$ and $d\gamma$ we have

$$dP = C \exp\left[-\frac{1}{2} \sum_{i} e_i \gamma_i^2\right] d\gamma$$

which is now a product of independent one-dimensional Gaussian distributions. Thus

$$\overline{\gamma_a \gamma_b} = \delta_{ab} \, e_a^{-1}$$

and hence

$$\overline{\beta_i \beta_j} = \sum_a \sum_b \overline{\gamma_a \gamma_b} \, u_{ai} u_{bj}$$
$$= \sum_a u_{ia}^{-1} e_a^{-1} u_{aj}$$
$$= (u^{-1} e u)^{-1}_{ij}$$

and so we obtain the result

$$\overline{(a_i - a_i^*)(a_j - a_j^*)} = (E^{-1})_{ij}$$

and E^{-1} is known as the error matrix.

It is possible, using the χ^2 function to derive a quantitative condition for a "good" fit. If $\bar{x}_i$ is the true mean of x_i, the normalised probability of observing x, in dx, x_2 in dx_2, etc., is

$$P(x_1, x_2 \cdots x_N) \, dx_1 \cdots dx_N = \prod_{i=1}^{N} \frac{1}{\sqrt{2\pi} \, \sigma_i} \exp\left[-\frac{1}{2} \sum_{i=1}^{N} q_i^2\right] dx_i$$

where

$$q_i = \frac{1}{\sigma_i}(x_i - \bar{x}_i)$$

If we define $\quad Q(q_i) = (2\pi)^{N/2} \exp\left[-\frac{1}{2}\sum_{i=1}^{N} q_i^2\right]$

then $\quad Q(q_i) \, dq_1 \cdots dq_N = P(x_i) \, dx_1 \cdots dx_N$

and Q depends on the q_i only through

$$\sum_{i=1}^{N} q_i^2 = \chi^2$$

It therefore has the same value everywhere on a spherical surface in N dimensions and the probability distribution of χ has the form

$$F(\chi^2) \, d\chi^2 = \int_{\text{spherical shell } \chi, d\chi} Q(q_i) \, dq_1 \cdots dq_N = (2c) \, e^{-\chi^2/2} \chi^{N-1} d\chi$$
$$= c \, e^{-\chi^2/2} \chi^{N-2} \, 2\chi \, d\chi .$$

C is determined by the normalisation

$$\int_0^\infty F(\chi^2)\, d\chi^2 = 1$$

And thus

$$F(\chi^2)\, d\chi^2 = \frac{1}{2^{N/2}\,\Gamma(\frac{N}{2})}\, e^{-\chi^2/2}\, (\chi^2)^{\frac{N}{2}-1}\, d\chi^2$$

The probability that χ^2 exceeds the observed value χ_0^2

is

$$P_N(\chi^2 > \chi_0^2) = \int_{\chi_0^2}^\infty F(\chi^2)\, d\chi^2$$

Tables of this function are given in ref.(60). If

it is large, the fit is good. In a more thorough

probability analysis it turns out that the number N

should be the difference of the number of data points

and the number of parameters i.e. the number of degrees

of freedom.

REFERENCES

1. M. Gell-Mann and Y. Ne'eman: The Eightfold Way
    Benjamin (1964).

2. F. Gursey and L.A. Radicati: Phys. Rev. Letters
    13, 173-175 (1964).
    A. Pais: Phys. Rev. Letters 13, 175-177 (1964).

3. W. Heisenberg: Z. Physik, 120, 513 673 (1943).

4. See for example E.J. Squires: Complex Angular
    Momenta and Particle Physics, Benjamin, New
    York (1963).

5. P. Nath and G.L. Shaw: Phys. Rev., 138, B702-
    B706,(1965).

6. G.F. Chew, M.L. Goldhaber, F.E. Low and Y. Nambu:
    Phys. Rev., 106, 1337 (1957).

7. See for example G. Kallen: Elementary Particle
    Physics, Addison-Wesley (1964).

8. S. Gasiorowicz: Fort. der Phys., 8, 665 (1962).

9. M. Jacob and G.C. Wick: Ann. Phys., 7, 404 (1959).

10. See for example M. Jacob and G.F. Chew: Strong
    Interaction Physics, Benjamin (1964).

11. S. Mandelstam: Phys. Rev. Letts., 4, 84 (1959);
    Phys. Rev., 112, 1344 (1958); Phys. Rev. 115,
    1741, 1752 (1959).

12. R.H. Dalitz and S.F. Than: Ann. Phys. 10, 307
    (1960).

13. R.H. Dalitz: Rev. Mod. Phys., 33, 471 (1961).

14. M. Jacob and G.C. Wick: Ann. Phys., 7, 404 (1959).

15. S.W. MacDowell: Phys. Rev., 116, 774 (1959).

16. R.G. Moorhouse: Nuovo Cimento (10), 20, 123 (1961).

17. M. Ross and G. Shaw: Ann. Phys., $\underline{9}$, 391 (1960);
    Ann. Phys., $\underline{13}$, 147 (1961).

18. P. Nath and G. Shaw: Phys. Rev., $\underline{138}$, B702-B706
    (1965).

19. J.K. Kim: Phys. Rev. Letts., $\underline{19}$, 1074, 1079 (1967).

20. G. Barton: Dispersion Techniques in Field Theory
    Benjamin

21. J. Bjorken and S. Drell: Relativisitic Quantum
    Fields P260   McGraw-Hill (1964).

22. S. Pomeranchuk: JETP, $\underline{7}$, 499 (1958).

23. R.J.N. Phillips and W. Rarita: Phys. Rev., $\underline{139}$,
    B1336 (1965).

24. S. Goldhaber, W. Chinowsky, G. Goldhaber, W. Lee,
    T. O'Halloran, T. Stubbs, G. Pjerrou, D. Stork,
    H. Ticho: Phys. Rev. Letts., $\underline{9}$, 135 (1962).

25. A.D. Martin and R. Perrin: Nuc. Phys., $\underline{B10}$, 125 (1969).

26. R.J. Glauber: Phys. Rev. $\underline{100}$, 242 (1955).

27. C. Wilkin: Phys. Rev. Letts., $\underline{17}$, 561 (1966).

28. V.J. Stenger et al.: Phys. Rev. $\underline{134B}$, 1111 (1964).

29. H.P.C. Rood: Nuovo Cimento $\underline{50A}$, 493 (1967).

30. W. Kittel and G. Otter: Phys. Letters $\underline{22}$, 115 (1966).

31. N. Zovko: Z. Phys. $\underline{192}$, 346 (1966).

32. M. Lusignoli, M. Restignoli, G.A. Snow and G. Violini:
    Phys. Letts., $\underline{21}$, 229 (1966).

33. A.A. Carter: Phys. Rev. Letts., $\underline{18}$, 801 (1967).

34. G.H. Davies, N.M. Queen, M. Lusignoli, M. Restignoli
    and G. Violini: Nuc. Phys. $\underline{B3}$, 616 (1967).

35. A.D. Martin and F. Poole: Phys. Letters $\underline{25B}$, 343 (1967).

36. A.A. Carter: Cambridge University report HEP 68-
    10 (1968).

37. N.M. Queen, S. Leeman and F.E. Yeomans: Nuclear Phys. (to be published).

38. Ya. I. Granovskii and V.N. Starikov: Sov. J. Nuc. Phys., $\underline{6}$, 444 (1968).

39. See for example J.J. de Swart: NIRL LN/5 (Lecture Notes).

40. N.F. Nelipa: Nuc. Phys. $\underline{82}$, 680 (1966).

41. H. Thom: Phys. Rev. $\underline{151}$, 1322 (1966).

42. C.A. Levinson, H.J. Lipkin and S. Meshov: Phys. Letts. $\underline{7}$, 81 (1963).

43. V.B. Elings et al.: Phys. Rev. $\underline{156}$, 1433 (1967).

44. A.M. Boyarski et al.: Phys. Rev. Letts., $\underline{22}$, 1131 (1969).

45. K. Igi: Phys. Rev. Letts., $\underline{9}$, 76 (1962).

46. Bateman Manuscript Project, Vol. 1   McGraw-Hill (1955).

47. A.D. Martin and F. Poole: Nuc. Phys., $\underline{B4}$, 467 (1968).

48. L. Sertorio and M. Toller: Phys. Letts., $\underline{18}$, 191 (1965).

49. A.D. Martin and G.G. Ross: Phys. Letts., $\underline{26B}$, 527, (1967).

50. A.D. Martin, N.M. Queen, G. Violini: Nuc. Phys., $\underline{B10}$, 131 (1969).

51. N.M. Queen, S. Leeman and F.E. Yeomans: Nuc. Phys., to be published.

52. C.H. Chan and F.T. Meiere: Phys. Rev. Letts. $\underline{20}$, 568 (1968).

53. T.D. Lee and C.N. Yang: Phys. Rev. $\underline{108}$, 1645 (1957).

54. Y.C. Lin: Phys. Rev., $\underline{172}$, 1564 (1968).

55. B.R. Martin and M. Sakitt: to be published.

56. F. Von Hippel and J.K. Kim: Phys. Rev. Letts., 20, 1303 (1968).

57. J.D. Jackson and H. Wyld: Nuovo Cimento (10), 13, 84 (1959).

58. B.R. Martin: Phys. Rev., 138B, 1136 (1965).

59. D.W. Merrill and J. Button-Shafer: Phys. Rev. 167, 1202 (1968).

60. M. Abramowitz and I. Stegun: Handbook of Mathematical Functions Dover (1964).

61. T.D. Lee, J. Steinberger, G. Feinberg, P.K. Kabir and C.N. Yang: Phys. Rev., 106, 1367 (1957).

E1   W.E. Humphrey and R.R. Ross: Phys. Rev. <u>127</u>, 1305 (1962).

E2   M. Sakitt et al.: Phys. Rev. <u>139</u>, B719

E3   J.K. Kim: Columbia University Report, Nevis-149 (1969).

E4   W. Kittel, G. Otter and I. Wacek: Phys. Letts. <u>21</u>, 349 (1966).

E5   M.B. Watson, M. Ferro-Luzzi and R.D. Tripp: Phys. Rev. <u>131</u>, 2248 (1963).

E6   J.A. Kadyk et al.: Phys. Rev. Letts. <u>17</u>, 599 (1966).

E7   G. Sayer et al.: Phys. Rev. <u>169</u>, 1045 (1968).

E8   R.L. Cool et al.: Phys. Rev. Letts. <u>16</u>, 1228 (1966), <u>17</u>, 102 (1966).
       J.D. Davies et al.: Phys. Rev. Letts. <u>18</u>, 62 (1967).
       R.J. Abrams et al.: Phys. Rev. Letts. <u>19</u>, 259 (1967), <u>19</u>, 678 (1967).
       D.V. Bugg et al.: Phys. Rev. <u>168</u>, 1466 (1968).

E9   V. Cook et al.: Phys. Rev. <u>123</u>, 320 (1961); Phys. Rev. Letts., <u>7</u>, 182 (1961).
       W.F. Baker et al.: Phys. Rev. <u>129</u>, 2285 (1963); Proc. Sienna Intern. Conf. on Elementary Particles (1963) P.634.
       A.N. Diddens, E.W. Jenkins, T.F. Kycia and R.F. Riley: Phys. Rev., <u>132</u>, 2721 (1963).

E10   W. Galbraith et al.: Phys. Rev. <u>138B</u>, 913 (1965).

E11   J.A. Kadyk et al.: UCRL 18325 (1968).